THE UNIVERSITY *of* EDINBURGH

Estimating the above-ground biomass of mangrove forests in Kenya

Rachel Cohen

Doctor of Philosophy

The University of Edinburgh

2014

Declaration

I declare that the work contained in this thesis is my own, unless indicated otherwise. No part of this thesis has been previously submitted or accepted for a degree or professional qualification.

Rachel Cohen

October 2014

Abstract

Robust estimates of forest above-ground biomass (AGB) are needed in order to constrain the uncertainty in regional and global carbon budgets, predictions of global climate change and remote sensing efforts to monitor large scale changes in forest cover and biomass. Estimates of AGB and their associated uncertainty are also essential for international forest-based climate change mitigation strategies such as REDD+. Mangrove forests are widely recognised as globally important carbon stores. Continuing high rates of global mangrove deforestation represent a loss of future carbon sequestration potential and could result in significant release into the atmosphere of the carbon currently being stored within mangroves.

The main aims of this thesis are 1) to provide information on the current AGB stocks of mangrove forests in Kenya at spatial scales relevant for climate change research, forest management and REDD+ and 2) to evaluate and constrain the uncertainty associated with these AGB estimates. This thesis adopted both a ground-based statistical approach and a remote sensing based approach to estimating mangrove AGB in Kenya.

Allometric equations were developed for Kenyan mangroves using mixed-effects regression analysis and uncertainties were fully propagated (using a Monte Carlo based approach) to estimates of AGB at all spatial scales (tree, plot, region and landscape). In this study, species and site effects accounted for a large proportion (41%) of the total variability in mangrove AGB. The generic biomass equation produced for Kenyan mangroves has the potential for broad application as it can be used to estimate the AGB of new trees where there is no pre-existing knowledge of the specific species-site allometric relationship. The 95% prediction intervals for landscape scale estimates of total AGB suggest that between 5.4 and 7.2 megatonnes (Mt) of AGB is currently held in Kenyan mangrove forests.

An in-depth evaluation of the relative contribution of various components of uncertainty (measurement, parameter and residual uncertainty) to the magnitude of the total uncertainty of AGB estimates was carried out. This evaluation was undertaken using both the mixed-effects regression model and a standard ordinary

least squares (OLS) regression model. The exclusion of measurement uncertainty during the biomass estimation process had negligible impact on the magnitude of the uncertainty regardless of spatial scale or tree size. Excluding the uncertainty due to species and site effects (from the mixed-effects model) consistently resulted in a large reduction (~ 70%) in the overall uncertainty. Estimates of the uncertainty produced by the OLS model were unrealistically low which is illustrative of the general need to account for group effects in biomass regression models.

L-band Synthetic Aperture Radar (SAR) was used to estimate the AGB of Kenyan mangroves. There was an observable relationship ($R^2 = 0.45$) between L-band HH and AGB with HH backscatter found to decrease as a function of increasing AGB. There was no significant relationship found between L-band HV and AGB. The negative relationship between HH and AGB in this study can possibly be attributed to enhanced backscatter at lower AGB due to strong double-bounce and direct surface scattering from short stature/open forests and attenuation of the SAR signal at higher AGB. The SAR-derived estimate of total AGB for Kenyan mangroves was 5.32 Mt ± 18.6%. However, due to the unexpected nature of the HH-AGB relationship found in this study the SAR-derived estimates of mangrove AGB in this study should be considered with caution.

Acknowledgements

Firstly I would like to thank my principal supervisor Prof. Maurizio Mencuccini for his endless encouragement, support, patience and above all, faith in me over the past years. I was never afraid to knock on your door and that was more important than I can say. I would also like to thank my other supervisors Prof. Mark Huxham, Dr. James Kairo and Prof. Iain Woodhouse for providing their advice throughout. I am very grateful to Dr. Ed Mitchard for guiding me through the complicated world of radar, to Dr. Karin Viergever for contributing some of her SPOT work to this thesis and to Dr. Giles Innocent for patiently answering numerous statistical questions.

The funding for this PhD was provided by the Natural Environment Research Council (NERC), UK to whom I am very grateful. This research was made possible through close collaboration with Kenya, Marine and Fisheries Research Institute (KMFRI) who provided access to datasets and help with organising some of the logistical aspects of conducting research in Kenya. I would also like to thank Kenya Forest Service (KFS) for allowing their forest rangers to participate in the fieldwork for this study and Sheelali Abdallah Athman for his help in organising the logistical aspects of working in Lamu.

I met so many great people during my time in Kenya that not only helped me with carrying out the fieldwork for this project but also made my time in Kenya an unforgettable experience. I wish to thank Dr. Joseph Lang'at who was a friendly face in Gazi, put up with my many mangrove questions and empathised with the difficulties of the '**P**ermanent **h**ead **D**amage' process. Collecting the field data for this study was challenging to say the least and was only made possible by the hard work and dedication of KFS rangers: Bwanaheri Ali Sizi, Kris, Mohammed Bachari, Mwagasambi Gasare Said, Moses Makau Kilale and KMFRI staff: Alfred Obinga, Nema Pasua, Hamisi Ali Kiruani and Laitani Suleiman Kumbambanya. I would also like to thank Mohammed Jale for his hard work in the field in Lamu.

I wish to make special mention of Yussef Jale whose exceptional skill as coxswain kept us all safe at sea, whose dedication kept us safe on land and whose entire family extended their warmth and hospitality to me during my time in Lamu. Last but by no

means least I would like to express my sincere gratitude and admiration for Mr. Bernard Kivyatu whose experience and knowledge about all things mangrove was undoubtedly my greatest asset in the field. Without Bernard's tireless hard work, enthusiasm and commitment much of the fieldwork for this project would not have been possible and it definitely would not have been so much fun! Thank you to all those who shared my mangrove adventure you kept my spirits up and gave me so many great memories.

I would not have made it through this process without the friends I met at Edinburgh University. Thanks to Gemma Cassells for patiently introducing me to the concept of remote sensing over numerous long coffee breaks. A massive thank you to Bron, Sam, Tom, John, Iain and Abbie for helping me through more low points than I care to remember and for generally being my mateys – it wasn't often sensible but it was always fun! To Luke, thank you for your friendship, help and support throughout (it is no exaggeration to say I would not have made it this far without you) but above all thank you for just being in my life, I can't express how much it means to me but I hope you know.

Finally, I would not be where I am now without the unwavering love and support of my family, in particular that of my mum Helen Cohen. Your strength, hard work and above all, your care and concern for others are an inspiration to me. This PhD is dedicated to you.

"…. at current rates of deforestation, and in response to rising sea levels mangrove forests will be virtually gone by the year 2100, and during that same year 4.3 million papers will be published about them."

Ellison (2002)

Contents

1. Introduction

Atmospheric concentration of CO_2 now exceeds pre-industrial levels by ~ 40% and increasing CO_2 concentration is the single biggest driver of global climate change (IPCC, 2013). Land use change is the second biggest contributor (after fossil fuel emissions) to global anthropogenic CO_2 emissions (IPCC, 2013). An estimated 15% (range 8-20%) of annual global anthropogenic CO_2 emissions results from deforestation, forest degradation and conversion of forest land to other uses occurring primarily in the tropics (FAO and JRC, 2012; van der Werf et al., 2009). Recent estimates suggest that during the period 2000-2005 mean net forest loss in the tropics was ~ 9 million ha yr^{-1} with Africa recording the second highest rate of forest loss (~ 2.7 million ha yr^{-1}) (FAO and JRC, 2012).

Concern regarding the impact of CO_2 emissions arising from deforestation and degradation on the global climate has led to increased emphasis being placed on estimating current carbon stocks[1] within the world's forests and changes to these stocks. Robust estimates of forest carbon stocks and stock changes are crucial in order to constrain uncertainties in regional and global carbon budgets and predictions of climate change made using earth systems models (Valentini et al., 2014). Such estimates are also a key requirement for international forest-based climate change mitigation strategies such as Reducing Emissions from Deforestation and Forest Degradation (REDD+).

REDD+ envisages achieving CO_2 emissions reductions, forest conservation and sustainable development by placing an economic value on forest carbon storage and facilitating the transfer of funds from developed to developing nations through international trade in carbon credits. In contrast to the Clean Development Mechanism (CDM[2]) initiated under the United Nations Framework Convention on Climate Change (UNFCCC) Kyoto Protocol; REDD+ emphasises the maintenance

[1] Carbon stocks can be converted to potential CO_2 emissions by multiplying the carbon stock by 3.67 (the molecular weight ratio of CO_2 to C).

[2] The CDM allows for developed countries to partially achieve their CO_2 emissions reduction targets by initiating emission reduction projects in developing countries which produce tradable certified emission reduction (CER) credits. Forest-based activities covered under the CDM are limited to afforestation and reforestation projects and to date account for just 0.8% of all projects registered under the CDM (UNEP, 2014).

and enhancement of current forest carbon stocks. Details of how REDD+ will operate at the national and international level under the UNFCCC are still under debate as there are a myriad of political, technical, financial and ethical issues (see Corbera, 2012; Streck, 2012; Venter and Koh, 2012) which are yet to be resolved and/or reconciled prior to wide-scale REDD+ implementation. Despite this, numerous REDD+ 'readiness' activities (e.g. demonstration projects and development of national REDD+ strategies) are already taking place across the globe with some of the funding provided by voluntary carbon markets but the bulk provided by voluntary carbon funds administered by various international organisations (e.g. the REDD+ partnership) (Streck, 2012).

Above-ground biomass (AGB[3]) is one of five forest carbon pools (IPCC, 2006) which is measurable and reportable for forest carbon projects operating under existing voluntary or future international compliance carbon markets (i.e. REDD+). Providing estimates of forest AGB which are accompanied by an appropriate measure of the associated uncertainty is a key requirement for REDD+ Measurement, Reporting and Verification (MRV) programs (Maniatis and Mollicone, 2010). Furthermore, much of the uncertainty in remote sensing derived estimates of AGB is due to the uncertainty in the ground-based AGB estimates ('ground truth' data) used to calibrate remote sensing algorithms (Ahmed et al., 2013). Therefore it is essential to produce statistically robust AGB estimates accompanied by a realistic estimate of the uncertainty in order to constrain the uncertainties involved with remote-sensing based approaches to large-scale monitoring of biomass dynamics (Venter and Koh, 2012).

1.1 Estimating above-ground biomass

Estimates of the AGB of trees are most commonly obtained through the use of allometric biomass equations which relate one or more measured variables (e.g. tree diameter) to total AGB (Ciais et al., 2011). In order to parameterise an allometric model it is usually necessary to destructively harvest and weigh a representative sample of individual trees for which these variables have been measured. Regression

[3] For simplicity estimates of above-ground biomass (dry weight) can be converted to carbon content using the IPCC default carbon fraction value of 0.47 i.e. carbon content = biomass*0.47(IPCC, 2006).

analysis is used to obtain a predictive relationship between the measured variable (s) and total AGB. This relationship is then applied to forest inventory data in order to produce estimates of AGB at larger spatial scales (e.g. plot, regional and landscape scale).

Allometric models are usually developed within a classical regression framework where ordinary least squares (OLS) regression techniques are applied to estimate the regression coefficients. However, a key limitation of such approaches is that they tend to ignore any correlations (or 'group effects') in the underlying dataset used to fit the model. This typically results in an underestimation of the standard error of regression coefficients and thus the uncertainty on final predictions made using such models (Steele, 2008). In contrast mixed-effects regression models offer an efficient means by which to analyse datasets which display a complex structure where data from individuals within populations are nested or grouped by one or more factors. For example, such grouping factors could include the species or site which the individual belongs to or an experimental treatment applied to a subset of individuals. Mixed-effects models allow for investigation of the variance in the response variable (e.g. total AGB) due to such group effects.

In mixed-effects models the regression coefficients are estimated by partial pooling. This process involves fitting the overall mean regression for the response variable (the complete pooling estimate) and a separate regression for each group (the no-pooling estimate) simultaneously. Model residuals are split into group-level and individual level residuals, thus the total variance is divided into 'between group' and 'within group' (between individuals) variance (Steele, 2008). Partial pooling estimates of a regression coefficient are calculated as a weighted average of the mean of the observations within a group (the no-pooling estimate) and the mean across all groups (the complete pooling estimate) relative to the sample size in each group and the estimated between group and within group variance parameters (Gelman and Hill, 2007). Thus, mixed-effects models allow for robust estimation of regression parameters and their uncertainty (Steele, 2008).

Previous studies have highlighted the importance of the choice of allometric model (i.e. model form) used to derive estimates of AGB (Parresol, 1999; Ryan, 2009;

Soares and Schaeffer-Novelli, 2005). In addition to issues regarding model specification the biomass estimation process (following choice of the 'best' model) introduces various other sources of uncertainty. The uncertainty of an estimate of AGB for a single tree is comprised of the uncertainty in the measurement of inventoried trees (measurement uncertainty) and the uncertainty due to the use of the allometric model for predicting the biomass of a new individual (predictive uncertainty) (Chave et al., 2004). These uncertainties are in turn propagated to estimates of AGB at larger spatial scales. Failing to account for uncertainties during the biomass estimation process ultimately leads to an under-estimation of the uncertainty on final predictions of AGB (Dietze et al., 2008). Accounting for predictive uncertainty is particularly important in biomass estimation as allometric equations are often applied outwith the data range for which they were originally intended (Chave et al., 2005) and are always applied outside the particular trees (and often sites) from which they were developed.

An important issue in practical biomass studies is the species and site specific nature of allometric relationships in trees (Zianis and Mencuccini, 2004). Given that it is impractical to construct a new allometric equation for every species encountered at every new site (particularly in species-rich tropical forests) this problem has mostly been approached by using compilations of species-specific equations (thus ignoring site specificity), using generic allometric models which combine data from various species and sites into a single equation or by re-sampling existing allometric equations to produce 'generalised' models (Chave et al., 2005; Komiyama et al., 2005; Zapata-Cuartas et al., 2012; Zianis, 2008). Generic allometric equations have been widely used to estimate AGB (in particular the set of pan-tropical equations developed by Chave et al., (2005)) however; in applying such equations the uncertainty introduced by variability in the allometric relationship due to species and site effects is often simply ignored.

1.1.1 Remote sensing and AGB

Remote sensing provides a powerful tool for fast and repeatable monitoring of land cover and above-ground carbon (i.e. AGB) dynamics at local, regional and global scales. To date a variety of remote sensing techniques have been used to produce

forest classification maps, estimates of forest cover (and changes in cover through time), to map deforestation and degradation and to estimate AGB biomass (Asner et al., 2012; FAO and JRC, 2012; Giri et al., 2011; Ryan et al., 2012; Saatchi et al., 2011b).

The use of optical remote sensing data for biomass studies in the tropics is often hampered by the presence of cloud cover, and relationships derived between optically sensed spectral metrics (e.g. NDVI) and AGB are generally of limited use (Patenaude et al., 2005). In contrast, active remote sensing techniques (LiDAR and radar) have shown greater potential for AGB estimation (Asner et al., 2012; Mitchard et al., 2009) however currently LiDAR data from space-borne sensors are not widely available and the cost of collecting airborne LiDAR data are prohibitive.

Synthetic Aperture Radar (SAR) systems actively transmit microwave energy (at various wavelengths) and measure the amount of energy that is returned to the sensor by the underlying ground surface. SAR systems operating at longer wavelengths (e.g. L-band) can penetrate the forest canopy and interact with the branches and stems below thereby providing information on the structural characteristics of the forest components which hold the greatest proportion of AGB (Lucas et al., 2007). Relationships between SAR backscatter and AGB have previously been derived for a variety of different forest types including boreal forest in Alaska (Rignot et al., 1994); savanna and miombo woodland in Africa (Mitchard et al., 2009); tropical forest in Costa Rica (Saatchi et al., 2011a) and mangroves in French Guiana (Mougin et al., 1999). Comparatively few previous studies have attempted to use SAR for the retrieval of AGB in mangroves and only one such study has been undertaken in Africa (Carreiras et al., 2012).

1.2 Mangroves – ecosystems of global importance

Mangroves are intertidal forests composed of saline tolerant tree and shrub species, which occur at the interface between land and sea, in tropical and subtropical latitudes (Fig. 1.1). Although they constitute just 0.1% of the earth's continental land surface (Giri et al., 2011) and 0.4% of the world's forested areas (FAO and JRC, 2012), mangroves play an important role in the global carbon cycle.

Fig. 1.1: Global distribution of mangrove forests. Modified from the UNEP Blue Carbon report (Nellemann et al., 2009).

1.2.1 Mangroves and carbon

Fixation of atmospheric CO_2 during photosynthesis by mangrove plant species often constitutes the bulk of organic carbon input to the mangrove system (Alongi et al., 2004). Mangroves are highly productive ecosystems with an estimated global net primary production (NPP[4]) of 218 ± 72 Tg C yr^{-1} (Bouillon et al., 2008). There is a general latitudinal trend in mangrove productivity such that it is highest in forests near the equator and decreases with increasing latitude (Saenger and Snedaker, 1993). At finer spatial scales mangrove productivity is influenced by a variety of factors such as; climatic conditions, species composition, forest age and structure, hydrology, salinity and soil characteristics (Day et al., 1996; Twilley et al., 1992).

Comparison of ecosystem carbon stocks suggests that at the global scale the amount of carbon stored by mangroves as live AGB (7990 g C m^{-2}) is second only to that

[4] Net Primary productivity (NPP) is commonly defined as the difference between total photosynthesis (gross primary productivity (GPP)) and plant respiration (R) i.e. NPP = GPP-R (Clark et al., 2001). Therefore, a positive value of NPP implies that there has been net fixation of carbon above and beyond what has been lost to the atmosphere via plant respiration. NPP equates to the increase in standing biomass and tissue turnover (above and below-ground) plus any losses (e.g. via litterfall, herbivory) over a given period of time (Clark et al., 2001; Chapin et al., 2006; Hogarth, 1999).

stored by terrestrial tropical forests (12045 g C m^{-2}) (Laffoley and Grimsditch, 2009). Levels of mean AGB have been found to vary considerably between mangrove forests across the globe (see review by Komiyama et al., 2008) reflecting not only variability in the factors which influence productivity (as mentioned above) but also varying levels of disturbance (Fromard et al., 1998). Global estimates of total mangrove AGB vary depending on the methodologies employed for estimating AGB and extrapolating estimates to the global scale but range between ~ 2.5 to 5 Pg AGB (Hutchison et al., 2013; Laffoley and Grimsditch, 2009; Siikamaki et al., 2012; Twilley et al., 1992). Thus despite accounting for just 0.7% of the world's tropical forest cover (Giri et al., 2011) mangroves hold up to 1.2% of the estimated 193 Pg C currently stored in tropical forest AGB (Saatchi et al., 2011b).

Comparatively few studies have focused on quantifying the amount of mangrove carbon stored as below-ground biomass. However, root production has been suggested to be equally if not more important than litterfall in terms of overall contributions to the soil carbon pool in mangroves (Gleason and Ewel, 2002; Kristensen, 2007). Previous studies have found that live below-ground root biomass accounted for between 18 to 37% of total mangrove biomass (Ong et al., 2004; Tamooh et al., 2009). A very high proportion (up to 97%) of mangrove below-ground biomass is composed of dead roots (Alongi and Dixon, 2000; Tamooh et al., 2008). The refractory nature of mangrove roots means that there is a large potential for carbon storage and accumulation in soils over time (Middleton and McKee, 2001). Biomass from *in situ* plant production constitutes the bulk of the carbon accumulating in mangrove sediments (Kristensen, 2007; Middleton and McKee, 2001), however, there can be additional inputs from land and sea (Jennerjahn and Ittekkot, 2002).

Carbon burial rates in mangroves can be substantial where sediment accretion rates and organic matter input are high and sediments are largely anoxic (Henrichs, 1992). Estimates of global mangrove carbon burial rates suggest that as much as 0.02 Pg C yr^{-1} is buried within mangrove sediments which equates to ~ 10% of the total carbon buried annually in global ocean sediments (Duarte et al., 2005). Analysis of peat cores suggests that mangroves in some areas have the capacity to accumulate deep

stores of organic material over exceptionally long time periods. Peat deposits from mangroves on the Caribbean coast can be up to 10m deep and have been dated between 7000 and 8000 years old (McKee et al., 2007). Recent estimates of whole ecosystem carbon stocks suggest that as much as 20 Pg of carbon is currently being stored in mangrove biomass, sediments and peat world-wide and that carbon density (ha^{-1}) within mangroves is several times that found within other tropical and temperate forest biomes (Donato et al., 2011).

Mangroves do not merely sequester carbon but represent an important link between the biogeochemical cycles of land and sea as they not only receive inputs of organic matter from terrigenous sources but due to tidal flooding and draining also exchange material with surrounding coastal waters. At the global scale, it has been estimated that mangroves export 0.05 Pg C yr^{-1} in the form of litter detritus to the coastal zone, which accounts for 11% of total annual terrestrial input of carbon to the oceans (Jennerjahn and Ittekkot, 2002). In addition, mangrove-derived dissolved organic carbon (DOC) exported primarily as a result of tidal flushing of sediment porewaters can be a major source of offshore DOC (Bouillon et al., 2007b; Dittmar et al., 2006; Lee, 1995). Bouillon et al., (2004) estimated that exported mangrove carbon accounted for 21-70% of the seagrass sedimentary organic C pool in Gazi Bay, Kenya indicating that a large proportion of benthic mineralization within nearby seagrass habitats may be sustained by mangrove-derived carbon (Bouillon et al., 2004).

1.2.2 Beyond carbon

In addition to their role within global biogeochemical cycles mangroves also provide a number of other key ecosystem services which are of ecological, economical and societal importance at local, regional and global scales. The mangrove environment plays host to both aquatic and terrestrial faunal communities providing habitat, refuge and food for a wide variety of benthic and pelagic species at different stages in their life cycle (Kristensen et al., 2008). Indeed, there is evidence to suggest that mangroves support offshore fisheries production (Aburto-Oropeza et al., 2008; Mumby et al., 2004). Local human communities often rely heavily on adjacent

mangroves for fishing, timber, fuelwood and traditional medicines (Dahdouh-Guebas et al., 2000).

In recent years, the role of mangroves in mitigating the effects of 'natural disasters' (e.g. tsunamis) has also been recognised (Dahdouh-Guebas et al., 2005; Zhang et al., 2012). Mangroves can not only act as physical 'buffers' during extreme weather events but their presence along coastal rivers and estuaries regulates the exchange of sediment between land and sea (Duarte et al., 2005). The process of coastal sedimentation and accretion is highly variable in space and time but in general mangroves appear to promote the net deposition of sediments (Alongi, 2009). The degradation and destruction of mangroves in some areas has resulted in substantial coastal erosion (Mazda et al., 2002).

1.3 Mangroves under threat

Mangroves have been systematically lost over recent decades primarily due to an increasing human population, wide-scale over-exploitation of wood resources and conversion to aquaculture, coastal development and human settlement (Alongi, 2002; Primavera, 2005). Current global mangrove cover has been estimated at ~ 14 million hectares (Giri et al., 2011) however, estimates of mangrove loss at the global scale indicate that ~ 20 to 35% of global mangrove cover has been lost since 1980 (FAO, 2007; Valiela et al., 2001). Rates of mangrove deforestation may be slowing in some countries however, they generally remain high at the global scale with an estimated loss of ~ 1 to 2% yr^{-1} (FAO, 2007; Valiela et al., 2001). The extent to which mangrove forests have suffered degradation is harder to quantify but is likely substantial and continued loss of cover, forest fragmentation and loss of species diversity may result in mangroves becoming functionally extinct within the next 100 years (Duke et al., 2007; Polidoro et al., 2010). In addition to the more immediate threat of deforestation and degradation; global climate change in general and sea level rise in particular poses a significant threat to remaining mangrove forests (Alongi, 2008; McLeod and Salm, 2006). The ability of mangroves to keep pace with future sea level rise will depend primarily on site specific rates of sediment accretion (relative to sea level rise) and thus mangroves in settings where there is low

sediment input, low topographic relief and limited options for landward migration will be at high risk of disappearing (Alongi, 2002; 2008; McLeod and Salm, 2006).

Given that mangroves represent a globally important carbon sink (Donato et al., 2011) their continued degradation and loss world-wide not only represents a loss of future C sequestration potential (and other important ecosystem services) but could result in significant release into the atmosphere of C currently stored within mangrove biomass, sediments and peat (Pendleton et al., 2012). Indeed, recent estimates indicate that between 0.02 and 0.12 Pg C yr^{-1} is emitted to the atmosphere as a result of global mangrove deforestation (Donato et al., 2011; Pendleton et al., 2012). This equates to as much as 10% of the 1.2 Pg C yr^{-1} emitted due to global deforestation (van der Werf et al., 2009).

1.4 Mangroves in Kenya

Mangroves occur along the entire Kenyan coastline between 4°40'S, 39°12'E in the South bordering Tanzania and 1°40'S, 41°33'E in the North bordering Somalia (see Chapter 2; Fig 2.1). The climate along the coast of Kenya is influenced by seasonal change in the Intertropical Convergence Zone (ITCZ) which produces a bimodal pattern of rainfall; the long rains (March - May) and the short rains (September/October – December) (Mutai and Ward, 2000). Mean annual rainfall varies along the coast but ranges between 600 – 1600 mm, mean minimum and maximum temperature ranges between 24°C and 30°C and relative humidity is generally high (~ 60 to > 90%) (GoK, 2009).

The bulk of Kenya's mangroves lie within the Lamu Archipelago in the North coast sheltered by barrier islands and coral reefs. There are also substantial tracts of mangrove forest found within the permanent Tana River estuary and delta (Bouillon et al., 2007a). The fringing coral reef which stretches along the coastline from Vanga (Tanzanian border) to Malindi provides shelter from strong wave action to the smaller areas of mangrove found in the South coast which occur in creeks and bays and receive variable inputs of freshwater from seasonal rivers (GoK, 2009).

Approximately 3.3 million people live in Kenya's coastal region (~ 8.6% of Kenya's total population) (GoK, 2009) of which 60-70% are classified as living below the

poverty line (GoK, 2003). The estimated annual population growth rate in the coastal region is high (~ 3%) and thus natural coastal resources are under increasing pressure (GoK, 2009). There is a long history of mangrove loss and degradation in Kenya due to over-exploitation of timber resources, conversion to salt works (Malindi area), coastal development (for industry and tourism), damming of the Tana River, dredging of water channels (Lamu) and oil pollution (Mombasa) (GoK, 2009). A recent estimate by Kirui et al., (2012) suggests that Kenya experienced a mean areal loss of mangroves of ~ 0.7% yr^{-1} during the period 1985-2010. However, mangrove reforestation programs have been successful in rehabilitating degraded forests in some areas of the South coast (Kairo et al., 2008).

The system of mangrove governance in Kenya is complicated and confused by the fact that Kenya Forest Service (KFS) and Kenya Wildlife Service (KWS) have an overlapping mandate over mangrove forests. Although mangroves in Kenya are gazetted as forest reserves under the Republic of Kenya Forests Act, 2005 and are officially managed by KFS (GoK, 2009); KWS appears to have almost complete jurisdiction over mangroves located within marine protected areas (MPAs). Where harvesting of mangroves is permitted KFS are responsible for the issue and regulation of cutting licences. However, logging practices are often poorly managed (Kairo et al., 2002) and continue unchecked even in areas where logging is prohibited by law (e.g. Mida Creek) (see Fig. 1.2). Mangroves located within designated MPAs along the Kenyan coast are offered some level of protection however, regulations regarding coastal development and logging within MPAs are often poorly enforced (GoK, 2009).

Fig. 1.2: Harvested mangrove trees in Mida Creek, Kenya. Photo taken by R. Cohen on 10th July 2011.

1.5 Thesis scope and main objectives

Producing robust estimates of forest above-ground biomass at spatial scales which are relevant for climate change research, forest management and REDD+ is now a key challenge facing environmental scientists. Kenya is one of many developing nations currently in the process of developing a national strategy for REDD+ implementation. This process involves (amongst other things) establishing national baseline carbon stocks and an effective MRV system. Mangroves are both globally important carbon stores and one of the most threatened ecosystems on the planet. As such, there is definite scope for their inclusion within a REDD+ framework.

The over-arching objective of this thesis is to provide spatially explicit information on the current AGB stocks of Kenyan mangrove forests and to evaluate and constrain the uncertainty of these estimates of AGB stocks. For this purpose this thesis adopts two approaches to estimating the above-ground biomass of mangrove forests in Kenya: a ground-based statistical approach and a remote sensing based approach. This thesis utilises two unique datasets; one represents the largest tree harvest dataset compiled for African mangroves to date and the other is an extensive forest inventory dataset spanning the entire Kenyan coastline. A schematic overview of the main structure of this thesis and the main outcomes of each research chapter is provided in Fig. 1.3.

Chapter 2 focuses on 1) developing new allometric equations for Kenyan mangroves within a mixed-effects regression modelling framework 2) demonstrating a methodology for uncertainty propagation during the biomass estimation process which ensures that AGB estimates are accompanied by a realistic estimate of the total uncertainty and 3) producing estimates of mangrove AGB at different spatial scales (tree, plot, regional and landscape) which are accompanied by an appropriate measure of uncertainty.

Chapter 3 builds on the work carried out within chapter 2 and focuses in depth on evaluating the relative contribution of various components of uncertainty (propagated during the biomass estimation process) to the magnitude of the total uncertainty of AGB estimates. This evaluation is carried out using the mixed-effects regression

model introduced in chapter 2 and for comparative purposes is also carried out using a standard ordinary least squares regression model.

Chapter 4 represents the first attempt to utilise L-band SAR data for the purpose of estimating mangrove AGB in East Africa. This chapter utilises the ground-based estimates of plot AGB obtained in chapter 2 and SAR data acquired by JAXA's (Japan Aerospace Exploration Agency) Advanced Land Observing Satellite Phased Array L-band Synthetic Aperture Radar (ALOS PALSAR) sensor. The chapter focuses on 1) investigating the nature of the backscatter-AGB relationship in Kenyan mangrove forests and 2) producing SAR-derived estimates of mangrove AGB at the regional and national scale 3) quantifying the uncertainty of these estimates.

Finally, chapter 5 provides a general summary and discussion of the work carried out in chapters 2 to 4.

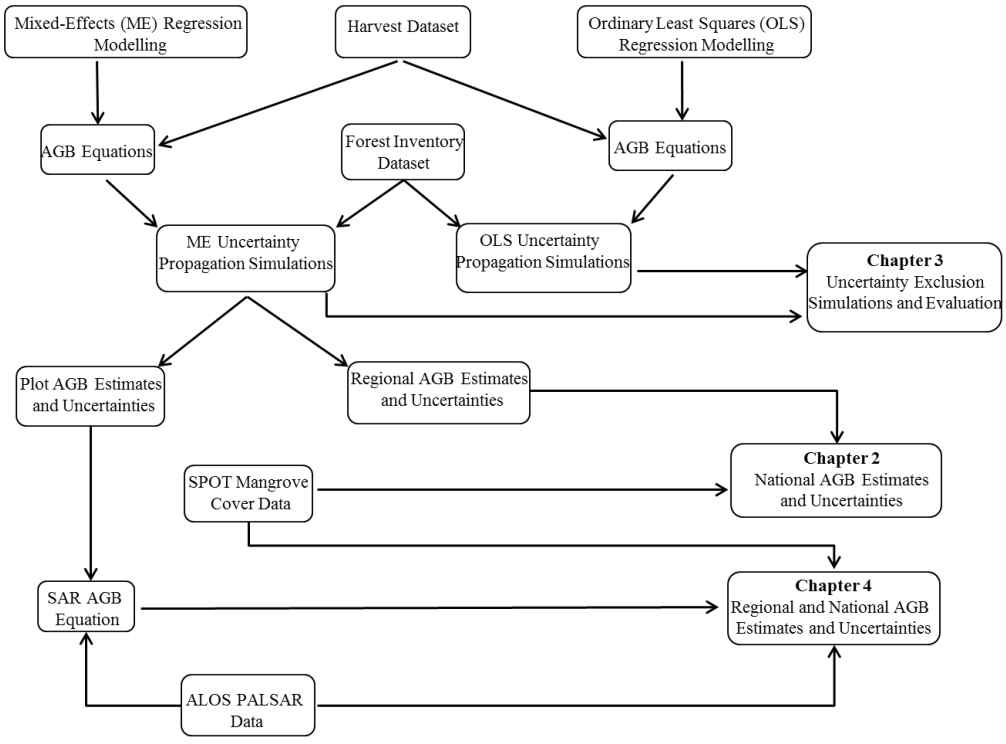

Fig. 1.3: Schematic overview of thesis structure. Abbreviations are: AGB = above-ground biomass; SAR = Synthetic Aperture Radar; ALOS PALSAR = Advanced Land Observing Satellite Phased Array L-band Synthetic Aperture Radar; SPOT = Satellite Pour l'Observation de la Terre.

2. Propagating uncertainty to estimates of above-ground biomass for Kenyan mangroves: a scaling procedure from tree to landscape level

R. Cohen[a], J. Kaino[b], J. A. Okello[b,c], J. O. Bosire[b], J. G. Kairo[b], M. Huxham[d], M. Mencuccini[a]

[a] *School of GeoSciences, University of Edinburgh, Crew Building, West Mains Road, Edinburgh, EH9 3JN, United Kingdom*
[b]*Kenya Marine and Fisheries Research Institute, P.O. Box 81651, Mombasa, Kenya*
[c]*Department of Plant Biology and Nature Management (APNA), Vrije Universiteit Brussels, Pleinlaan 2, 1050, Brussels, Belgium*
[d]*School of Life, Sport and Social Sciences, Edinburgh Napier University, Edinburgh, United Kingdom*

Author Contributions:

R. Cohen provided some of the data used in this study (as detailed in the manuscript), carried out the data analysis and wrote the manuscript. Additional raw data were provided by J. Kaino and J. A. Okello. Comments on this manuscript were provided by J. O. Bosire, J. G. Kairo and M. Huxham. Advice on data analysis and comments on the manuscript were provided by M. Mencuccini.

This manuscript is published in Forest Ecology and Management as:

Cohen, R., Kaino, J., Okello, J.A., Bosire, J.O., Kairo, J.G., Huxham, M., Mencuccini, M., 2013. Propagating uncertainty to estimates of above-ground biomass for Kenyan mangroves: a scaling procedure from tree to landscape level. Forest Ecology and Management 310, 968-982.

Appendix 1 shows the manuscript as it appears in published format.

Abstract

Mangroves are globally important carbon stores and as such have potential for inclusion in future forest-based climate change mitigation strategies such as Reducing Emissions from Deforestation and Forest Degradation (REDD+). Participation in REDD+ will require developing countries to produce robust estimates of forest above-ground biomass (AGB) accompanied by an appropriate measure of uncertainty. Final estimates of AGB should account for known sources of uncertainty (measurement and predictive) particularly when estimating AGB at large spatial scales. In this study, mixed-effects models were used to account for variability in the allometric relationship of Kenyan mangroves due to species and site effects. A generic biomass equation for Kenyan mangroves was produced in addition to a set of species-site specific equations. The generic equation has potential for broad application as it can be used to predict the AGB of new trees where there is no pre-existing knowledge of the specific species-site allometric relationship: the most commonly encountered scenario in practical biomass studies. Predictions of AGB using the mixed-effects model showed good correspondence with the original observed values of AGB although displayed a poorer fit at higher AGB values, suggesting caution in extrapolation. A strong relationship was found between the observed and predicted values of AGB using an independent validation dataset from the Zambezi Delta, Mozambique ($R^2 = 0.96$, $p = <0.001$). The simulation based approach to uncertainty propagation employed in the current study produced estimates of AGB at different spatial scales (tree – landscape level) accompanied by a realistic measure of the total uncertainty. Estimates of mangrove AGB in Kenya are presented at the plot, regional and landscape level accompanied by 95% prediction intervals. The 95% prediction intervals for landscape level estimates of total AGB stocks suggest that between 5.4 and 7.2 megatonnes of AGB is currently held in Kenyan mangrove forests.

2.1 Introduction

Mangrove forests are now widely recognised as globally important carbon (C) stores (Bouillon et al., 2008; Chmura et al., 2003; Donato et al., 2011; McKee et al., 2007). Despite accounting for just 0.7% of the world's tropical forest cover (Giri et al., 2011) mangroves play a disproportionately important role in the global C cycle. Recent estimates suggest that as much as 20Pg of C is currently being stored in mangrove biomass, sediments and peat world-wide (Donato et al., 2011). Mangroves do not merely sequester and store C they also provide a number of other key ecosystem services which are ecologically and economically important at local, regional and global scales. Such services include but are not limited to; coastal defence (Zhang et al., 2012), fisheries production (Aburto-Oropeza et al., 2008), habitat provision for terrestrial and aquatic fauna (Kathiresan and Bingham, 2001), timber and fuelwood production (Dahdouh-Guebas et al., 2000), pollution abatement (Wickramasinghe et al., 2009) and regulation of sediment exchange between land and sea (Duarte et al., 2005).

The continued degradation and destruction of mangroves world-wide has been highlighted in recent years (Alongi, 2002; Giri et al., 2011). Mangroves are considered to be one of the most threatened ecosystems on the planet with an estimated decline in global areal cover of ~35% during the period 1980 - 2000 (Valiela et al., 2001). This decline is largely due to over-exploitation of wood products, conversion to aquaculture, coastal development and human settlement (Primavera, 2005). Although rates of destruction may be slowing in some countries they generally remain high; for example Kenya experienced an estimated mean areal loss of mangroves of ~ 0.7% yr^{-1} during the period 1985 to 2010 (Kirui et al., 2012). Continued degradation and loss of mangrove cover not only represents a loss of future C sequestration potential but could result in significant release into the atmosphere of C currently being stored by mangroves (Pendleton et al., 2012).

An estimated 8 - 20% of annual global anthropogenic CO_2 emissions result from land-use changes occurring primarily in the tropics (van der Werf et al., 2009). This realisation has led to proposals for forest-based climate change mitigation strategies

such as Reducing Emissions from Deforestation and Forest Degradation (REDD+). In essence REDD+ envisages achieving CO_2 emissions reductions, forest conservation and sustainable development by placing an economic value on forest carbon storage and facilitating the transfer of funds from developed to developing nations through international trade in carbon credits. Details of how REDD+ will operate at the national and international level under the United Nations Framework Convention for Climate Change (UNFCCC) are still under debate. However many developing nations (including Kenya) are already in the process of formulating national REDD+ readiness strategies in partnership with the World Bank's Forest Carbon Partnership Facility (FCPF). There is definite scope for mangroves to be included in national and/or local scale forest carbon projects operating either under existing voluntary or future compliance carbon markets. Indeed, a recent study by Siikamaki et al. (2012) suggested that at the global scale reducing CO_2 emissions by avoiding further loss of mangroves could prove to be an economically viable option in comparison with the cost of reducing emissions from other sources (e.g. industry) even under scenarios of low mangrove carbon offset supply.

Participation in REDD+ (under the UNFCCC) will require countries to produce accurate estimates of their forest carbon stocks and stock changes through robust Measurement, Reporting and Verification (MRV) programs. The most recent Intergovernmental Panel on Climate Change (IPCC) Guidelines for National Greenhouse Gas Inventories (IPCC, 2006) provide the current methodological framework for REDD+ MRV requirements (Maniatis and Mollicone, 2010). In accordance with these guidelines all estimates should be accompanied by an appropriate measure of uncertainty (95% confidence interval) and should account for and reduce all known sources of uncertainty as far as is possible (IPCC, 2006). Above-ground biomass (AGB) is one of five forest carbon pools (identified by the IPCC) which will be estimable and reportable for REDD+. Providing robust estimates of AGB is important both in terms of future REDD+ reporting but also in providing the link between ground and remote sensing efforts to monitor changes in forest biomass and land cover at local, regional and global scales.

The above-ground biomass of trees is commonly estimated by the use of allometric equations (derived using regression analysis) which relate one or more easily measurable tree variables (e.g., stem diameter at breast height (DBH)) to total above-ground biomass. These equations are then applied to forest inventory data in order to estimate biomass at larger spatial scales. Allometric equations have been developed for a variety of mangrove species occurring across a broad geographical range (Clough and Scott, 1989; Kairo et al., 2009; Komiyama et al., 2005; Poungparn et al., 2002; Soares and Schaeffer-Novelli, 2005). However, African mangroves are under-represented in the current literature with published equations existing for Kenya (Kairo et al., 2009; Kairo et al., 2008; Kirui et al., 2006; Slim et al., 1996; Tamooh et al., 2009) and South Africa (Steinke et al., 1995) only.

Allometric relationships in trees are generally considered to be both species and site-specific. However, the infeasibility of constructing a new allometric equation for every species encountered at every new site has led to increasing interest in the development of generic equations for biomass estimation (Brown et al., 1989; Chave et al., 2005; Zianis and Mencuccini, 2004). Existing generic equations for mangroves have used wood density as the species-specific component of the relationship (Chave et al., 2005; Komiyama et al., 2005). The generic equation developed by Komiyama et al. (2005) was deemed to perform within acceptable levels of precision (as measured by the relative error) in comparison with site-specific equations for selected species (Komiyama et al., 2008).

Uncertainties are introduced at all stages of the biomass estimation process (from single tree to landscape level). Total uncertainty at the single tree level is comprised of uncertainty in the measurement of tree variables (measurement uncertainty) and uncertainty due to the use of the allometric model for predicting the biomass of a new individual (predictive uncertainty) (Chave et al., 2004; Zianis, 2008). These uncertainties are, in turn, propagated to plot and landscape level biomass estimates. Failing to account for uncertainty during the biomass estimation process ultimately leads to an underestimation of the uncertainty on final predictions (Dietze et al., 2008).

Accounting for predictive uncertainty is particularly important in biomass estimation as allometric equations are often applied outwith the data range for which they were originally intended (Chave et al., 2005) and are always applied outside the particular trees (and often sites) from which they were developed. Uncertainty in the parameters of a regression model is often represented by simply quoting the standard error of the allometric constants whilst the coefficient of determination (R^2) is the usual means by which to evaluate both the 'fit' of the model and its predictive power (e.g. Komiyama et al., 2005; Soares and Schaeffer-Novelli, 2005). However, over reliance on the use of R^2 in regression analysis as a measure of model predictive accuracy and for model comparison (between datasets) has been criticised in recent years (Gelman and Pardoe, 2006; Johnson and Omland, 2004). In contrast to model selection criteria such as the Akaike Information Criteria (AIC) (Akaike, 1987) the R^2 statistic is not a direct measure of model predictive accuracy and model selection made solely on the basis of maximising the R^2 statistic can lead to imprecise predictions as no account is taken of model complexity (Johnson and Omland, 2004).

The issue of uncertainty in biomass estimation has been addressed in the literature for forests in general (Brown, 2002; Chave et al., 2004; Ketterings et al., 2001; Parresol, 1999; Phillips et al., 2000; Zianis, 2008). Methodologies for propagating uncertainty have been presented based on summing the variances of component sources of uncertainty (see Chave et al., 2004; Ketterings et al., 2001; Phillips et al., 2000) and simulation techniques such as Monte Carlo (Heath and Smith, 2000; Ryan, 2009). To the best of our knowledge such methodologies have never been applied for the purpose of propagating uncertainty to biomass estimates in mangroves. With this in mind and in the context of future REDD+ requirements for biomass/carbon accounting this study focused on: 1) the development of new allometric equations to estimate the above-ground biomass of Kenyan mangroves using linear mixed-effects models and based on a meta-analysis of all the available harvest data for Kenyan mangrove species 2) demonstrating a simulation based methodology for propagating uncertainty during the biomass estimation process and 3) demonstrating the practical application of said equations and simulations to a large forest inventory dataset spanning the entire Kenyan coastline for the purpose of producing estimates of

above-ground biomass at different spatial scales (tree, plot, region and landscape) with an appropriate measure of uncertainty.

2.2 Methods

2.2.1 Harvest dataset – model development and validation

The harvest data used in this study is detailed in Table 2.1 and represents the largest dataset compiled to date for African mangroves. The bulk of the harvest data originates from the Gazi Bay area (4°25'S, 39°30'E) which is located ~ 55 km south of the city of Mombasa in Kenya (Fig. 2.1) and was made available through collaboration with Kenya Marine and Fisheries Research Institute (KMFRI). The Gazi Bay data has been divided into two sub-sites; Gazi (the area next to Gazi village) and Kinondo (the area next to Kinondo village). An additional study within the Gazi Bay area by Slim et al., (1996) was considered for inclusion but discounted as it was not possible to obtain the raw data. Attempts were made to source additional datasets from outwith Africa in order to expand the range of stem diameter and height data available for each species and also to provide some data for species (e.g. *Xylocarpus* sp.) not included in any of the African studies. An extensive literature search was carried out to look for raw harvest data which were 1) from the same species that occur in Kenya and 2) freely available in the publication. It was only possible to find one study which met both these criteria; that of Poungparn et al. (2002) from South-East Asia.

The harvest dataset used in this study to develop regression models comprises the raw data from 337 individually harvested trees (see section 2.2.2 for harvest methodology) and includes data for seven of the nine mangrove species known to occur in Kenya. The harvest dataset is unbalanced with very few data points for some species (Table 2.1). However, *Rhizophora mucronata* and *Avicennia marina* are well represented in the dataset in terms of sample size and these are two of the most dominant (in number) and widely distributed mangrove species in Kenya. In common with most allometric studies, there is a paucity of data from large diameter size classes with 97% of the harvested trees in the current dataset < 20cm in

diameter. This means that the data range in the harvest dataset does not fully encompass the upper values of diameter and height recorded in the existing forest inventories.

Harvest data from a recent study conducted by WWF, Mozambique and KMFRI in 2011 in the Zambezi Delta, Mozambique (Bosire et al., unpublished results) were used in this study for validation purposes only and were not used to develop regression models (data summarised in Table 2.1). The Zambezi validation dataset comprises harvest data from 23 trees from six mangrove species occurring in both Mozambique and Kenya. In addition, the coastlines of Mozambique and Kenya occur within the same Köppen-Geiger climate classification (Peel et al., 2007).

2.2.2 Summary of harvest methodology

All of the studies listed in Table 2.1 employed similar methodologies for tree harvesting and determination of total live above-ground biomass (but see individual papers for details). Harvested trees were selected randomly and prior to harvest, the stem diameter (cm) and total height (m) of each tree was recorded. Stem diameter was measured at 1.3m above-ground (DBH) except in the case of *Rhizophora* trees where the highest prop root occurred > 1.3m above-ground in which case diameter was measured at ~30cm above the highest prop root. Trees were then harvested at ground level and the fresh weight of component parts (stem, branches, leaves and prop roots in the case of *Rhizophora* sp.) was measured in the field. Sub-samples of component parts were then oven dried to constant weight (80 - 85°C in the case of all studies apart from Poungparn et al. (2002) where fresh material was dried at 110°C) in order to calculate wet-dry weight ratios (conversion factors). Conversion factors were then applied to convert the fresh weight of each tree component to dry weight in kilograms (kg DW) and summed giving total above-ground biomass in kg DW. The study by Kirui (2006) employed a slightly different methodology for determining the total above-ground biomass of multi-stemmed *Avicennia* trees. Each stem arising from a common butt was treated as an individual tree and the biomass of

each stem was calculated separately following a procedure outlined in Clough et al. (1997) involving apportionment of the common butt.

2.2.3 Statistical analyses

2.2.3.1 Rationale for using mixed-effects models

Ecological datasets often display a complex structure where data from individuals within populations are nested or grouped by one or more factors. Such grouping factors could include for example; the species and/or site which the individual belongs to, an experimental treatment applied to a subset of individuals and time series data. If such correlations or group effects are not accounted for during analysis the standard errors of the regression coefficients will tend to be underestimated due to inflation of the effective sample size (Steele, 2008). Mixed-effects models not only account for but explicitly model the variance due to group effects.

In mixed-effects models the intercept and regression coefficients can be assigned their own probability models and allowed to vary by group (as random effects) around the overall population mean (the fixed effects). This is particularly useful in studies where the main target of inference is the wider population and predictions are sought for new individuals within new groups, with an appropriate measure of predictive uncertainty (Gelman and Hill, 2007). In addition, mixed-effects models deal well with unbalanced datasets (especially common in meta-analysis studies) and provide a more robust estimation of regression coefficients for groups where there is little information (i.e. a small sample size) as additional information on the probability distribution of coefficients can be gained from the dataset as a whole (Dietze et al., 2008).

Table 2.1: Provenance and summary of the tree harvest dataset used in this study to develop and validate biomass equations for Kenyan mangroves. [a]

Study	Location	Forest Type	Species	Stem Diameter Range (cm)	Height Range (m)	Above-ground Biomass (kg DW)	Sample Size
Lang'at (2008)	Ramisi, Kenya	Plantation (12 yrs old)	*Bruguiera gymnorrhiza*	1.1 - 4.8	2.7 - 6.6	0.5 - 7.3	15
Kairo et al., (2008)	Kinondo (Gazi Bay), Kenya	Plantation (12 yrs old)	*Rhizophora mucronata*	2.4 - 11.5	3.5 - 8.9	0.6 - 68.9	50
Kirui et al., (2006)	Gazi (Gazi Bay), Kenya	Natural	*Rhizophora mucronata*	5.7 - 21.4	4.3 - 11.3	13.4 - 269.5	15
Kirui (2006)	Kipini, Kenya	Natural	*Rhizophora mucronata*	2.3 - 23.6	2.8 - 16.1	0.6 - 383.7	15
			Avicennia marina	2.5 - 15.8	3.9 - 11.7	4.6 - 71.4	28 (19)
	Gazi (Gazi Bay), Kenya	Natural	*Avicennia marina*	3.7 - 21.8	2.1 - 11.3	7.2 - 127.3	51 (15)
Tamooh et al., (2009)	Gazi (Gazi Bay), Kenya	Plantation (6yrs old)	*Rhizophora mucronata*	0.9 - 6.4	0.8 - 3.9	0.08 - 16.2	12
Kairo et al., (2009)	Gazi (Gazi Bay), Kenya	Plantation [b]	*Avicennia marina*	5.2 - 10.2	4 - 5.8	6.8 - 22.5	10
			Sonneratia alba	5.3 - 11.3	4 - 5	3.8 - 9.4	10
			Ceriops tagal	5 - 5.5	1.8 - 2.6	1.5 - 6.1	10
			Rhizophora mucronata	3 - 8	2.8 - 5	3 - 25.8	58
Steinke et al., (1995)	Mgeni estuary, South Africa	Natural	*Bruguiera gymnorrhiza*	3.4 - 11.5	4.6 - 13.5	3.2 - 107.2	12
			Avicennia marina	5.4 - 9.9	4.9 - 7.7	5.3 - 31.9	4
Poungparn et al., (2002)	Thailand	Natural	*Sonneratia alba*	4.2 - 12.7	3.4 - 13.4	3.1 - 79.3	10
			Bruguiera gymnorrhiza	4.8 - 33.4	9.2 - 24.9	8.3 - 943.5	10
			Rhizophora mucronata	4.7 - 11.2	6.9 - 16	7.7 - 73.7	11
			Xylocarpus granatum	3.7 - 12.7	4.1 - 8	3.2 - 66.8	8
	Indonesia	Natural	*Sonneratia alba*	6.7 - 21.7	7.3 - 22.6	13.1 - 256	2
			Bruguiera gymnorrhiza	9.7 - 48.9	11.1 - 30.6	54.7 - 1411.1	4
			Xylocarpus granatum	18.6	13.4	162.2	1
			Xylocarpus moluccensis	11.8	13.5	47.4	1
WWF/KMFRI (Validation Dataset)	Zambezi Delta, Mozambique	Natural	*Ceriops tagal*	5.3 - 15.4	3.6 - 6.5	6.55 - 68.2	3
			Bruguiera gymnorrhiza	5.6 - 24.6	5.5 - 8.1	11.7 - 161.8	4
			Xylocarpus granatum	5.2 - 14.9	4 - 7.8	6.7 - 49	3
			Sonneratia alba	5.9 - 35	5.9 - 13.5	8.8 - 453.4	6
			Avicennia marina	8 - 28	5.3 - 13.5	14.9 - 248	4
			Heritiera littoralis	5 - 22.5	4.9 - 9.5	3.9 - 121.2	3

[a] Above-ground biomass is given in kg dry weight (kg DW) and includes stem, branch, leaf and prop root (in the case of *Rhizophora* sp.) components. An exception is the study by Lang'at (2008) where above-ground biomass comprises stem weight only. In the study by Kirui (2006) sample sizes for *Avicennia* sp. are the total number of stems (treated separately during analysis) and numbers in parentheses are the actual number of harvested trees. The study by Poungparn et al., (2002) included data sourced from other studies; see original paper for details. [b] Plantation age at time of harvest in Kairo et al., (2009) was 5 years old for *R. mucronata* and *S. alba* and 8 years old for *C.tagal* and *A. marina*.

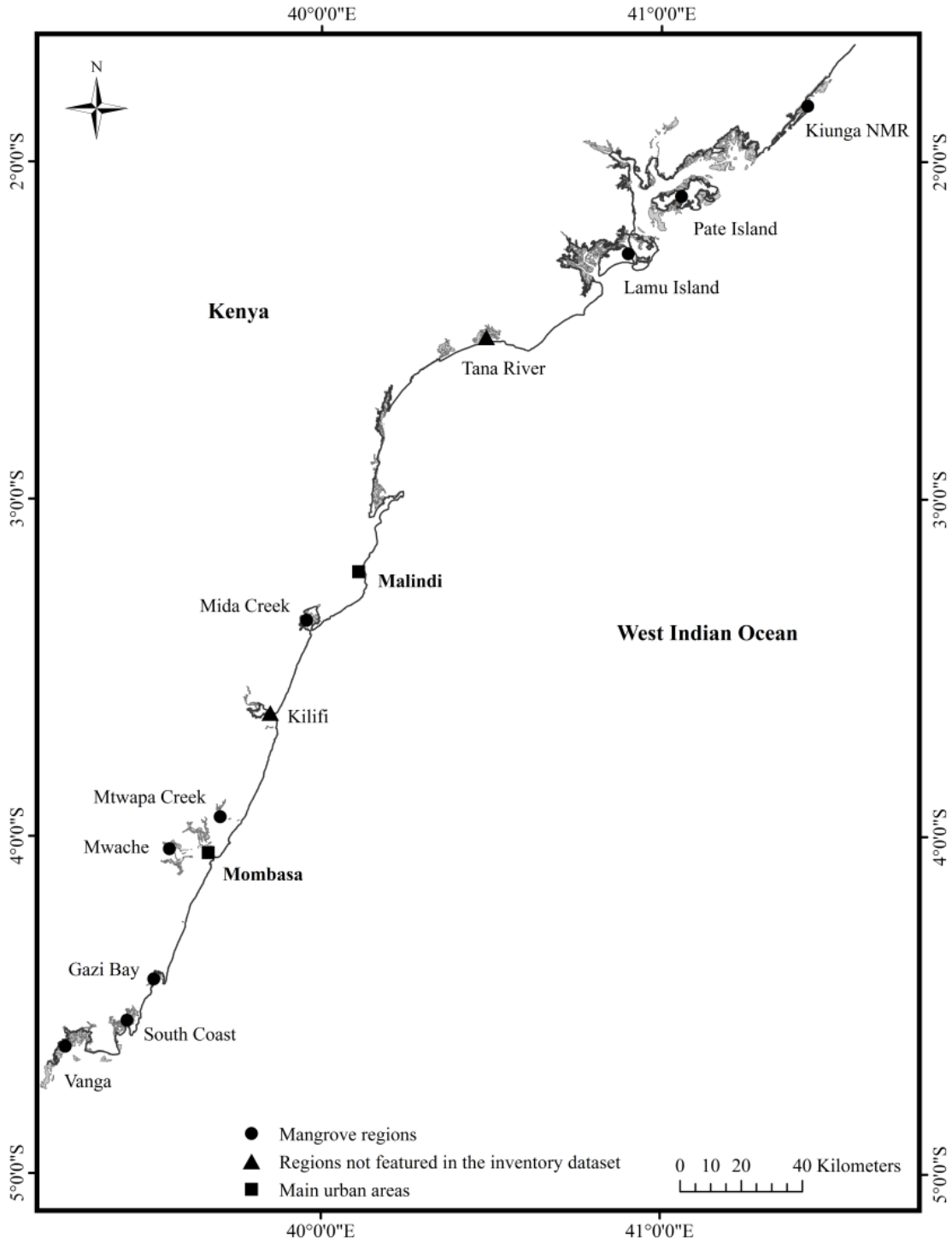

Fig. 2.1. Kenya coastline showing areas of mangrove forest where inventory data has been collected (dots). Inventory data collected within the general area of Lamu Island and Pate Island constitute the "South Lamu" study region. Kiunga NMR stands for Kiunga National Marine Reserve. Please note that the mangrove area defined as the Tana River region in this study spans the official districts of Kilifi and Tana River in Kenya and encompasses the mangroves just North of Malindi to the border of Lamu District. Kenya GIS base-map and mangrove shape-file obtained from the World Resources Institute (available at: <http://www.wri.org/>).

2.2.3.2 Model specification and selection process

The power function equation (Eq. (2.1)) or its linearized form (Eq. (2.2)) is commonly used as the underlying allometric scaling relationship for biomass regression models (e.g. Brown et al., 1989; Chave et al., 2005; Komiyama et al., 2008; Parresol, 1999).

$$y = ax^b \tag{2.1}$$

$$\ln(y) = \ln(a) + b\ln(x) + e_i \tag{2.2}$$

where y is the response variable, x is the predictive variable and a and b are the allometric constants. Specifically, a is the scaling coefficient (or intercept), b is the scaling exponent (or slope) and e_i is the error term which is assumed to be normally distributed $e^i \sim N(0,\sigma^2)$. For mangroves, biomass regression models have been developed using stem diameter (D) as the sole predictive variable (Clough and Scott, 1989; Steinke et al., 1995). However, many studies have found that the inclusion of additional biometric variables (e.g. tree height (H)) either fitted independently or as a combined variable such as $x = D*H$ or $x = D^2*H$ have improved model fit (Chave et al., 2005; Komiyama et al., 2002; Soares and Schaeffer-Novelli, 2005). The relationship between stem diameter and total tree height can be highly variable and hence for some types of mangrove forest (e.g. short stature shrub and dwarf mangroves) and for some species such as *A. marina* which commonly display an irregular branching architecture; the inclusion of tree canopy characteristics such as crown volume or crown area as predictive variables in allometric models (where such data is available) has been recommended (Kauffman and Donato, 2012; Ross et al., 2001). The inclusion of wood density as a predictive variable has also been recommended particularly for the development of generic allometric models (Chave et al., 2005; Komiyama et al., 2005).

In the current study, a linear relationship was obtained between predictive variables (stem diameter and height) and the response variable (total above-ground biomass (AGB)) after transforming all variables by natural log (Fig. 2.2) allowing for the use

of regression models of the form shown in Eq. (2.2). Wood density was not included as a potential predictive variable as tree level wood density data were not available in the harvest dataset used for model development. The individual level grouping factor used in the current study was a combined species_site indicator which grouped the harvest data from individuals within each species at each site in the dataset. For example data from *Rhizophora* trees at Kinondo (Table 2.1) formed the group Rhiz_Kin and so on. In total there were eighteen species_site groupings present within the harvest dataset. It was necessary to combine species and site into one grouping factor due to the unbalanced nature of the harvest dataset which has insufficient replication of species data at each site to allow separation of any possible variation in AGB attributable solely to either factor. In addition, Zianis and Mencuccini (2004) showed that within-species variability in allometric coefficients across sites is just as large as the variability in coefficients across species. Given that the harvest dataset comprises data from various studies any differences between the species_site groupings could also potentially incorporate an effect of study origin. However, harvest methodologies are broadly consistent across studies therefore it is likely the case that the random effects predictions are largely reflective of the differences across groups due to species and site effects.

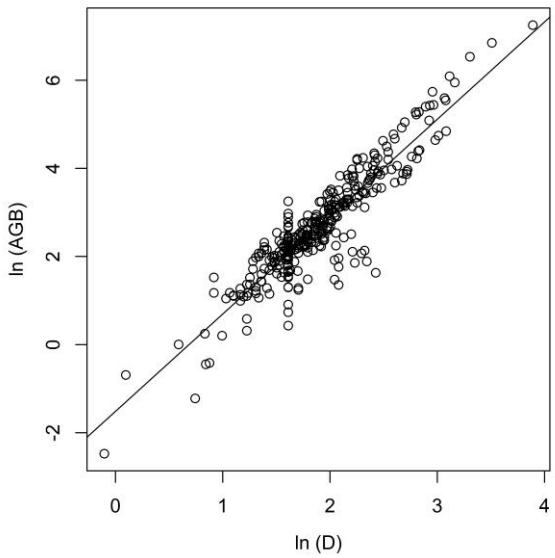

Fig. 2.2. Relationship between above-ground biomass (AGB) and stem diameter (D) of harvested mangrove trees after transformation by natural log. The vertical arrangement of data points at approximately ln (D) = 1.6 is mostly due to data from the study by Kairo et al., (2009) which focused on harvesting trees from plantation forests of known age whereby a large proportion of data points arising from this study were of similar stem diameter (~ 5cm).

Linear mixed-effects models were fitted using the lme4 package within R statistical software version 2.15.0 (Bates et al., (2011), http://CRAN.R project.org/package=lme4). Prior to model fitting the logged predictive variables were centred at their mean to reduce any correlation between intercept and slope coefficients. Models were initially fitted using maximum likelihood (ML) estimation and compared using the Deviance Information Criterion (DIC) as outlined in Gelman and Hill (2007). In order to identify the best fixed and random effects terms for inclusion in the final model eight candidate models were fitted to the data (Table 2.2). Model notation follows that of Gelman and Hill (2007) where $\ln(y_i)$ is the response (AGB in this study) for the *ith* individual, α is the intercept, β represents the coefficients for the predictive variables diameter ($\ln(x_i)$) and height ($\ln(z_i)$) and σ_y^2 is the residual or the unexplained 'within-group' variance. The subscript term $_{j[i]}$ indexes the *ith* individual within the *jth* group and denotes where the intercept or a coefficient has been allowed to vary across groups ($j = 1,..., J$) as a random effect.

Table 2.2: Comparison of candidate models fitted using maximum likelihood (ML) estimation, with corresponding DIC values [a]

Model	DIC
I. $\ln(y_i) \sim N(\alpha_{j[i]} + \beta\ln(x_i) + \beta\ln(z_i), \sigma_y^2)$, for $i = 1,\ldots,n$,	274.1
II. $\ln(y_i) \sim N(\alpha_{j[i]} + \beta_{j[i]}\ln(x_i) + \beta\ln(z_i), \sigma_y^2)$, for $i = 1,\ldots,n$,	231.5
III. $\ln(y_i) \sim N(\alpha_{j[i]} + \beta\ln(x_i) + \beta_{j[i]}\ln(z_i), \sigma_y^2)$, for $i = 1,\ldots,n$,	220.3
IV. $\ln(y_i) \sim N(\alpha_{j[i]} + \beta_{j[i]}\ln(x_i), \sigma_y^2)$, for $i = 1,\ldots,n$,	260.5
V. $\ln(y_i) \sim N(\alpha_{j[i]} + \beta_{j[i]}\ln(z_i), \sigma_y^2)$, for $i = 1,\ldots,n$,	603.7
VI. $\ln(y_i) \sim N(\alpha_{j[i]} + \beta_{j[i]}\ln(x_i z_i), \sigma_y^2)$, for $i = 1,\ldots,n$,	299.1
VII. $\ln(y_i) \sim N(\alpha_{j[i]} + \beta_{j[i]}\ln(x_i^2 z_i), \sigma_y^2)$, for $i = 1,\ldots,n$,	240.1
VIII. $\ln(y_i) \sim N(\alpha_{j[i]} + \beta_{j[i]}\ln(x_i) + \beta_{j[i]}\ln(z_i), \sigma_y^2)$, for $i = 1,\ldots,n$,	206.1*

[a] The asterisk symbol denotes that model VIII was the best model overall.

Model I was the simplest model and included a random effects term for the intercept only whilst the slopes of both predictive variables were kept constant across groups (Table 2.2). The inclusion of a random effects term for $\ln(x_i)$ and $\ln(z_i)$ coefficients in models II and III respectively led to a reduction in the DIC value in comparison with model I. In order to ascertain if both diameter and height were needed as predictive variables within the model; models IV and V excluded each variable as a fixed effect (and hence as a random effect) in turn. As shown in Table 2.2 there is

clearly a need to include both variables as fixed effects within the model. This is especially evident in the case of model V where exclusion of diameter from the model had a large impact on the DIC value. Models were also fitted using two new combined predictive variables: $\ln(x_i z_i)$ and $\ln(x_i^2 z_i)$, both of which were logged and centred prior to model fitting as before. However, as shown in Table 2.2 models VI and VII using the combined variables displayed a poorer overall fit in comparison with models II and III (Table 2.2). Model VIII had the lowest DIC value of all the models under consideration indicating that the inclusion of a random effects term for the coefficients of both $\ln(x_i)$ and $\ln(z_i)$ was needed in order to account for variability in AGB across groups.

Model VIII was considered to be the most appropriate model overall and was subsequently re-fitted using restricted (or residual) maximum likelihood (REML) estimation in order to produce the best unbiased estimates of variance and co-variance parameters (Pinheiro and Bates, 2000). In model VIII the terms $\alpha_{j,}\beta_{jx}$ and β_{jz} signify that these parameters have themselves been modelled yielding a partial pooling estimate of α and the coefficients β_x and β_z for each group along with an estimate of the overall population mean and the 'between-group' variance (estimated from the data). The group-level model for model VIII can be written as:

$$\begin{pmatrix} \alpha_j \\ \beta_{jx} \\ \beta_{jz} \end{pmatrix} \sim N\left(\begin{pmatrix} \mu_\alpha \\ \mu_{\beta x} \\ \mu_{\beta z} \end{pmatrix}, \begin{pmatrix} \sigma_\alpha^2 & \rho_1\sigma_\alpha\sigma_{\beta x} & \rho_2\sigma_\alpha\sigma_{\beta z} \\ \rho_1\sigma_\alpha\sigma_{\beta x} & \sigma_{\beta x}^2 & \rho_3\sigma_{\beta x}\sigma_{\beta z} \\ \rho_2\sigma_\alpha\sigma_{\beta z} & \rho_3\sigma_{\beta x}\sigma_{\beta z} & \sigma_{\beta z}^2 \end{pmatrix} \right), \text{for } j = 1, \ldots\ldots\ldots, J, \tag{2.3}$$

where the overall mean across all groups (the fixed effects estimates) for the intercept, slope of $\ln(x_i)$ and the slope of $\ln(z_i)$ are denoted by μ_α, $\mu_{\beta x}$ and $\mu_{\beta z}$ respectively. The between-group variance in the intercept, slope of $\ln(x_i)$ and the slope of $\ln(z_i)$ are given as σ_α^2 and $\sigma_{\beta x}^2$ and $\sigma_{\beta z}^2$ respectively. The parameters ρ_1, ρ_2 and ρ_3 are also estimated as the between-group correlations of the α's and β's (e.g. $\rho_1\sigma_\alpha\sigma_{\beta x}$ is the correlation between the group intercepts and slopes of $\ln(x_i)$).

2.2.3.3 Simulation-based approach to biomass estimation

In order to estimate the biomass of mangroves along the entire Kenyan coastline the equations developed in this study were applied to a forest inventory dataset (detailed in section 2.2.3.2) comprising 498 plots inventoried during the period 2007 – 2012. The modelling process described in section 2.2.3.2 generated a mean biomass equation and a suite of specific equations; one for each of the eighteen species_site groups. The mean equation is comprised of the fixed effects estimates and can be regarded as a generic equation for Kenyan mangroves. The group specific equations represent the group departures from the fixed effects estimates (fixed effect estimates ± the group specific random effects) and are only valid for the specific groupings from which they were originally derived. Eight of the group specific equations can potentially be applied to the forest inventory dataset to estimate biomass as the remaining ten equations are only valid for species_site combinations occurring outwith Kenya. Therefore, group specific equations were applied to estimate the biomass of individual trees within the inventory dataset if those trees fell into one of the pre-existing groups identified within the harvest dataset. For example the group specific equation for Rhiz_Kin was applied to inventoried *Rhizophora* trees at Kinondo and so forth. In cases where inventoried trees did not fall into one of the pre-existing groups their biomass was estimated using the generic equation. The simulation-based approach adopted in this study allows for the propagation of measurement, parameter and residual uncertainty to estimates of biomass at the individual tree, plot and regional level.

2.2.3.4 Simulations for individual tree biomass

The above-ground biomass of each tree in the inventory dataset was simulated 10,000 times using a new set of simulated values for each iteration. In order to propagate measurement uncertainty possible values of stem diameter $\ln(D_{sim})$ and height $\ln(H_{sim})$ for each tree were randomly sampled from a normal distribution with mean equal to the observed value and one standard deviation conservatively assumed to be 5% and 10% of the observed diameter and height respectively. These assumed

values of measurement uncertainty are consistent with the findings of previous studies (Chave et al., 2004; Gregoire et al., 1990; Phillips et al., 2000).

To propagate parameter uncertainty, possible values of the fixed effects intercept (α_{fixsim}) and coefficients for stem diameter ($\beta_{xfixsim}$) and height ($\beta_{zfixsim}$) were sampled from a multivariate normal distribution around means equal to μ_{α}, $\mu_{\beta x}$ and $\mu_{\beta z}$ from model VIII using the variance-covariance matrix of the fixed effects. In cases where the generic equation was applicable (to estimate the biomass of new trees in new groups) simulated values of the random effects for the intercept (α_{ransim}) and the coefficients for stem diameter ($\beta_{xransim}$) and height ($\beta_{zransim}$) were generated by sampling from a multivariate normal distribution around means equal to zero using the variance-covariance matrix of the group level (or mean) random effects (Eq. (2.3)). In cases where a group specific equation was applicable (to estimate the biomass of new trees in existing groups) possible values of the random effects were simulated as for the generic equation, however values were sampled around means equal to the group specific random effects for the intercept and coefficients and used the variance-covariance matrix of the group specific random effects. Simulated values were then used in Eq. (2.4) to calculate AGB biomass ($\ln(AGB_{pred})$) for each tree:

$$\ln(AGB_{pred}) = \alpha_{sim} + ((\beta_{xfixsim} + \beta_{xransim})\ln(D_{sim})) + ((\beta_{zfixsim} + \beta_{zransim})\ln(H_{sim}) \quad (2.4)$$

where α_{sim} is the un-centred intercept (calculated as shown in Eq. (2.5)) and corrects for the use of mean centred predictive variables diameter and height during model development (section 2.2.3.2).

$$\alpha_{sim} = (\alpha_{fixsim} + \alpha_{ransim}) - ((\beta_{xfixsim} + \beta_{xransim})\bar{x}) - ((\beta_{zfixsim} + \beta_{zransim})\bar{z}) \quad (2.5)$$

where $\bar{x}$ and $\bar{z}$ are the mean logged values of diameter and height respectively from the harvest dataset. In order to account for residual uncertainty in biomass estimates; possible values of biomass ($\ln(AGB_{Est})$) were randomly sampled from a normal distribution with mean equal to $\ln(AGB_{pred})$ and standard deviation equal to σ_y (the standard deviation of σ_y^2) from model VIII. Values of $\ln(AGB_{Est})$ were then back-

transformed by taking the exponent; producing 10,000 estimates of AGB (in kg DW) for each tree. The estimates for all trees within a plot were then summed at each iteration point yielding a distribution of 10,000 possible estimates of total biomass for each plot. The median was taken as the plot level biomass estimate as this provided the most typical value from skewed distributions of the simulations. The quantiles from the distribution of plot estimates were used for calculating the 95% prediction interval (95% PI) at the plot level.

2.2.3.5 Calculation of regional level prediction intervals

In order to upscale biomass estimates from plot to regional level, plots were first grouped according to the mangrove regions identified in the inventory dataset (Table 2.3). Plots within Lamu District were further sub-divided into those within Kiunga National Marine Reserve (NMR) and those outwith the reserve (hereafter "South Lamu"). Due to their close geographical proximity plots from Shirazi, Ramisi, Funzi and Bodo were aggregated to form the region "South Coast". The mean biomass estimate was calculated for each iteration (across all plots within a region) yielding a distribution of 10,000 possible mean biomass estimates. The mean of this distribution was taken as the regional level biomass estimate (Mg ha^{-1}) and provides the expected value of AGB taking into account the whole scale of values present in a specific geographical area. The quantiles from the distribution were used to calculate the 95% PI at the regional level.

2.2.3.6 Model validation

The predictive performance of model VIII was evaluated using a harvest dataset from the Zambezi Delta, Mozambique (Table 2.1). The simulation process detailed in section 2.2.3.4 was repeated for the 23 trees in the Zambezi dataset. For each tree the median fitted value of AGB (kg) was obtained along with the 95% PI for the median.

Table 2.3: Provenance and summary of mangrove forest inventory dataset [a]

Region	Study	Date	No. of Plots	Plot Size (ha)	Stem Diameter Range (cm)	Height Range (m)
Mida Creek	This Study	2010/2011	14	Variable (ranging from 0.01 to 0.5 ha)	2.5 - 58	1.5 - 17.7
Lamu District:	This Study	2010/2011				
South Lamu			25		2.4 - 54	1.8 - 28.5
Kiunga			16		2 - 49.8	1.3 - 23.7
Gazi Bay	This Study	2010/2011	28		5 - 64	1.8 - 20.2
	CAMARV	2009	18	0.01	0.5 - 51	0.6 - 15
	UNDP	2009	70	0.01	2.2 - 63.3	2 - 21
Mtwapa Creek	Okello (unpublished results)	2010	54	0.01	2.5 - 46.9	0.5 - 15
Mwache	Kaino (2013)	2011	67	0.01	2 - 53	1 - 15
South Coast:	KMFRI	2007				
Shirazi			43	0.01	5 - 47.5	2 - 16
Ramisi			22	0.01	5 - 48.4	2.5 - 15
Funzi			24	0.01	5 - 43.2	1.5 - 15
Bodo			34	0.01	5 - 60.5	2 - 14
Vanga	KMFRI	2012	83	Variable (ranging from 0.0025 to 0.04 ha)	2.5 - 72.5	1 - 25

[a] Study abbreviations are as follows; United Nations Development Programme (UNDP); Capacity Building for Mangrove Assessment, Restoration and Validation (CAMARV) and Kenya Marine and Fisheries Research Institute (KMFRI).

2.2.4 Forest inventory dataset

A summary of the forest inventory dataset is provided in Table 2.3, recent estimates of mangrove cover by region are provided in Table 2.4 and the location along the Kenyan coastline of each region is shown in Fig. 2.1. The cover estimates in Table 2.4 were derived from 2.5m resolution SPOT remote sensing imagery acquired over the Kenyan coastline during 2009-2011 (see chapter 4 for further details). The inventory dataset is a combination of data collected by this and other studies. All studies conducted prior to 2010/2011 had the objectives of characterising and investigating mangrove structural variability and change in the southern coastal region. However, in the current study sampling strategy was tailored (as much as was practicable) towards facilitating both a statistical and remote sensing based approach to biomass estimation along the entire coastline. Thus studies within the inventory dataset differ in terms of sampling strategy and plot size. There is also an obvious bias in total sampling effort towards sites in the south coast (Table 2.3).

In general all inventory studies followed a standardised methodology of within-plot data collection. In all studies the species, stem diameter and total height of all trees within each plot which met the diameter measurement threshold were recorded. Stem diameter was recorded to the nearest millimetre and was measured at 1.3m

aboveground (DBH) except in the case of *Rhizophora* sp. where stem diameter was measured at ~30cm above the highest prop root if this occurred above 1.3m. In cases where trees branched below 1.3m (common in *Avicennia* sp.) and branches met the diameter measurement threshold; the diameter and height of each branch was recorded separately. In the current study total tree height was measured using an ultrasonic vertex hypsometer (Haglöf, Sweden). In all other studies tree height was measured using a graduated pole.

Table 2.4: Mangrove cover estimates for inventory regions derived from high-resolution SPOT satellite imagery [a]

Region	Mangrove Cover Estimate (ha)	Proportion of Total Cover (%)
Mida Creek	1657.8	3.6
South Lamu	26609.1	57.1
Kiunga NMR	4763.8	10.2
Gazi Bay	589	1.3
Mwache	2667.1	5.7
Mtwapa Creek	519.4	1.1
South Coast	2253.1	4.8
Vanga	3440	7.4
Kilifi *	640.2	1.4
Tana River *	3433	7.4
Total Cover	**46572.5**	

[a] Regions marked with asterisks' do not feature in the forest inventory dataset. For details of SPOT image processing see chapter 4.

2.2.4.1 Mida Creek and Lamu District

Forest inventory data from the Mida Creek area and Lamu District was collected as part of this study during June – August 2010 and 2011. Mida Creek (3°20'S, 40°00'E) is situated mid-way along the Kenyan coast ~ 23km south of the town Malindi in Kilifi District. Some of the mangrove forest in this area falls within the boundaries of Watamu Marine National Park (WNMP); however the majority is outwith the protected area. Regardless of location (within or outside of WNMP) harvesting of mangroves is currently prohibited in the Mida Creek area. In total 14 plots within the Mida Creek area were inventoried comprising nine 0.04ha (20 x 20 m) plots, four 0.25ha (50 x 50 m) plots and one 0.5ha (100 x 50 m) plot. None of the inventoried plots were located within the marine park.

The Lamu archipelago extends between 2°22'S, 40°48'E in the South and 1°44'S, 41°30'E in the North and is part of Lamu District. Lamu District currently holds the greatest proportion of remaining mangrove cover in Kenya (Table 2.4). Mangroves in the extreme north, close to the border with Somalia are part of Kiunga NMR and are considered to be the only remaining examples of relatively "pristine" mangrove forest in Kenya. Forty-one plots within Lamu District were inventoried comprising twenty-five 0.04ha plots, fifteen 0.25ha plots and one 0.5ha plot. Within Lamu District sites visited included: Kiunga NMR (n = 16 plots), Pate Island area (n = 15) and Lamu Island area (n = 10).

Plots inventoried in Mida Creek (n = 6) and Lamu District (n = 8) during 2010 were all 0.04ha in size. Plots were positioned at random within *Rhizophora* zones and all trees within each plot with stem diameter ≥ 2.5 cm were measured. Plots inventoried during 2011 were a mixture of 0.04ha plots (Mida Creek: n = 3, Lamu District: n = 17) located at random within randomly chosen map grid squares (grid resolutions of 500 x 500 metres and 1000 x 1000 metres) and larger plots (0.25ha and 0.5ha) which were positioned at random within larger areas pre-identified using optical and radar remote sensing imagery. These pre-identified areas were judged to be potentially distinct from each other in terms of forest structure/biomass and also to broadly represent the main levels of structural variation within the study region as a whole. This more targeted plot location strategy was for the purpose of facilitating future remote sensing work. All plots inventoried in 2011 included all trees within each plot which met the criteria of having stem diameter ≥ 5 cm.

2.2.4.2 Gazi Bay

The Gazi Bay inventory consists of 116 plots in total. As part of this study twenty-four 0.01ha (10 x 10 m) plots were inventoried during July 2010 and four 0.25ha plots were inventoried during August 2011. The smaller plots inventoried in 2010 were positioned randomly within the main identifiable mangrove zones and included all trees DBH ≥ 5 cm. The larger plots collected in 2011 were positioned using the same procedure as detailed above for the large plots in section 2.2.4.1 and included all trees within each plot stem diameter ≥ 5 cm.

The remaining plot data (n = 88) from the Gazi Bay area were collected in 2009 as part of two internationally funded short-term projects. Eighteen 0.01ha plots were inventoried in the area adjacent to Gazi village as part of a project entitled CAMARV (Capacity Building for Mangrove Assessment, Restoration and Valuation in East Africa) funded by the Natural Environment Research Council (NERC) of the United Kingdom. Seventy 0.01ha plots were inventoried as part of a UNDP-GEF Small Grants Programme project co-ordinated by Gazi Womens Group. In both projects plots were randomly positioned along a transect within each identifiable mangrove zone and all trees within each plot were included in the inventory.

2.2.4.3 Mwache and Mtwapa Creek

Mwache (4°2'S, 39°33'E) and Mtwapa Creek (3°57'S, 39°43'E) are both examples of peri-urban mangroves due to their close proximity to the city of Mombasa and the town of Mtwapa respectively. Both areas are considered to be degraded due to a combination of sewage pollution, timber over-exploitation and in the case of Mwache; the heavy sedimentation and flooding associated with the *El Niño* event of 1997-1998 (Kitheka et al., 2002). Inventory data from Mtwapa Creek (n = 54) was collected in 2010 as part of a study by Okello (unpublished results) and funded by the Flemish Interuniversity Council - University Development Cooperation VLIP-UOS. Data from Mwache (n = 67) was collected in 2011 as part of a study conducted by Kaino (2013) and funded by the Western Indian Ocean Marine Science Association (WIOMSA). Both studies used plot sizes of 0.01ha. Plots at Mtwapa Creek were positioned along transects running perpendicular to the shoreline at ~50 m intervals and all trees with stem diameter ≥ 2.5 cm were measured. At the Mwache site plots were positioned along transects running perpendicular to the shoreline at 100m intervals using a stratified sampling scheme based on observed differences in forest composition and structure. All trees with stem diameter ≥ 2 cm within each plot were measured.

2.2.4.4 South Coast

Forest inventory data from the South Coast (Shirazi, Ramisi, Funzi and Bodo) was collected in 2007 by KMFRI as part of a Kenya government funded project. In total there are data from one hundred and twenty-three 0.01ha plots comprising; Shirazi (n = 43), Ramisi (n = 22), Funzi (n = 24) and Bodo (n = 34). Plots were positioned at ~ 20m intervals along transects running perpendicular to the shoreline and all trees with stem diameter ≥ 5cm were included in the inventory.

2.2.4.5 Vanga

Mangroves close to the Kenya-Tanzania border were inventoried by KMFRI during January 2012. Plots inventoried within the Vanga mangrove system number 83 in total and are of variable size (sixty-nine 0.01ha, six 0.04ha and eight 0.0025ha (5 x 5 m) plots). Plots were positioned within each identifiable mangrove zone using a stratified random sampling strategy and all trees ≥ 2.5cm in diameter were recorded.

2.3 Results

2.3.1 Model VIII summary and key features

Overall, there is good correspondence between the fitted values of AGB (as estimated from model VIII) and the original observed values of AGB for trees in the harvest dataset (Fig. 2.3 (a) and (b)). The mean absolute error (MAE) in predictions of AGB from model VIII is 6.3 kg and the mean bias (observed-fitted) in predictions is an underestimate of just 0.06 kg. The model performs well at values of observed AGB ≤ 50 kg (Fig. 2.3 (b)) which comprise 85% of the total dataset. There is some divergence from the reference line for the few trees in the harvest dataset with higher AGB values (Fig. 2.3 (a)). Poorer model fit at higher AGB is likely due to the paucity of harvest data from larger trees with just 11 out of 337 trees in the dataset having an observed AGB ≥ 200 kg. Further diagnostic plots (data not shown) revealed no systematic trend in model residuals when plotted against the fitted values and against each of the predictive variables.

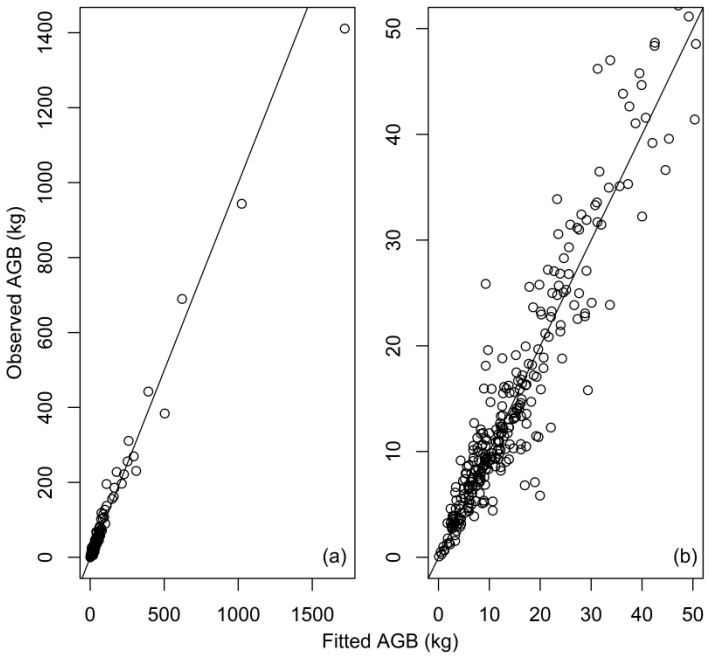

Fig. 2.3. (a) Total above-ground biomass (AGB) in kg as measured for each tree in the harvest dataset versus the corresponding fitted value (kg) from model VIII and (b) as (a) but re-scaled to show in detail the correspondence between observed and fitted values at the lower range of AGB. The reference lines shown in (a) and (b) represent a 1:1 correspondence between observed and fitted values.

Mixed-effects models partition the total variance in the response variable (AGB in this study) between the main components of the model (Fig. 2.4). The proportional contribution of the random effects terms (σ_α^2,$\sigma_{\beta x}^2$,$\sigma_{\beta z}^2$) and the residual variance ($\sigma_y{}^2$) to the total variance was calculated for each term as:

$$\% \text{ contribution} = ((\sigma_\alpha^2/\text{tot\_var})100) \quad (2.6)$$

where e.g. σ_α^2 is the variance in the model attributed to between-group differences in the intercept and tot_var is the total variance from model VIII calculated as the variance of the logged values of total above-ground biomass of the 337 trees in the harvest dataset. Thus, the contribution to the total variance attributable to the combined fixed effects terms was calculated as:

$$\% \text{ contribution} = (((\text{tot\_var} - (\text{sum}(\sigma_\alpha^2 + \sigma_{\beta x}^2 + \sigma_{\beta z}^2 + \sigma_y{}^2)))/\text{tot\_var})100) \quad (2.7)$$

As expected, most of the variability in AGB was accounted for in model VIII by the fixed effects terms (Fig. 2.4). Together the random effects terms accounted for 41%

of the variance in AGB. Between-group variability in the slopes of the predictive variables diameter and height was very similar accounting for 18% and 19% of the total variance respectively. In combination the fixed and random effects explained 94% of the variability in AGB leaving a relatively small residual variance of 6% (Fig. 2.4).

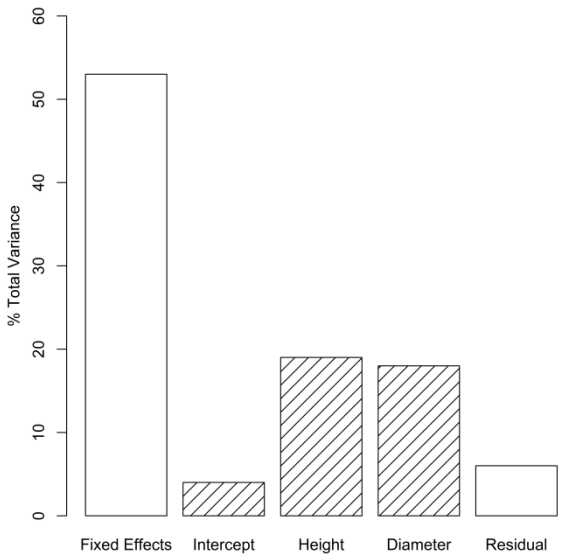

Fig. 2.4. Proportion of the total variability in AGB of harvested trees associated with the fixed effects terms, the random effects terms (hatched bars) and the remaining unexplained (residual) variance from Model VIII.

The random effects represent the group-specific departures (either ±) from the fixed effects estimate of the intercept and the coefficients for diameter and height. There is clearly some between-group variability in the random effects for the eight species_site groups occurring in Kenya (Fig. 2.5). The 95% PI around the random effects is more constrained for groups with a larger sample size (Fig. 2.5) and there is some degree of overlap in the prediction intervals between most groups.

The random effects for most groups fall within the bounds of the 95% confidence interval (95% CI) of the fixed effects estimate of each parameter (Fig. 2.5). However, the predicted random effect for the intercept of group Rhiz_Gaz and the coefficient of height for group Avic_Gaz show no overlap with the fixed effects estimates for these parameters. For group Sonn_Gaz there is a pronounced departure from both the fixed effects estimates and from the predicted random effects for the other groups. Such deviation from the fixed effects estimates suggest that the

allometry for these species_site groupings may be distinct from that of the other groups in the harvest dataset and highlights the general need for the inclusion of group effects in regression models.

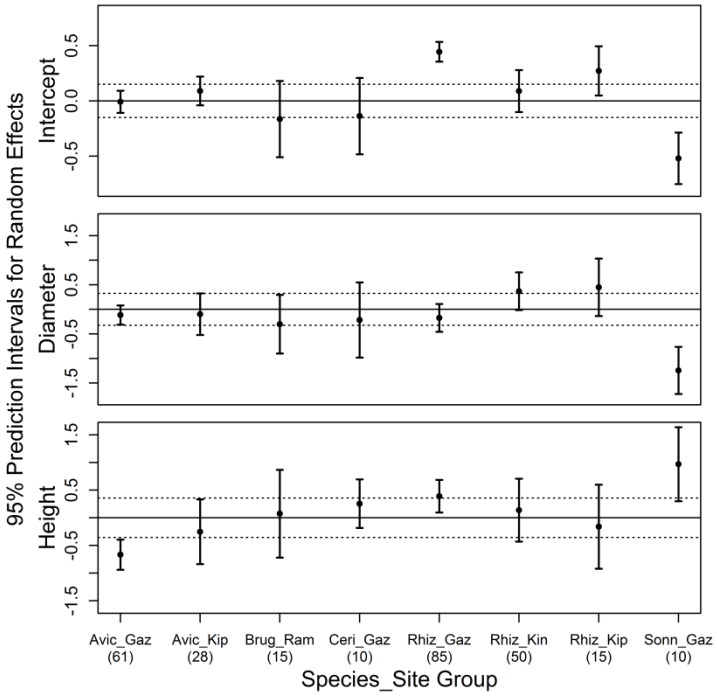

Fig. 2.5. Group-specific random effects (± 95% PI) for the intercept and the coefficients of diameter and height. The solid line at zero represents no departure from the fixed effects estimate for each parameter and the dashed lines on either side are the upper and lower limits of the 95% CI of the fixed effects estimate. Species_site groups correspond to the first four letters of the species followed by the first three letters of the site (see Table 2.1). Numbers in parentheses denote sample size for each group.

2.3.2 Model validation

For harvested trees in the Zambezi Delta predictions of median AGB (± 95% PIs) from model VIII correspond well with the original observed values of AGB (Fig. 2.6). A linear regression between the logged observed values and predicted median values of AGB was used to further assess the predictive ability of model VIII (R^2 = 0.96, p = <0.001). The 95% confidence interval for the intercept includes zero (-0.23 ± 0.37) and for the regression slope includes one (1.01 ± 0.09). The uncertainty around predictions is well constrained for trees with lower AGB but increases with increasing predicted AGB.

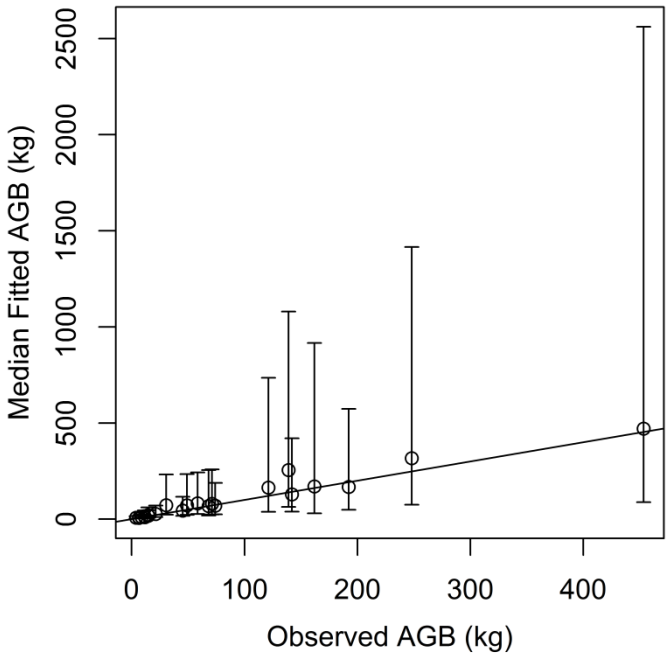

Fig. 2.6. Total above-ground biomass (AGB) in kg as measured for each tree in the Zambezi harvest dataset versus the corresponding median fitted value (kg ± 95% PI) from model VIII. The 95% PI is the difference between the 97.5% and 2.5% quantiles of the simulated distribution of possible values of median AGB for each tree. The reference line represents a 1:1 correspondence between observed and fitted values.

2.3.3 Plot level AGB estimates

Plot level estimates of mangrove AGB vary greatly within and between regions (Fig. 2.7). Within each study region (except Kiunga) there are two orders of magnitude difference between the smallest and largest plot estimates. If the 95% PIs are considered then the scale of maximum AGB across regions ranges between ~200 Mg ha^{-1} at Mida Creek to > 2000 Mg ha^{-1} at Vanga. For each region the uncertainty in estimates is tightly constrained for plots with low values of AGB but there appears to be a general pattern of larger prediction intervals around estimates for plots with higher AGB (Fig. 2.7). For some regions there is considerable variation in the PIs of plots with similar median AGB estimates (e.g. see Mwache plots 45 and 46 in Fig. 2.7). It is likely that larger PIs around the estimates of some plots is not associated with higher biomass *per se* but is due to the presence of large diameter trees in these plots for which the biomass has been estimated with relatively greater uncertainty.

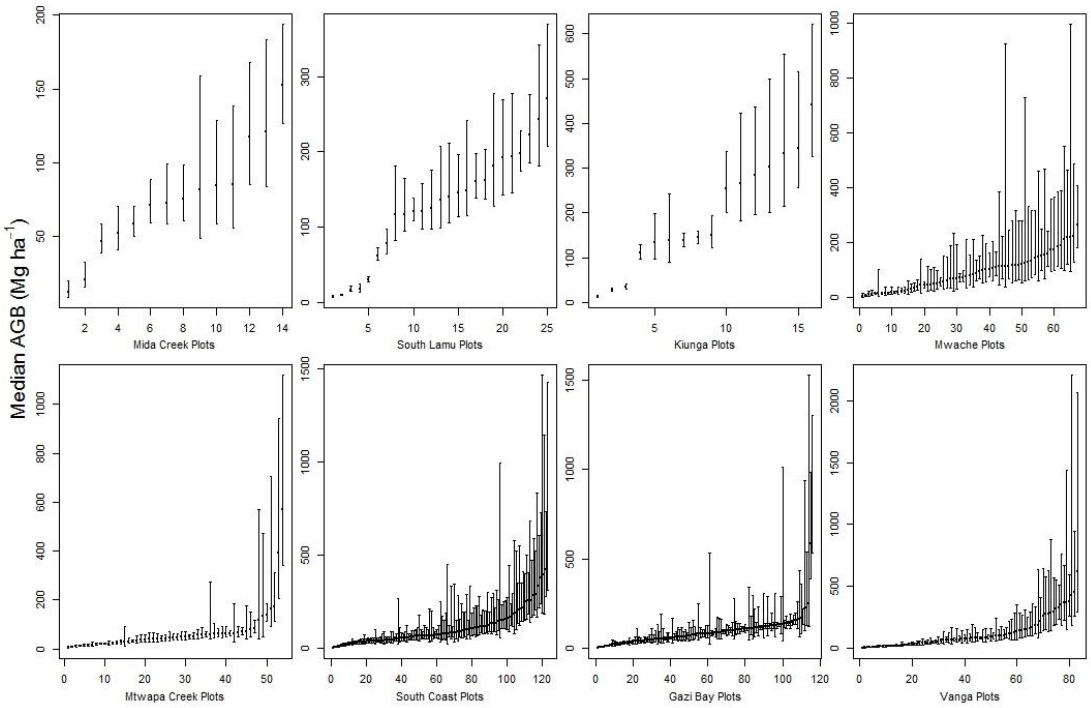

Fig. 2.7. Estimated median above-ground biomass (AGB) of each plot within the forest inventory dataset (± 95% PI). Plots have been grouped according to the eight regions identified in the inventory dataset. For each region plots appear in ranked order from low to high estimated AGB. The 95% PI is the difference between the 97.5% and 2.5% quantiles of the simulated distributions of possible values of median AGB for each plot.

2.3.4 Regional level AGB estimates

As expected, estimates of mean AGB vary amongst the study regions which span the entire Kenyan coastline (Fig. 2.8). There is a difference of > 120 Mg ha^{-1} between the lowest estimate for mangroves at Mtwapa Creek near Mombasa (73 Mg ha^{-1}) to the highest for mangroves within Kiunga NMR (200 Mg ha^{-1}). However, there is a general overlap between the prediction intervals of most regions and the estimates of mean AGB do not differ substantially between the regions Mwache, Gazi, South Coast, Vanga and South Lamu. Uncertainty around the estimates of mean AGB is reasonably well constrained with an absolute difference between upper and lower prediction limits of < 50 Mg ha^{-1} for all regions.

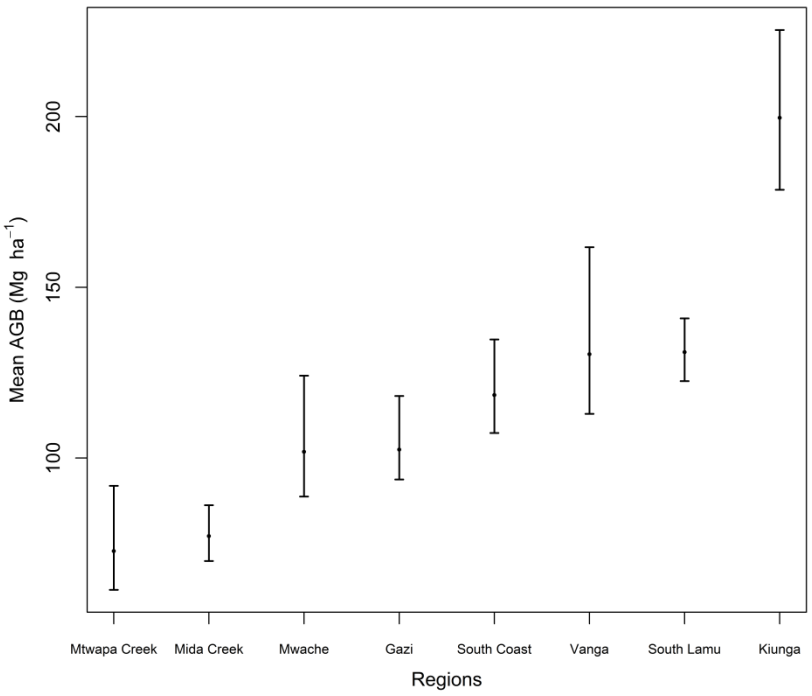

Fig. 2.8. Estimated mean AGB (± 95% PI) of mangroves within each region. The 95% PI is the difference between the 97.5% and 2.5% quantiles of the simulated distribution of possible values of mean AGB for each region.

The regional level estimates of mean AGB (Fig. 2.8) and mangrove cover (Table 2.4) were used in a basic up-scaling exercise in order to give an indication of the total AGB of mangroves within each region and within Kenya as a whole (Table 2.5). Up-scaled values of total mangrove AGB in megatonnes (Mt) were calculated by multiplying the regional level estimates of mean AGB (Mg ha^{-1}) shown in Fig. 2.8 by the corresponding estimate of total mangrove cover (ha) for each region (Table 2.4). There was no inventory data available for mangroves at Kilifi and Tana River therefore it was not possible to estimate mean AGB for these regions. For the purposes of up-scaling it was assumed that the mean AGB of mangroves at Kilifi and Tana River lies somewhere between that of Mtwapa Creek (the lowest regional mean) and Kiunga (the highest regional mean). Thus for sites Kilifi and Tana River two sets of possible values of total AGB ('Low' and 'High') were calculated using the lowest (Mtwapa Creek) and the highest (Kiunga) of the regional level estimates of mean AGB. Consequently there are also two sets of estimates of the total AGB of Kenyan mangroves; one in which the lowest estimates for Kilifi and Tana River were added to the total AGB of the other regions ('Kenya Low') and one in which the highest estimates were used ('Kenya High'). Lamu District (South Lamu + Kiunga)

holds the highest proportion (~ 69 - 75% dependent on Kenya total) of mangrove AGB in Kenya (Table 2.5). Despite having one of the lowest estimates of mean AGB the estimated total AGB of mangroves at Mida Creek is more than double that of Gazi Bay due to the higher mangrove cover at Mida Creek.

Table 2.5: Estimated total mangrove above-ground biomass (AGB) for Kenya and for each region within Kenya [a]

Region	2.5% Quantile of Total AGB (Mt)	Mean of Total AGB (Mt)	97.5% Quantile of Total AGB (Mt)
Mtwapa Creek	0.032	0.038	0.048
Mida Creek	0.116	0.128	0.143
Mwache	0.237	0.272	0.331
Gazi Bay	0.055	0.060	0.070
South Coast	0.242	0.267	0.304
Vanga	0.388	0.449	0.556
South Lamu	3.260	3.486	3.749
Kiunga	0.851	0.951	1.073
Kilifi (Low)	0.039	0.047	0.059
Kilifi (High)	0.114	0.128	0.144
Tana River (Low)	0.211	0.250	0.315
Tana River (High)	0.613	0.685	0.774
Kenya Total (Low)	5.431	5.947	6.648
Kenya Total (High)	5.908	6.464	7.192

[a] 1 megatonne (Mt) = 1 million tonnes. The uncertainty around estimates of total AGB for each region is represented by the 2.5% and 97.5% quantiles of the mean.

The uncertainty around the estimates of total AGB are generally well constrained for all regions (Table 2.5). However, the Low and High estimates of total AGB for Kilifi and Tana River differ by a factor of ~2.7. This constitutes another level of uncertainty for these regions and consequently the overall total for Kenya which differs by ~8% between Low and High estimates.

2.4 Discussion

2.4.1 Applicability and interpretation of Model VIII

This study used mixed-effects modelling to account for both species and site variability in the allometric relationship for mangroves producing a generic equation for Kenyan mangroves and a set of species-site specific equations. The procedure for uncertainty propagation employed in the current study ensures that estimates of AGB at different spatial scales are accompanied by a realistic measure of the total uncertainty. It is important to note that although mangroves have been used as a case

study here, the kind of models and methodologies presented can be regarded as broadly applicable to forests in general.

The practical application of the equations developed in the current study is dependent on the target of inference. The set of species-site specific equations are only applicable to four species within the Gazi Bay region and simulations using these equations account for the uncertainty in predicting the AGB of a new tree within a pre-existing group. In contrast, the generic equation has a much broader application as it can be used to predict the AGB of new trees where there is no pre-existing knowledge of the specific species-site allometric relationship: the most commonly encountered scenario in practical biomass studies. The generic equation offers a far better solution than simply disregarding the additional uncertainty involved in applying an equation that was perhaps derived for a different species and/or a different site.

The predictions of AGB from model VIII show good correspondence with the observed values of AGB used to fit the model (Fig. 2.3). Perhaps more importantly, the median fitted values of AGB (± 95% PIs) from model VIII show good overall correspondence with the observed values of AGB for trees within the Mozambican validation dataset (Fig. 2.6). This would seem to indicate that accounting for variance due to species and site effects in biomass regression models is important if they are to be used effectively elsewhere to predict AGB. Indeed, a large proportion of the total variance in model VIII was attributed to between-group variability in the coefficients of the predictive variables diameter and height (Fig. 2.4). Both species and site specificity in the allometric relationship for mangroves is indicated by the group-specific random effects (Fig. 2.5). Most groups show some overlap in predicted random effects but there are some differences between species at the same site (species_Gaz groups) and between sites for the same species (Rhiz_site groups). However the use of a combined species_site grouping factor precludes any conclusion regarding the relative contribution of each factor (species and site) to the total variance in the allometric relationship. It is also not possible to formally assess the potential contribution of a study effect to the predicted random effects in this

study. However, as mentioned in section 2.2.3.2 any such effect is assumed to be minimal due to the general agreement in methodology across studies included in the harvest dataset. The only study which differed notably in methodology was that of Lang'at (2008) where total above-ground biomass comprised stem weight only (Table 2.1). In this case the sample size was fairly small (15 trees) and re-fitting model VIII after excluding this dataset did not substantially alter the fixed effects estimates, predicted random effects or residual variance.

In modelling the covariance of the distribution of random effects, the constraints imposed by the mixed-effects model used in the current study on the estimated correlation parameters may be considered too restrictive when more than two coefficients vary by group **(**Gelman and Hill, 2007). Although outwith the scope of the current paper; an alternative approach for future study would be to use a scaled inverse-Wishart distribution as the prior for modelling the covariance matrix of the random effects in a fully Bayesian model (Dietze et al., 2008; Gelman and Hill, 2007).

Ideally regression models should not be applied outwith the data range for which they were derived (Chave et al., 2005; Chave et al., 2004). The lack of large tree harvest data means that extrapolation is often a practical necessity when estimates of AGB are needed for large trees within forest inventory datasets. In this study, it is assumed that the log-log linear relationship will hold for trees beyond the original data range. It is, however, acknowledged that this may not be the case and that the estimates of AGB for trees outwith the data range recorded in harvest dataset will include additional uncertainty due to extrapolation. Only a very small proportion of trees in the inventory dataset (0.1%) had a recorded diameter exceeding that found within the harvest dataset and none exceeded the height range. However, the effect of having limited information regarding the allometric relationship for large trees is apparent in the poorer model fit at higher AGB values (Fig. 2.3). It is also apparent (to some degree) in the width of the prediction intervals around the larger trees in the validation dataset and the estimates of AGB at the plot, regional and landscape level. This is presumably due to the fact that by accounting for the covariance of the

predictive uncertainty at the single tree level in producing estimates of AGB at aggregated levels (e.g. a plot) the aggregated predictive uncertainty is realistically larger than if the AGB of multiple trees had simply been summed (Wutzler et al., 2008). In addition, the greater width of the PIs for larger trees is an inevitable consequence of using a log-normal model where the variability is related to the mean on the linear scale. An approach to consider for future study would be to investigate the use of alternative distributions for the variability.

The 95% PIs in the current study are generally well constrained given that measurement and predictive uncertainty have been fully propagated to estimates. In addition, prediction intervals take into account both the uncertainty in estimating the conditional mean of the response and the variability in the conditional distribution of the response and as such are generally larger than the frequentist confidence intervals employed to represent uncertainty in most other studies. However, for a few of the plots in the inventory dataset the upper limit of the PI around the median estimate of AGB is exceptionally high (Fig. 2.7) and exceeds the highest levels of AGB previously reported for mangroves. The effects of both extrapolation and small plot size could possibly explain these extreme upper PI values for selected plots. All of the affected plots measure just 10 x 10 m and contain two or more large diameter trees which in some cases exceed the maximum diameter (48.9 cm) found in the harvest dataset. The presence of a few large trees in a small plot can skew results, however tree level and sampling uncertainties tend to be reduced in larger plots (Chave et al., 2004).

2.4.2 Comparison and interpretation of large-scale AGB estimates

Previous allometry/biomass studies conducted in Kenya have focused on the development and application of species-specific allometric equations to mangroves at a particular site. As a result existing published estimates of AGB for Kenyan mangroves are on a species by site basis and in many cases refer to monoculture plantation forest established at Gazi Bay (Kairo et al., 2009; Kairo et al., 2008; Tamooh et al., 2009). Estimates of AGB for natural mangrove forest in Kenya vary

considerably between sites but also between studies conducted at the same site. Within the Mida Creek area Gang and Agatsiva (1992) estimated the AGB of *Rhizophora* forest as 11.8 Mg ha $^{-1}$. However, their estimate is based on the data from just one plot and there is no mention of how this estimate was derived (Gang and Agatsiva, 1992). For the same species at Gazi Bay Slim et al., (1996) and Kirui et al., (2006) produced substantially higher estimates of mean AGB at 249 Mg ha^{-1} (± s.d. 40.1) and 452.02 Mg ha^{-1} respectively. Similar to the study by Gang and Agatsiva (1992) the estimate of AGB from Slim et al., (1996) was based on the application of their allometric equation to *Rhizophora* trees within one 20 x 20 m mono-specific plot and therefore cannot reasonably be assumed to represent the variability of *Rhizophora* forest within Gazi Bay. The highest estimate from Kirui et al., (2006) is more akin to the level of AGB found in mangroves in South East Asia (Komiyama et al., 2008) and it is not clear how their mean estimate was derived. In contrast to previous studies, this study has focused on providing estimates of mangrove AGB at varying spatial scales. This different approach means that the estimates provided here are not readily comparable with those from previous biomass studies conducted in Kenya. However, to facilitate some kind of comparison the outputs of the simulation procedure (section 2.2.3.4) were sub-set to provide an estimate of mean AGB for just *Rhizophora* forest at Gazi Bay of 134.5 Mg ha^{-1} (95% PI range 125.1 – 146.8 Mg ha^{-1}).

Estimates of biomass density (mean Mg ha^{-1}) at large spatial scales such as those produced in the current study can be regarded as a comparative tool by which to assess the level of AGB at different sites/regions or between countries or forest types. Levels of mean AGB have been found to vary considerably between mangrove forests across the globe (see review by Komiyama et al., 2008) ranging between 31.5 Mg ha^{-1} (± s.d. 2.9) for pioneer mangrove forest in French Guiana (Fromard et al., 1998) to 536.6 Mg ha $^{-1}$ (95% CI range 327.6 – 743.5 Mg ha^{-1}) for mangroves in Micronesia (Donato et al., 2012). Such broad-scale variability can be attributed to differences in floristic composition, climatic conditions, hydrology, geomorphology, successional stage and disturbance history (Fromard et al., 1998).

The regional estimates of mean AGB (± 95% PI) shown in Fig. 2.8 represent a best attempt at summarising the level of AGB within different mangrove regions in Kenya. The two regions with the lowest estimated mean AGB were Mtwapa Creek (72.8 Mg ha $^{-1}$, 95% PI range 61.4 – 91.9 Mg ha^{-1}) and Mida Creek (77.1 Mg ha^{-1}, 95% PI range 69.9 – 86.2 Mg ha^{-1}) and are comparable to the level of AGB (71 – 85 Mg ha $^{-1}$) found in mixed mangrove forests dominated by *R. mucronata* and *A. marina* in Sri Lanka (Amarasinghe and Balasubramaniam, 1992). The estimate for Mida Creek is somewhat lower than expected and could be due to insufficient inventory data from this region (n = 14 plots) but it is also likely reflective of the level of forest degradation in this area due to illegal and poorly managed logging practices (Kairo et al., 2002). The region with the highest estimate of mean AGB was Kiunga NMR (199.6 Mg ha^{-1}, 95% PI range 178.6 – 225.3 Mg ha^{-1}). This level of AGB is comparable to that reported for mangroves in Micronesia (Donato et al., 2012; Kauffman et al., 2011) and mature coastal mangroves in French Guiana (Fromard et al., 1998) and exceeds the estimate by Donato et al., (2011) of 169.9 Mg ha^{-1} for oceanic mangroves in the Indo-Pacific region.

Although the estimates of AGB produced in this study are statistically robust, it is important to note the underlying assumption that estimates at large spatial scales have been obtained using a sample which is representative of the variability in forest composition and structure within the area in question (Chave et al., 2004). The estimates of mean AGB in this study were derived using all available current inventory data for each region. It seems reasonable to assume that due to the sampling strategy employed (stratified random) and the comparatively large sampling effort (total number of plots sampled) that the mangrove areas in the South of Kenya (Gazi Bay, Mwache, Mtwapa Creek, South Coast and Vanga) have been adequately sampled. In addition, the large within-region variability in estimates of median AGB at the plot level (Fig. 2.7) would suggest that there has been no sampling bias in terms of plot location, for example by preferentially locating plots in areas likely to yield high biomass and that the range of possible biomass values within each region has been adequately captured.

The regional estimates for Mida Creek and Lamu District (South Lamu and Kiunga) are based on relatively small inventory datasets (n = 14 plots in Mida Creek, 25 in South Lamu and 16 in Kiunga) due to the larger resource requirement and practical difficulties (e.g. accessibility) associated with sampling areas in the North. While the sampling strategies employed in these regions (random and stratified random) are appropriate from a statistical point of view; it is recommended that further data collection is undertaken in order to increase sample size and ensure representivity in these regions. This is particularly important in the case of Lamu District which covers a large geographical area and is worthy of further division into smaller sub-regions. For example, the mangroves of Dodori Creek (Dodori National Reserve, Lamu District) were not sampled in the current study but should probably be considered as a distinct mangrove system.

In considering the regional and Kenya-wide estimates of total AGB provided in Table 2.5 it is acknowledged that: 1) the estimates of mean AGB (± 95% PIs) used in up-scaling are assumed to be regionally representative as discussed above and 2) the uncertainty associated with the estimates of mangrove cover derived from the remote sensing data has not been accounted for. Bearing in mind these caveats the estimates (± 95% PIs) shown in Table 2.5 can still be viewed as a useful comparative overview of the level of total AGB stocks currently held within each region. There is undoubtedly scope for large-scale estimates to be further refined in the future. In particular there is a need for current inventory data to be collected within the regions Kilifi and Tana River (as defined in this study) not only to constrain the regional estimates but also the Kenya-wide estimate of total AGB. In addition, if and when future remote sensing work allows for the detailed mapping of mangrove cover and structural characteristics in each region it may become possible (and desirable) to produce large-scale estimates of AGB based on up-scaling by forest strata.
The stratification of forest cover is recommended for the reporting of forest carbon pools (IPCC, 2006) and there are a variety of stratification options still under consideration for future REDD reporting (Maniatis and Mollicone, 2010). Mangroves are generally considered to display species zonation and have traditionally been stratified by such ‘zones’ (Hogarth, 1999). However, not all

mangroves display well-defined patterns of zonation (e.g. Mida Creek) and other options for stratification for example based on structural characteristics may be more appropriate in some situations. Various remote sensing techniques have been used in recent years to map mangroves at fine to large spatial scales (see review by Kuenzer et al., 2011). Such techniques offer the potential for fast and repeatable estimates of cover, and in the case of radar remote sensing above-ground biomass to be made based on mangrove structural parameters (Fatoyinbo et al., 2008; Held et al., 2003; Lucas et al., 2007).

It is anticipated that if required and pending any further collection of new harvest data, the model and methodology for uncertainty propagation presented in the current study could be used to produce estimates of mean AGB for use in future up-scaling exercises based on some stratification system with only minor modification to the existing procedures.

Acknowledgements

This research was funded by the Natural Environment Research Council (NERC), UK to which we are very grateful. We are also very grateful for the support provided by our collaborating partner Kenya Marine and Fisheries Research Institute (KMFRI) and additional support in the field provided by Kenya Forest Service (KFS). Many thanks to all those who provided the raw data used for model development and application and to WWF, Mozambique/KMFRI for providing us with a validation dataset. Data collection in Mwache was supported by the WIOMSA-MASMA regional project on "Resilience of mangroves and dependent communities in the WIO region to climate change", Grant No: MASMA/CC/2010/08. Data collection in Mtwapa Creek was supported by the Flemish Interuniversity Council – University Development Cooperation VLIR-UOS. Satellite imagery was provided by Spot Image through the Planet Action initiative as part of a larger project funded by the Ecosystem Services for Poverty Alleviation (ESPA) programme [under the Swahili Seas NE/I003401/1 project]. The ESPA programme is funded by the Department for International Development (DFID), the Economic and Social Research Council (ESRC) and the Natural Environment

Research Council (NERC) of the UK. Additional SPOT imagery was provided under the European Space Agency (ESA) Category-1 scheme (Project ID: 8177). All processing of satellite imagery was carried out by Dr. Karin Viergever at ecometrica (Edinburgh, UK) and Neha Joshi to whom we are very grateful for lending their expertise. We wish to thank all those involved for their hard work in collecting the inventory data for the current study, in particular Mr Bernard Kivyatu. Many thanks to Dr. Luke Smallman (University of Edinburgh, UK) for help with programming in R and to Dr. Giles T. Innocent (Biomathematics and Statistics Scotland (BioSS)) for providing statistical advice. Finally, we wish to thank two anonymous reviewers for their comments and suggestions for improvement to the manuscript.

3. The effect of excluding uncertainty components during the biomass estimation process

R. Cohen[a] and M. Mencuccini[a]

[a] *School of GeoSciences, University of Edinburgh, Crew Building, West Mains Road, Edinburgh, EH9 3JN, UK*

Author Contributions:

R. Cohen provided some of the data used in this study (as detailed in Table 3.2), carried out the data analysis and wrote the manuscript. Advice on data analysis and comments on the manuscript were provided by M. Mencuccini.

Abstract

All estimates of forest above-ground biomass (AGB) should be accompanied by a realistic measure of uncertainty. Estimates of AGB should account for the uncertainty in the measurement of inventoried trees (e.g. measurements of stem diameter) and the parameter and predictive uncertainty associated with the use of the allometric model. This study evaluates the effect of excluding such components of uncertainty on predictions of the uncertainty of AGB estimates obtained using 1) a mixed-effects (ME) regression model and 2) a standard ordinary least squares (OLS) regression model. The exclusion of measurement uncertainty had relatively little impact on the magnitude of the overall uncertainty of an estimate of AGB regardless of spatial scale or tree size. The pattern of relative importance and the proportional change (in the magnitude of the uncertainty) attributed to the removal of each uncertainty component was generally consistent across landscape and regional spatial scales for both the ME and OLS models, largely reflecting the partitioning of variance in the underlying regression models. In the ME model the removal of the random effects during the biomass estimation process had the biggest impact on the magnitude of the uncertainty at all spatial scales (landscape and regional) and levels of estimated plot and tree AGB (low, medium and high AGB levels). In the current study use of the OLS model underestimated the total uncertainty in biomass estimates by > 300% in comparison with the ME model, reflecting the complete pooling approach to parameter estimation and the overestimation of the degrees of freedom typical of standard OLS models. This is illustrative of the potential to substantially underestimate the uncertainty of biomass values if group-effects are not considered in regression models.

3.1 Introduction

All estimates of forest above-ground biomass (AGB) should be accompanied by a realistic measure of uncertainty. This is essential in order to constrain uncertainty in global climate models, the reporting of forest carbon stocks and stock changes for the purposes of global climate change mitigation strategies such as Reducing Emissions from Deforestation and Forest Degradation (REDD+) and remote sensing based approaches to biomass monitoring (Ahmed et al., 2013; Brown et al., 1995; Chave et al., 2004; IPCC, 2006)

Estimates of AGB obtained by applying allometric equations to forest inventory data (the biomass estimation process) should account for the uncertainty in the measurement of inventoried trees (e.g. measurements of stem diameter) and the parameter and predictive uncertainty associated with the use of the allometric model. Failing to propagate such components of uncertainty during the biomass estimation process ultimately leads to an underestimation of the total uncertainty (Dietze et al., 2008).

A common approach to uncertainty propagation has involved summing the variances of individual uncertainty components derived using empirical expansion-based methods (e.g. Taylor series) to produce an estimate of the total uncertainty in addition to an estimate of the proportional contribution of each uncertainty component to the total (Ahmed et al., 2013; Chave et al., 2005; Ketterings et al., 2001; Phillips et al., 2000). A limitation of such methodologies is that they do not account for interactions between the various uncertainty components which affect the relative importance of each component to the total uncertainty (Smith and Heath, 2001). Simulation-based approaches to uncertainty propagation (e.g. Monte Carlo simulations) involve the simultaneous sampling of model parameters from specified distributions. Such approaches not only allow for a fuller representation of each uncertainty component (and thus the overall uncertainty) but also an evaluation of the relative influence of each component on the total uncertainty whilst taking into account the simultaneous effects of all other uncertainty components (Ryan, 2009; Smith and Heath, 2001).

Allometric equations used to estimate AGB have commonly been derived using standard ordinary least squares (OLS) regression models (Chave et al., 2005; Komiyama et al., 2005; van Breugel et al., 2011). However, the complete pooling approach to parameter estimation employed in such models ignores any correlations (or 'group-effects') in the underlying data used to fit the model resulting in an underestimation of the standard error of regression coefficients (Gelman and Hill, 2007; Steele, 2008). In contrast, mixed-effects regression models explicitly model the variance due to group-effects and the partial pooling approach to parameter estimation allows for more robust estimation of regression coefficients and their uncertainties (Steele, 2008). Thus the choice of allometric model can be expected to affect the magnitude of the total uncertainty (of AGB estimates) and the relative contribution of different components of uncertainty (propagated during the biomass estimation process) to the total uncertainty.

This study uses the mixed-effects (ME) regression model and simulation procedure for propagating uncertainty as detailed in Cohen et al., (2013) in order to evaluate the effect of excluding uncertainty components (measurement, residual and parameter uncertainties) during the biomass estimation process on predictions of the uncertainty of AGB estimates. For comparative purposes the current study also provides an evaluation of the effect of excluding uncertainty components during the biomass estimation process using a standard OLS regression model.

3.2. Methods

3.2.1 ME regression model

The linear ME model developed by Cohen et al., (2013) for estimating mangrove above-ground biomass in Kenya used a combined species_site grouping factor to account for variability in the allometric relationship due to both species and site effects:

$$\ln(y_i) \sim N(\alpha_{j[i]} + \beta_{j[i]}\ln(x_i) + \beta_{j[i]}\ln(z_i) + \sigma_y^2) \text{ for } i = 1,\ldots,n, \quad (3.1)$$

where $\ln(y_i)$ is the response (total AGB) for the *ith* individual, the term $\alpha_{j[i]}$ indexes the *ith* individual within the *jth* group and denotes that the coefficient for the intercept (α) varies across groups (j = 1,..., J) as a random effect. The terms $\beta_{j[i]}\ln(x_i)$ and $\beta_{j[i]}\ln(z_i)$ denote that the coefficients for the predictive variables stem diameter ($\ln(x)$) and tree height ($\ln(z)$) vary across groups as random effects and σ_y^2 is the residual or the unexplained 'within-group' variance. The terms $\alpha_{j,}$ β_{jx} and β_{jz} signify that these parameters were themselves modelled yielding a partial pooling estimate of α and of the coefficients β_x and β_z for each group along with an estimate of the overall population mean (the fixed effects) and the 'between-group' variance (estimated from the data). Full details of model development and validation can be found in Cohen et al., (2013). A large proportion (41%) of the total variance in the model was attributable to between-group variability in the intercept and the coefficients of *x* and *z* (the random effects terms), leaving a relatively small residual variance of just 6% (Fig. 3.1).

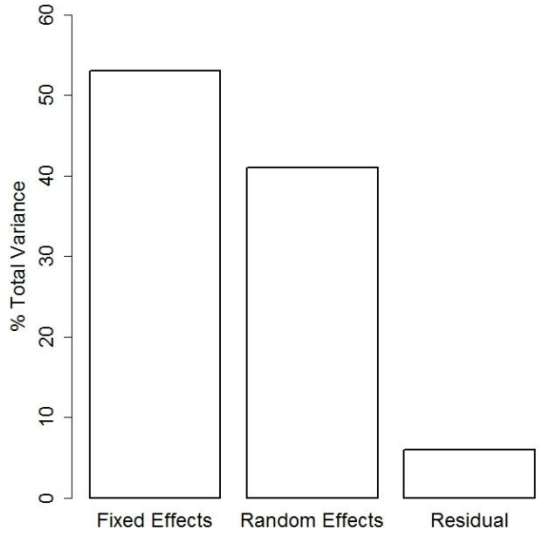

Fig. 3.1: Partitioning of the total variability in the AGB of harvested trees associated with the fixed effects terms, the random effects terms and the remaining unexplained (residual) variance from the ME regression model developed by Cohen et al., (2013).

The biomass estimation process described in Cohen et al., (2013) used the above model (Eq. (3.1)) in a statistical simulation procedure which propagated components of uncertainty (measurement, residual and parameter) to estimates of AGB for trees, plots and regions. In the current study, this simulation procedure was modified to exclude in turn each uncertainty component during the biomass estimation process.

Six uncertainty scenarios were simulated (Table 3.1) using the extensive forest inventory dataset detailed in Cohen et al., (2013) and summarised here in Table 3.2.

Table 3.1: Specifications for uncertainty simulations [a]

Uncertainty Scenario	Components of Uncertainty			
	Measurement	Residual	Random Effects	Fixed Effects
1	✓	✓	✓	✓
2	×	✓	✓	✓
3	✓	×	✓	✓
4	✓	✓	✓	×
5	✓	✓	×	✓
6	✓	✓	×	×

[a] ✓ and × symbols indicate whether an uncertainty component has been included (✓) or excluded (×) during each simulation.

Measurement uncertainty refers to the assumed uncertainty in diameter (5% of the observed value) and height (10% of the observed value) measurements of inventoried trees. The residual uncertainty (σ_y^2) is the unexplained variance from the ME regression model (Eq. 3.1). In this study parameter uncertainty is comprised of the random effects and the uncertainty in the estimates of the fixed effects. The random effects are technically a measure of the variability in the estimated fixed effects parameters due to group effects. However, in the context of this study the random effects are also considered to be a component of uncertainty, as their inclusion or exclusion from the biomass estimation process is equivalent to either recognising or ignoring the potential impact of accounting for between-group variability in the fixed effects estimates on the magnitude of the final uncertainty.

All statistical analyses were performed using R statistical software version 2.15.0 (R Development Core Team, 2012). The relative impact of removing each component of uncertainty during the biomass estimation process was assessed by comparing the difference in the magnitude of the 95% prediction interval (95% PI) under scenarios 2 to 6 against that of scenario 1 (total uncertainty).

Table 3.2: Provenance and summary of Kenyan mangrove forest inventory dataset[a]

Region	Origin of Data	Date	No. of Plots	Plot Size (ha)
Mida Creek	This Study	2010/2011	14	0.01 to 0.5
South Lamu			25	
Kiunga			16	
Gazi Bay	This Study	2010/2011	28	
	CAMARV	2009	18	0.01
	UNDP	2009	70	0.01
Mtwapa Creek	Okello (unpublished results)	2010	54	0.01
Mwache	Kaino (2013)	2011	67	0.01
South Coast	KMFRI	2007	123	0.01
Vanga	KMFRI	2012	83	0.0025 to 0.04

[a] Abbreviations are: Capacity Building for Mangrove Assessment, Restoration and Validation (CAMARV); United Nations Development Programme (UNDP) and Kenya Marine and Fisheries Research Institute (KMFRI).

3.2.1.1 Landscape scale simulations

The AGB of each tree within the forest inventory dataset was simulated 50,000 times. The AGB estimates for each tree within a plot were summed at each iteration point giving a distribution of 50,000 possible estimates of total AGB for every plot in the inventory dataset. The mean AGB was calculated at each iteration point across all 498 plots yielding a distribution of 50,000 possible estimates of mean AGB. The quantiles of this distribution of means were used to calculate the mean 95% PI (97.5% - 2.5% quantile) for an estimate of plot AGB at the landscape scale. This process was repeated for each of the six uncertainty scenarios (Table 3.1).

3.2.1.2 Regional scale simulations

In order to assess the impact of removing each uncertainty component at the regional scale; plots within the inventory dataset were first grouped according to their location within the mangrove regions along the Kenyan coastline identified in Table 3.2. Due to the small sample size in some regions (e.g. Mida Creek) uncertainty simulations were performed using the inventory data from the five most heavily sampled regions: Gazi Bay, Mtwapa Creek, Mwache, South Coast and Vanga (Table 3.2). To ensure comparability of results between regions all plots used in the regional scale

simulations measured 0.01 ha (10 x 10 m) in size. The total number of inventoried plots differs between the five regions, therefore for each region (under each uncertainty scenario) the entire simulation procedure was repeated 1000 times using fifty randomly selected plots for each new simulation run.

For each regional scale simulation run the AGB of each tree was simulated 10,000 times. The AGB estimates for each tree within a plot were summed at each iteration point giving a distribution of 10,000 possible estimates of total AGB for every plot. The mean AGB was calculated at each iteration point across all 50 plots yielding a distribution of 10,000 possible estimates of mean AGB. The quantiles of this distribution of means were used to calculate the mean 95% PI for each simulation run. This process generated a distribution of 1000 possible mean 95% PIs for each region under each uncertainty scenario. The mean of the distribution of possible PIs was taken to represent the overall mean 95% PI for an estimate of plot AGB at the regional scale under each uncertainty scenario.

3.2.1.3 AGB 'levels'

3.2.1.3.1 Plot AGB

In order to assess the possible impact of removing each uncertainty component at different levels of AGB the inventory dataset was divided into three sub-datasets ('low', 'medium' and 'high' AGB plots) consisting of 166 plots each. Apportioning of each plot in the inventory dataset to one of the sub-datasets was made based on the estimates of median AGB (Mg ha^{-1}) obtained from Cohen et al., (2013) for each plot (Fig. 3.2). The plots were ranked from lowest to highest estimated median AGB (Fig. 3.2) with the first 166 plots forming the 'low' AGB sub-dataset and so on. Estimates of median AGB ranged from 1.9 Mg ha^{-1} to 51.9 Mg ha^{-1} for plots within the low sub-dataset, 52.1 Mg ha^{-1} to 111.4 Mg ha^{-1} for plots in the medium sub-dataset and 112.1 Mg ha^{-1} to 812.8 Mg ha^{-1} for plots in the high sub-dataset.

For each of the sub-datasets the AGB of each tree within each plot was simulated 50,000 times. The AGB estimates for each tree within a plot were summed at each

iteration point giving a distribution of 50,000 possible estimates of total AGB for every plot. The mean AGB was calculated at each iteration point across all plots (n = 166) yielding a distribution of 50,000 possible estimates of mean AGB. The quantiles of this distribution of means were used to calculate the mean 95% PI for plots of low, medium and high estimated AGB under each uncertainty scenario.

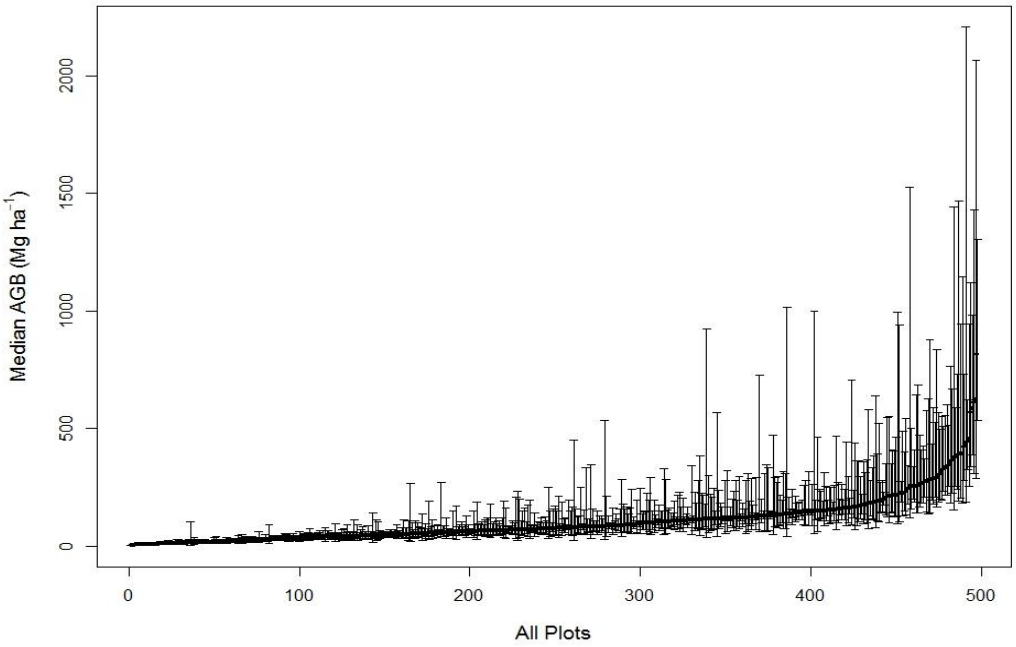

Fig. 3.2: Estimated median above-ground biomass (AGB) of each plot within the forest inventory dataset (± 95% PI). Plots appear in ranked order from low to high estimated median AGB. The 95% PI is the difference between the 97.5% and 2.5% quantiles of the simulated distributions of possible values of median AGB for each plot.

3.2.1.3.2 Tree AGB

Using the median estimates of AGB (kg) for each tree obtained from Cohen et al., (2013) the inventory dataset was divided into three sub-datasets comprising trees of 'low', 'medium' and 'high' AGB with each sub-dataset consisting of 6776 trees. Trees were ranked from lowest to highest estimated median AGB with the first 6776 trees forming the 'low' AGB sub-dataset and so on. Estimates of median AGB ranged from 0.05 kg to 8.65kg for trees within the low sub-dataset, 8.66 kg to 26.42 kg for trees in the medium sub-dataset and 26.45 kg to 2338.57 kg for trees in the high sub-dataset. For each of the sub-datasets the AGB of each tree was simulated 50,000 times. The mean AGB was calculated at each iteration point across all trees

(n = 6776) yielding a distribution of 50,000 possible estimates of mean AGB. The quantiles of this distribution of means were used to calculate the mean 95% PI for trees of low, medium and high estimated AGB under each uncertainty scenario.

3.2.2 OLS model

The tree harvest dataset detailed in Cohen et al., (2013) was used to fit a linear regression model using ordinary least squares (OLS) of the form:

$$\ln(AGB) = \ln(a) + b_1\ln(D) + b_2\ln(H) + \varepsilon \quad (3.2)$$

where a is the intercept, b_1 and b_2 are the coefficients of the explanatory variables stem diameter (D) and tree height (H) respectively and ε is the residual error term. The fixed-effects parameter estimates and associated regression statistics from the OLS model are provided in Appendix 2, Table A2.1. Estimates of AGB for trees in the inventory dataset (Table 3.2) using the OLS model were obtained using the procedure for propagating measurement, residual and parameter uncertainty (fixed effects only) detailed in Cohen et al., (2013).

The simulations described in sections 3.2.1.1 to 3.2.1.3 were repeated for uncertainty scenarios 1 to 4 (Table 3.1) using the OLS model. The simulations for AGB 'levels' were carried out as in section 3.2.1.3 however; plots and trees were divided into sub-datasets based on the ranked estimates of AGB obtained from the OLS model.

3.3 Results and Discussion

3.3.1 Landscape scale

The removal of the random effects during the biomass estimation process clearly had the biggest impact on the magnitude of the 95% PI in the ME model (Fig. 3.3a: scenarios 5 and 6). This is illustrative of the potential to substantially underestimate the uncertainty of biomass estimates if group-effects are not considered in regression models (Wutzler et al., 2008). Indeed there is considerable difference (> 300%) in

the magnitude of the total uncertainty (scenario 1) between the ME and OLS models (Fig. 3.3) such that in the OLS model the total uncertainty is approximately equal to that of the PI under scenario 5 in the ME model. This is due to the complete pooling approach to estimation of regression coefficients in the OLS model where correlations in the data structure are ignored and thus the effective sample size is inflated resulting in an under-estimation of the standard error of regression coefficients and consequently the total uncertainty of predictions (Steele, 2008).

The difference in the complete pooling (OLS model) vs. partial pooling (ME model) approach to estimating regression parameters is also evident in the small effect (-3.2%) of removing the uncertainty in the fixed effects parameters in the OLS model in comparison with the ME model (-9%). This is likely the result of the inflated number of degrees of freedom employed for the estimation of the fixed effects parameters in the OLS model, relative to the ME model. The removal of the residual variance in the ME model had a much smaller impact on the magnitude of the PI than in the OLS model (-11% versus -73% respectively); however this is to be expected as the large proportion of the variance explained by the random effects in the mixed model (Fig. 3.1) is attributed to residual 'unexplained' variance in the OLS model (Fig. 3.3b: scenario 3).

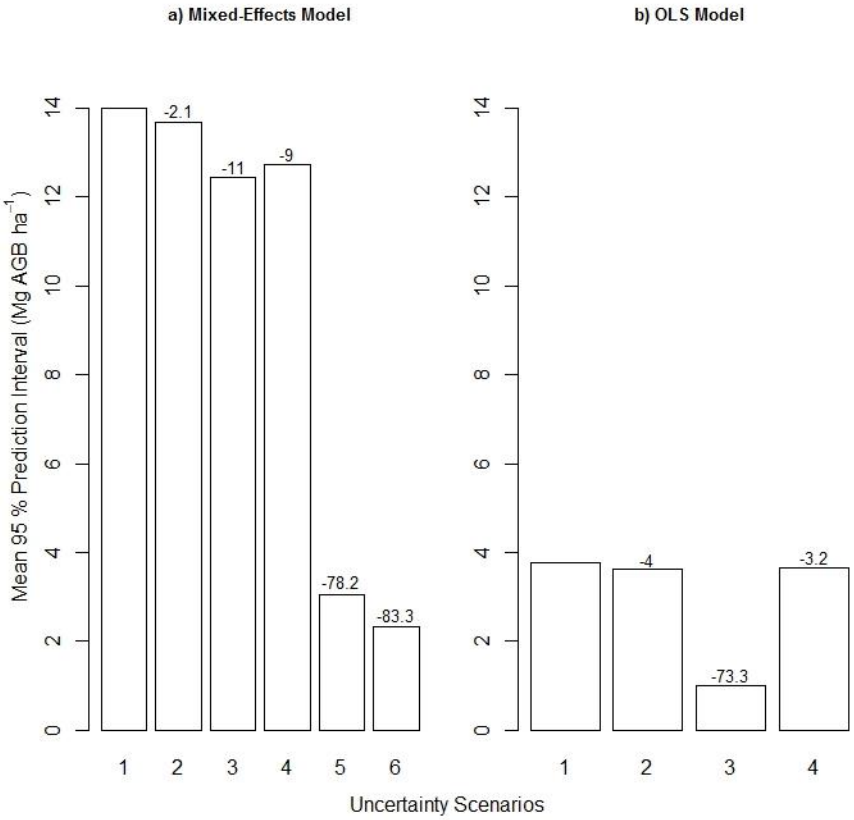

Fig. 3.3: Effect of removing components of uncertainty on the magnitude of the mean 95% prediction interval (95% PI) for an estimate of plot AGB at the landscape scale obtained using a) the ME model or b) the OLS model. Numbers along the x axis correspond to the uncertainty scenarios described in Table 3.1. Numbers above bars represent the percentage decrease in the mean 95% PI under each uncertainty scenario compared to scenario 1. Please note that % changes in the mean PIs between uncertainty scenarios 2 to 6 are not additive.

In this study the uncertainty in the measurements of stem diameter and height of inventoried trees was assumed to be 5 and 10% respectively. Despite these conservative assumptions there appears to be little impact on the PI of removing measurement uncertainty during the biomass estimation process using either model at the landscape scale (Fig. 3.3: scenario 2). This is in accordance with previous studies which found that the contribution of measurement uncertainty to the total uncertainty (whilst potentially important for an estimate of single tree AGB) generally averages out with increasing sample size (Chave et al., 2004; Phillips et al., 2000; Ryan, 2009). In addition, the partitioning of the variance in the models used here means that accounting for measurement uncertainty during the biomass estimation process is relatively unimportant in comparison with accounting for the

random effects (in the ME model) and residual uncertainty (in the OLS model) in terms of producing realistic prediction intervals.

3.3.2 Regional scale

The relative effect of removing each uncertainty component during the biomass estimation process (on the magnitude of the mean 95% PI) using the ME model is consistent between each of the five regions (Fig. 3.4). It is also consistent between the regional and landscape scale (Fig. 3.3a and Fig 3.4). Similarly, for each region the proportional change in the mean PI under each uncertainty scenario using the OLS model mirrors that at the landscape scale (see Appendix 2, Fig. A2.1). The general consistency between landscape and regional scale results in terms of the pattern of relative importance and the proportional change attributed to the removal of each uncertainty component is largely reflective of the partitioning of variance in the underlying regression models. There is however a difference in the overall magnitude of the total uncertainty (scenario 1) of an estimate of plot AGB between regions (Fig. 3.4). In particular the total uncertainty in Vanga (> 60 Mg ha^{-1}) is substantially larger than that of the other four regions. The most extreme values of diameter and height are found within the Vanga dataset and therefore the larger uncertainty in this region is presumably due to the influence of such values in a log-normal model where the variability is related to the mean on the linear scale. The small difference in scale of the PIs between the other four regions is similarly attributable to between region variability in the distribution of stem diameter and height measurements of inventoried trees.

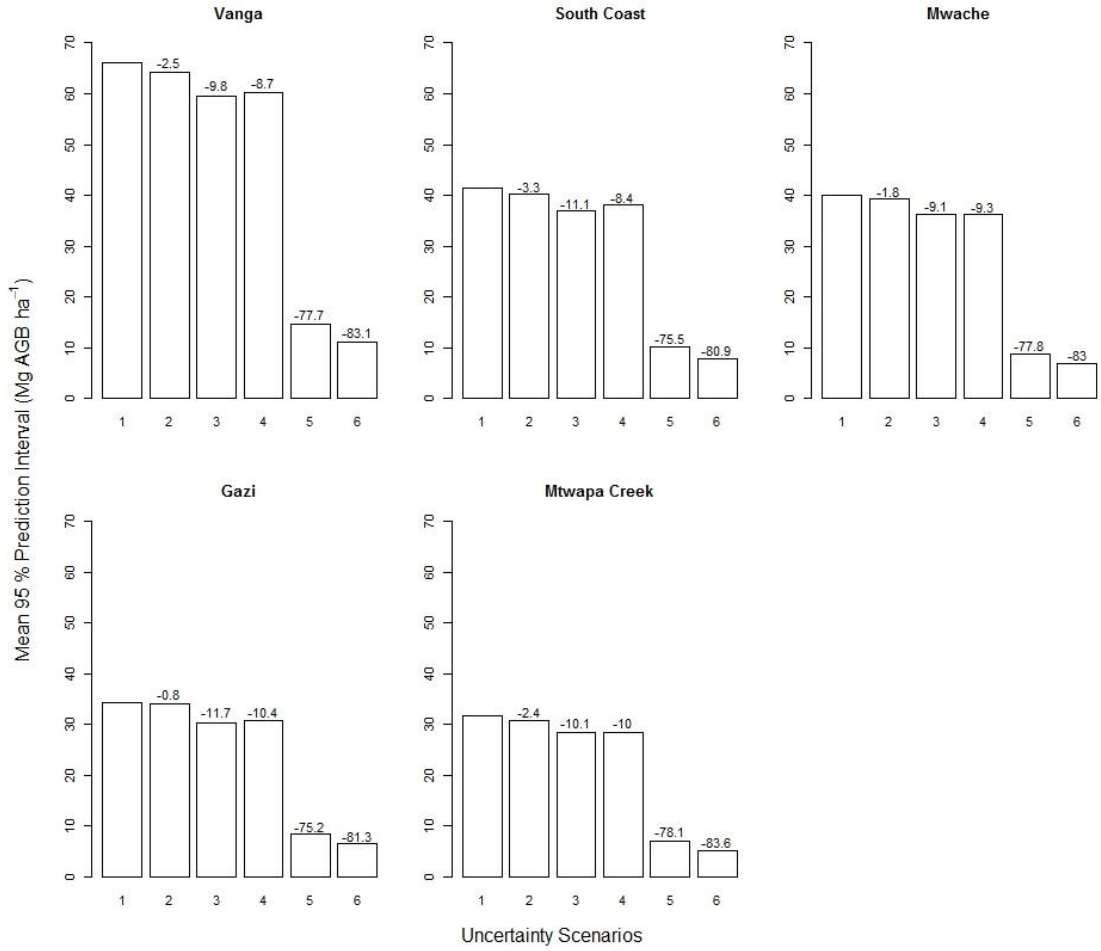

Fig. 3.4: Effect of removing components of uncertainty on the magnitude of the mean 95% prediction interval (95% PI) for an estimate of plot AGB at the regional scale obtained using the ME model. Numbers above bars represent the percentage decrease in the mean 95% PI under each uncertainty scenario compared to scenario 1. Please note that % changes in the mean PIs between uncertainty scenarios 2 to 6 are not additive.

3.3.3 AGB 'levels'

3.3.3.1 ME model

The predicted uncertainty for plots within the inventory dataset of comparatively high estimated AGB is an order of magnitude greater than the uncertainty for those plots with the lowest estimated AGB (Fig. 3.5). This large difference in the magnitude of the uncertainty between low and high AGB plots is due to the greater number of large trees (i.e. trees of larger diameter and height) present within the high AGB sub-dataset and the influence of such trees on the overall scale of the uncertainty. The effect of tree size on the overall uncertainty is further exemplified

by the large difference in the magnitude of the PIs between the low and high AGB trees (Fig. 3.6). The relative impact of removing each uncertainty component is generally consistent for plots of low, medium and high estimated AGB however the effect of removing the uncertainty in the fixed effects parameters (scenario 4) appears to be slightly larger (by ~ 4%) at levels of high plot AGB (Fig. 3.5).

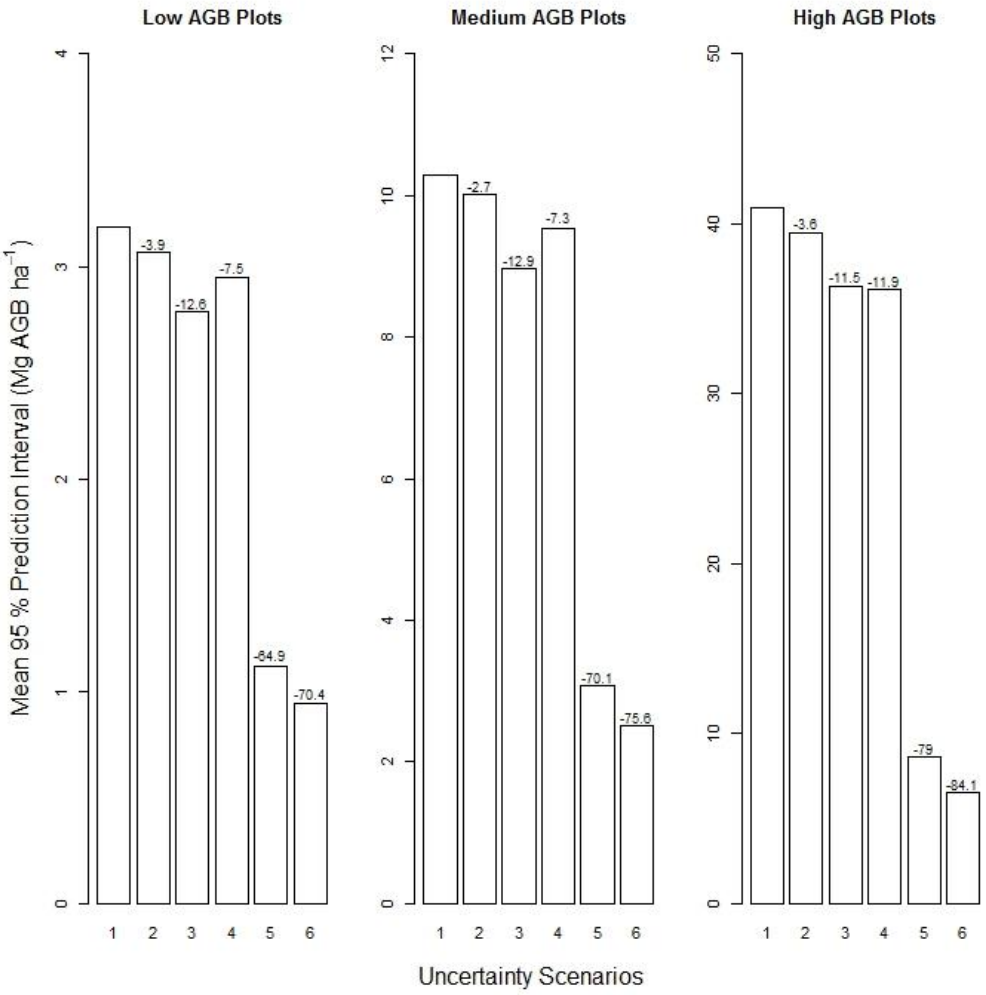

Fig. 3.5**:** Effect of removing components of uncertainty on the magnitude of the mean 95% prediction interval (95% PI) obtained using the ME model for plots of low, medium and high estimated AGB. Numbers above bars represent the percentage decrease in the mean 95% PI under each uncertainty scenario compared to scenario 1. Please note that % changes in the mean PIs between uncertainty scenarios 2 to 6 are not additive.

The pattern of relative importance of removing each uncertainty component is consistent across all levels of estimated tree AGB (Fig. 3.6). However, there is a pronounced difference in the proportional decrease in the PI under scenarios 5 and 6 for trees of low and medium AGB in comparison with high AGB trees. The

proportional impact of removing the random effects from the biomass estimation process is larger for high AGB trees (i.e. larger trees) in comparison with the low and medium AGB trees due to the multiplicative nature of the biomass equation where the random effects are added to the fixed effects and multiplied by the data (the diameter and height measurements of inventoried trees). The range of diameter and height measurements for trees within the high AGB sub-dataset is substantially larger than those within the low and medium AGB sub-datasets as indicated by the comparatively large range of estimated AGB for the high AGB sub-dataset (section 3.2.3.2). In the ME model the variance of the random effects for diameter and height is an order of magnitude greater (in log space) than that of the fixed effects and thus the proportional increase in the contribution of the random effects to the uncertainty of the biomass estimate is greater than that of the fixed effects in response to the increasing size of input data (i.e. with increasing tree size). This is consistent with the slight increase in the proportional impact on the PI of removing the random effects (scenarios 5 and 6) from low to high AGB plots as shown in Fig. 3.5, where the number of large trees present within the sub-datasets increases from low to high plot AGB. The impact (%) of removing the residual variance (scenario 3) during the biomass estimation process is comparatively larger for trees of low and medium estimated AGB (Fig. 3.6). This is a consequence of the reduced contribution of the random effects to the uncertainty of the biomass estimate of smaller trees (i.e. smaller input data).

The marked difference in the impact of removing the random effects for trees of low/medium AGB in comparison with those of high AGB is not apparent at the plot scale (Fig. 3.5). Given the influence of tree size on the contribution of the random effects to the uncertainty as seen in Fig. 3.6; the consistently larger contribution of the random effects at all AGB levels at the plot scale is illustrative of the dominant effect on the uncertainty of the presence of large trees within plots. The increase in the proportional effect of removing the uncertainty of the fixed effects parameters (scenario 4) for the high AGB plots (Fig. 3.5) is not seen within the high AGB trees (Fig. 3.6). Given the comparatively smaller variance of the fixed effects and the inclusion of the random effects under scenario 4; the small but appreciable increase

(~ 4%) in the effect of removing the fixed effects uncertainty within the high AGB plots in this study remains unresolved.

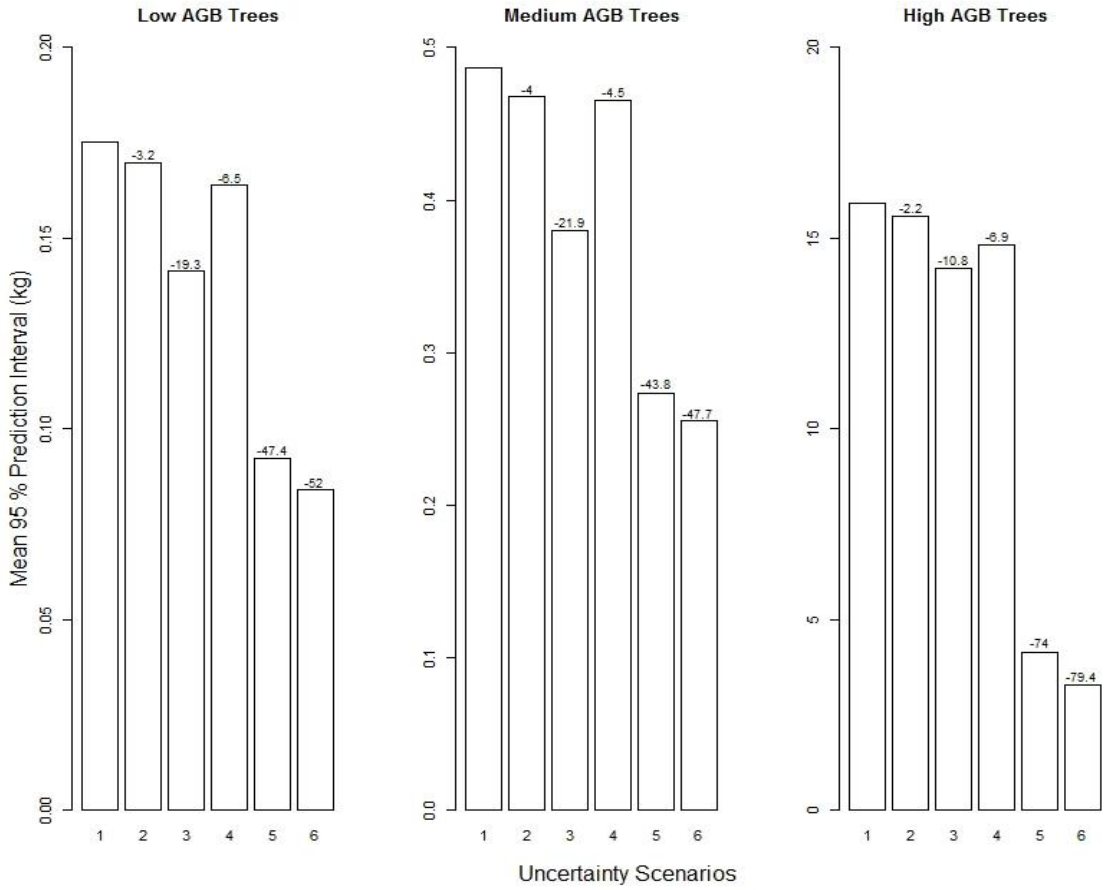

Fig. 3.6: Effect of removing components of uncertainty on the magnitude of the mean 95% prediction interval (95% PI) obtained using the ME model for trees of low, medium and high estimated AGB. Numbers above bars represent the percentage decrease in the mean 95% PI under each uncertainty scenario compared to scenario 1. Please note that % changes in the mean PIs between uncertainty scenarios 2 to 6 are not additive.

3.3.3.2 OLS model

The pattern of relative importance and the proportional change attributed to the removal of each uncertainty component in the OLS model (scenarios 2 to 4) mirrors the landscape scale results across all levels of estimated plot and tree AGB (see Appendix 2, Figs A2.2 and A2.3). As with the ME model there is a change in the magnitude of the uncertainty between AGB levels attributable to the use of a log-normal model and, as for the landscape scale, the overall magnitude of the PIs obtained using the OLS model was lower than that of the ME model. The variance

of the fixed effects parameters in the OLS model are an order of magnitude smaller than in the ME model and the residual variance is an order of magnitude larger, therefore any changes in the relative effect of excluding these uncertainty components due to tree size is obscured by the dominant impact of the large residual variance in the OLS model.

Comparison of the absolute magnitude of the predicted total uncertainty (scenario1) across the ME and OLS models (Figs. 3.5 and A2.2) indicates that the increase in uncertainty from low to high AGB plots is dependent on the regression model employed. For the ME model, the total uncertainty (scenario 1) increases from ~ 3 to > 40 Mg ha^{-1} from low to high AGB plots, however, for the OLS model, this increase is much smaller (from ~ 1.5 to ~ 10 Mg ha^{-1}). This difference is mirrored in the comparison between levels of estimated tree AGB (Figs. 3.6 and A2.3). This is again reflective of the impact of the inclusion of the random effects in the ME model whose effect on the uncertainty is magnified for trees of large size. Therefore, it appears that there is less difference in the magnitude of the total uncertainty (scenario 1) predicted by the OLS versus the ME model for trees of low and medium AGB however this difference increases for trees of high AGB and for all levels of plot AGB.

3.3.4 Conclusions

This study has clearly demonstrated the potential to produce unrealistically low estimates of uncertainty if group effects are ignored during regression analysis as is often the case when developing biomass models (Fig. 3.3). However, in assessing the relative impact of removing components of uncertainty during the biomass estimation process it should be noted that the findings of the current study are largely confined to the specific models (and the underlying datasets) used here. For the purposes of constraining the uncertainty on estimates of forest AGB at spatial scales relevant to environmental science, forest management and policy making (plot and above) the results presented in Figs 3.3 to 3.5 best represent the potential effect of excluding uncertainty components during the biomass estimation process.

The exclusion of measurement uncertainty had relatively little impact on the magnitude of the overall uncertainty regardless of spatial scale or tree size (as defined in this study). These results are consistent with the findings of previous studies and not only reflect the process of averaging over large sample sizes (of measured trees) but also the variance structure of biomass regression models where it can be expected that the uncertainty due to the use of the allometric model for making predictions of biomass for new individuals (i.e. predictive uncertainty) will dominate the total uncertainty. The random effects in the mixed-effects model used in this study represent the variability in the allometric relationship (of Kenyan mangroves) due to both species and site effects and their exclusion from the biomass estimation process consistently resulted in a large decrease in the predicted uncertainty. Future studies should investigate the use of additional covariates (e.g. wood density data) in a mixed-effects modelling framework to potentially account for some of the variance attributed to the random effects in the current model.

In this study, accounting for random effects was particularly important when producing estimates of uncertainty for the AGB of large trees and consequently the uncertainty of AGB estimates at larger spatial scales, as the presence of large trees within plots can have a considerable influence on the magnitude of the overall uncertainty. This is particularly relevant when producing realistic predictions of uncertainty for plots of a small size as the contribution to the overall uncertainty associated with estimates of individual tree AGB can be expected to reduce with increasing plot size.

Acknowledgements

This research was funded by the Natural Environment Research Council (NERC), UK. Data collection for the CAMARV and UNDP projects in Gazi Bay was funded by NERC and the UNDP-GEF Small Grants Programme respectively. Data collection in Mwache was supported by the WIOMSA-MASMA regional project on "Resilience of mangroves and dependent communities in the WIO region to climate change", Grant No: MASMA/CC/2010/08. Data collection in Mtwapa Creek was supported by the Flemish Interuniversity Council – University Development

Cooperation VLIR-UOS. We wish to thank all those who provided data for this study particularly our collaborating partner KMFRI. We would also like to thank all those involved in the collection of inventory data for the current study, in particular Mr Bernard Kivyatu. Finally we wish to thank Dr. Luke Smallman (University of Edinburgh, UK) for help with programming in R and Dr. Giles T. Innocent (Biomathematics and Statistics Scotland (BioSS)) for providing statistical advice.

4. Evaluating the use of ALOS PALSAR for estimating mangrove above-ground biomass in Kenya

R. Cohen[a], K. M. Viergever[b], I. H. Woodhouse[a], M. Mencuccini[a], E. T. A. Mitchard[a]

[a] *School of GeoSciences, University of Edinburgh, Edinburgh, EH9 3JN, UK*
[b] *Ecometrica, Unit3B, Kittle Yards, Edinburgh, EH9 1PJ, UK*

Author Contributions:

All ground data used in this study were provided by R. Cohen. All processing of radar data, statistical analysis and the writing of this manuscript were carried out by R. Cohen. Processing of SPOT imagery was carried out by K. M. Viergever, consequently K. M. Viergever contributed the first paragraph of text in section 4.3.3 describing this work. Comments on the manuscript were provided by I. H. Woodhouse and M. Mencuccini. Advice on data analysis and comments on the manuscript were provided by E. T. A. Mitchard.

Abstract

Large-scale estimation of forest above-ground biomass (AGB) stocks and stock changes are required for the effective implementation of forest-based climate change mitigation strategies such as Reducing Emissions from Deforestation and Forest Degradation (REDD+). The use of remote sensing data (particularly those acquired via space-borne sensors) allows for fast and repeatable large-scale monitoring of forest biomass dynamics. This study uses data acquired by JAXA's (Japan Aerospace Exploration Agency) Advanced Land Observing Satellite Phased Array L-band Synthetic Aperture Radar (ALOS PALSAR) for the purpose of estimating mangrove AGB along the entire Kenyan coastline. A reasonably strong relationship ($R^2 = 0.45$) was found between the ground-based estimates of AGB and radar backscatter in HH polarisation (σ^0_{HH}) with σ^0_{HH} found to decrease as a function of increasing AGB. No significant relationship was found between AGB and backscatter in HV polarisation. The negative relationship between σ^0_{HH} and AGB can be attributed to enhanced backscatter at low AGB levels due to strong double-bounce and direct surface scattering from short stature/open forests and attenuation of the radar signal by the forest canopy and complex root structures at high AGB levels. The relationship between σ^0_{HH} and AGB was used to estimate mangrove AGB along the entire Kenyan coastline. The relatively high uncertainty in radar-derived predictions of AGB at the 1ha pixel scale was constrained to between ~18 to 20% of the mean AGB estimate at the regional and national scale and is inclusive of the uncertainty associated with the ground-based approach to AGB estimation and the random errors associated with the up-scaling of SAR-derived predictions to larger spatial scales.

4.1 Introduction

Mangrove forests are globally important carbon stores (Donato et al., 2011). High rates of mangrove areal loss have been reported at the global (FAO, 2007; Giri et al., 2011; Valiela et al., 2001) and national level (Giri and Muhlhausen, 2008; Kirui et al., 2012; Leimgruber et al., 2005; Rodriguez and Feller, 2004) and are largely due to over-exploitation of wood products and conversion of mangroves for aquaculture and coastal development (Alongi, 2002). There is now international support for the maintenance and enhancement of forest carbon storage in the tropics through economic incentive schemes such as Reducing Emissions from Deforestation and Forest Degradation (REDD+). Estimation of baseline forest above-ground biomass (AGB) stocks and stock changes at large spatial scales (i.e. national level) will be required for the effective implementation of REDD+. The use of remote sensing data (particularly that acquired via space-borne sensors) allows for fast and repeatable large-scale monitoring of forest biomass dynamics.

The use of optical remote sensing data for biomass studies in the tropics is often hampered by the presence of cloud cover, and relationships derived between optically sensed spectral metrics (e.g. NDVI) and AGB are of limited use (Patenaude et al., 2005). In contrast, the acquisition of Synthetic Aperture Radar (SAR) data is not dependent on prevailing weather or light conditions and radar systems operating at longer wavelengths (e.g. L-band at ~ 23 cm) interact with the branches and stems below the canopy layer that hold the greatest proportion of AGB (Lucas et al., 2007).

SAR response from forests as measured by the amount of the transmitted microwave energy that is returned to the sensor (backscatter) is influenced by a number of factors such as: the configuration of the SAR system in use (wavelength, polarisation and incidence angle); forest structural parameters (size, density and geometry of vegetation); the physical characteristics of the underlying surface (topography and roughness) and the moisture content of the vegetation and soil (Quiñones and Hoekman, 2004). These factors determine the amount of incident microwave energy scattered (and the amount attenuated) by the underlying land cover and how that energy will be scattered.

Relationships have been derived between AGB and backscatter using SAR systems for a variety of different forest types including boreal forest in Alaska (Rignot et al., 1994); savanna and miombo woodland in Africa (Mitchard et al., 2009); tropical forest in Costa Rica (Saatchi et al., 2011a) and mangroves in French Guiana (Mougin et al., 1999). Previous studies have found that the use of L-band SAR in HV polarisation provided the strongest relationship with AGB with R^2 values ranging from 0.49 for forests in Bangladesh (Rahman and Sumantyo, 2013) to 0.92 in Australian savannas (Collins et al., 2009). The stronger relationship between aboveground biomass and L-band HV can be attributed in part, to the strong depolarisation of the incoming signal by larger vegetation components as biomass increases and volume scattering becomes dominant (Mougin et al., 1999). In addition, the HV polarisation is less sensitive to moisture conditions (soil and vegetation) and topographic changes than L-band HH (Quiñones and Hoekman, 2004; van Zyl, 1993).

Backscatter tends to increase with increasing AGB until a saturation point is reached and sensitivity to further increase in AGB is lost (Lucas et al., 2007). Saturation at higher biomass levels can be attributed to increased attenuation of the incident SAR signal within the canopy layer (Lucas et al., 2007; Mitchard et al., 2009). At L-band HV variable saturation points have been reported ranging from ~ 60 to ~ 200 Mg ha^{-1} (Luckman et al., 1997; Mitchard et al., 2009) indicating a potential limitation for the retrieval of high AGB and highlighting the lack of a consistent backscatter-AGB relationship (Woodhouse et al., 2012).

Previous studies focusing on backscatter-AGB relationships in mangroves have been limited in number (Carreiras et al., 2012; Li et al., 2007; Lucas et al., 2007; Mougin et al., 1999) with just one study undertaken in African mangroves (Carreiras et al., 2012). The backscatter-AGB relationship in mangroves can often be complicated by the presence of complex root systems and variable tidal regimes which can lead to unexpectedly low or high backscatter (Lucas et al., 2007). However, good relationships have previously been found between air-borne L-band HV and AGB for mangroves in French Guiana and Australia (Lucas et al., 2007; Mougin et al., 1999) with saturation occurring at ~140 Mg ha^{-1} and ~125 Mg ha^{-1} respectively.

To the best of our knowledge this is the first study to investigate the nature of the relationship between L-band SAR and mangrove AGB in East Africa. For this purpose the current study uses data acquired by JAXA's ALOS PALSAR sensor.

4.2 Methods

4.2.1 Field data

Forest inventory data from 25 plots were collected during June-August 2011 from four mangrove study regions located along the Kenyan coastline (Fig. 4.1 and Table 4.1). The Gazi Bay region (4°25'S, 39°30'E) is located ~55 km south of the city of Mombasa. The Mida Creek area (3°20'S, 40°00'E) is situated mid-way along the Kenyan coastline ~23 km south of the town of Malindi. The Lamu archipelago extends between 2°22'S, 40°48'E in the South and 1°44'S, 41°30'E in the North. For the purposes of this study the Lamu archipelago has been sub-divided into two study regions: South Lamu (area enclosed in braces in Fig. 4.1) and Kiunga National Marine Reserve (NMR) which encompasses the mangroves between South Lamu and the Kenya-Somalia border. Further details of all study regions can be found in Cohen et al., (2013).

A stratified random plot sampling scheme was used in order to capture the variation in mangrove structure within each of the study regions. For each region, plots were positioned within larger areas of mangrove deemed to 1) be homogeneous in terms of structure and 2) broadly represent the main levels of structural variation within the region as a whole. Such areas were pre-identified using an unsupervised classification of the radar data from 2010 (using HH, HV and HV/HH backscatter in the power domain at a pixel resolution of 100m) and visual comparison with corresponding 2.5m resolution SPOT imagery acquired during 2009-2011 covering each region. Figure 4.2 illustrates some of the main structural variations of mangrove forest identified in this study.

Within each plot, the stem diameter and height of all trees ≥ 5cm diameter at breast height (DBH) were measured. An exception was plots 10 and 19 (Table 4.1) which were both dominated by small stature trees hence all stems ≥ 2.5 cm were measured. Within some of the plots a 5 x 5m subplot was positioned at random and all stems <

5 cm DBH were counted giving an indication of the density of mangrove seedlings and saplings in the understorey. Stem diameter was measured at 1.3m above-ground (DBH) except in the case of *Rhizophora* sp. where stem diameter was measured at 30cm above the highest prop root if this occurred above 1.3m. In cases where trees branched below 1.3m (common in *Avicennia* sp.) and branches met the diameter measurement threshold; the diameter and height of each branch was recorded and treated separately during analysis. Tree height was measured using an ultrasonic vertex hypsometer (Haglöf, Sweden).

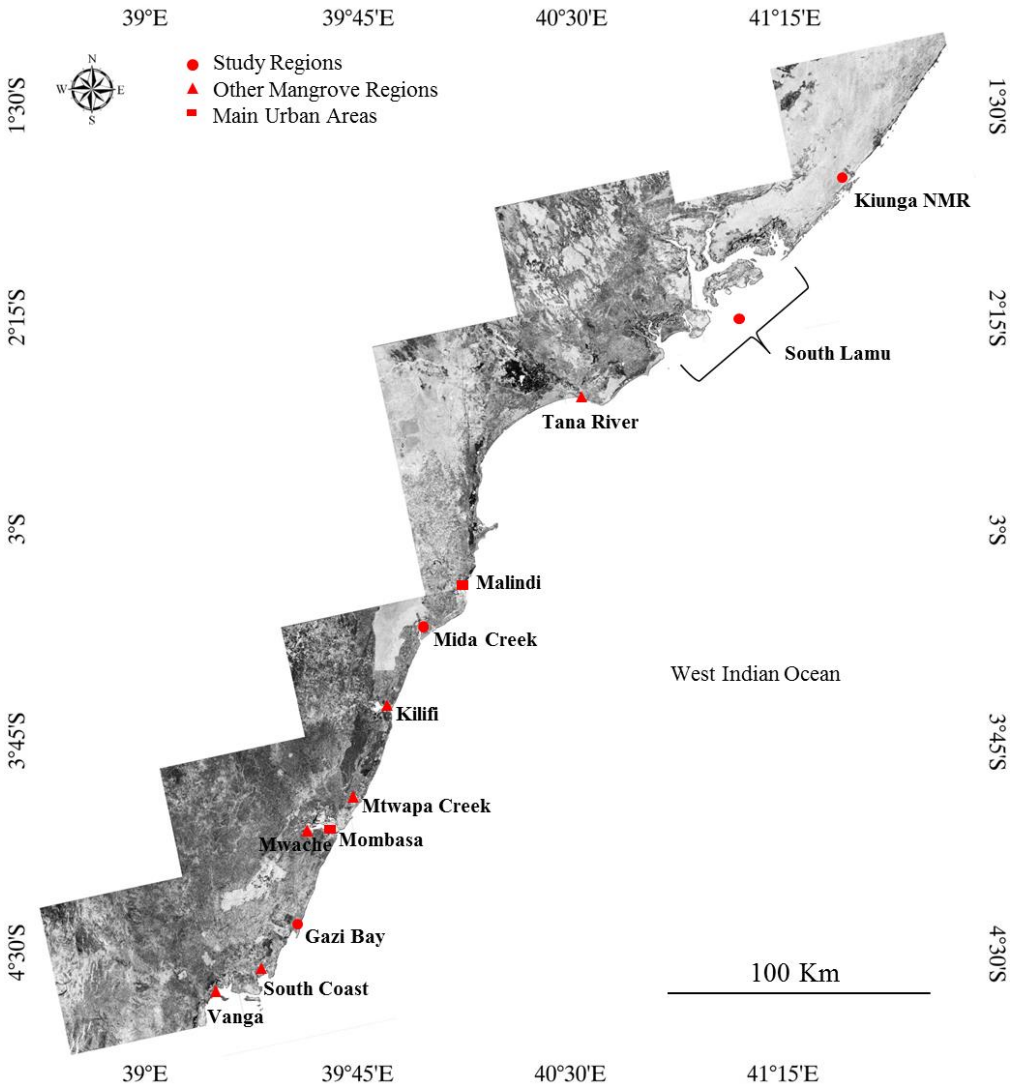

Fig. 4.1. ALOS PALSAR scenes displayed in HH polarisation showing the location of the mangrove study regions where forest inventory data were collected for this study (dots), other mangrove regions (triangles) and urban areas (squares) along the Kenyan coastline. Full definitions and descriptions of all mangrove regions are provided in Cohen et al., (2013).

4.2.2 Ground-based AGB estimates

Estimates of total AGB in Mg ha^{-1} were obtained for each field plot as detailed in Cohen et al., (2013). The allometric equations for Kenyan mangroves developed by Cohen et al., (2013) used stem diameter and height as the predictive variables in a linear mixed-effects modelling framework. The statistical simulation procedure employed by Cohen et al., (2013) for propagating uncertainty means that the estimates of plot AGB used here account for measurement and predictive uncertainty during the biomass estimation process.

4.2.3 SAR data

SAR data from the ALOS PALSAR sensor acquired over the Kenyan coastline during May-July 2010 were obtained through the European Space Agency (ESA) Category-1 scheme (Project ID: 8177). L-band SAR scenes were acquired in Fine-Beam Dual-polarisation (FBD) mode with an off-nadir incidence angle of 34.3°. SAR scenes were provided at processing level 1.5 with a pixel size of 12.5m (4 looks per pixel). All scenes were processed using the Alaska Satellite Facility's MapReady software (version 2.3.17) to correct geolocation and apply a geometric and radiometric terrain correction using the 90m resolution Digital Elevation Model (DEM) from the Shuttle Radar Topography Mission (SRTM). Geolocation accuracy was verified using the SPOT imagery and several ground control points (RMSE = ~16m (1.3 ALOS pixels)).

Digital numbers were converted to radiometrically calibrated values of sigma-nought (σ^0) using the coefficients and equations provided in Shimada et al., (2009). All further remote sensing analyses were carried out using ENVI version 4.8 (Exelis Visual Information Solutions, Boulder, Colorado). The mean HH and HV backscatter values (calculated in the power domain) were extracted for each of the 25 field plots and converted to σ^0 in dB prior to undertaking regression analyses using R statistical software version 2.15.0 (R Development Core Team, 2012).

Table 4.1: Structural characteristics of the inventoried plots within each mangrove study region.[a]

Plot ID	Study Region	Plot Size (ha)	Dominant Species	Mean Stem Diameter (cm)	Mean Height (m)	Stem Density ha^{-1} (trees ≥ 5cm DBH)	Stem Density ha^{-1} (trees < 5 cm DBH)	AGB (Mg ha^{-1})	Distance From Sea (m)
1	Gazi Bay	0.25 (50 x 50m)	AM	6.9	4.8	2140		33.2	464
2		0.25	RM	10.1	6.4	1936		132.8	226
3		0.25	RM, BG, CT	12.7	7.7	1056		128.4	738
4		0.25	RM	12.2	7.3	1116		105.4	750
5	Mida Creek	0.5 (100 x 50m)	AM	24	10.7	396		152.8	1828
6		0.25	CT	8.2	4.4	384	397 600	12.7	1008
7		0.25	CT	12.6	8.2	692	130 000	75.5	63
8		0.25	RM, CT	13.2	8	660		73	305
9		0.25	RM	13.6	6.9	632	32 800	59.1	74
10	South Lamu	0.25	CT	4.1	2.3	2084[b]		9.5	156
11		0.25	RM	11.7	8.5	1604		120.6	127
12		0.25	RM	13.2	9.3	1428		160.1	152
13		0.25	RM	7.8	6.6	2096		62.1	136
14		0.25	RM	22.5	15.5	572		223.1	104
15		0.25	CT	6.9	3.7	992	44 800	16.3	73
16		0.25	RM	17.1	10.7	1104		198.2	79
17		0.5	AM	6.3	3.2	694	7200	7.6	209
18	Kiunga NMR	0.25	RM	11.4	7.9	1920		138.4	72
19		0.25	AM	5	3.3	1672[b]		13.2	492
20		0.25	RM	32	20.7	320		254	166
21		0.25	RM	12.8	9	1656		144.4	68
22		0.25	RM	20.2	12.7	532		150.2	77
23		0.25	RM, CT	13.3	8.4	1192	7600	111.1	376
24		0.25	CT	7.5	4.1	1408	17 200	27.1	519
25		0.25	CT	8.4	4.3	1360		33.8	214

[a] Mangrove species codes are: AM = *Avicennia marina*; RM = *Rhizophora mucronata*; BG = *Bruguiera gymnorrhiza*; CT = *Ceriops tagal*. [b] For these plots the calculated stem density is for trees ≥ 2.5 cm DBH.

Fig. 4.2. Examples of the structural variation of inventoried plots; a) tall stature *R. mucronata* forest (Kiunga NMR 21st July 2011); b) dense short stature *C. tagal* forest (Mida Creek 8th July 2011); c) short stature *A. marina* forest (South Lamu 10th August 2011); d) tall stature *A. marina* forest (Mida Creek 7th July 2011). Plot numbers correspond with those in Table 4.1. All photos taken by R. Cohen.

4.3 Results

4.3.1 Backscatter-AGB regressions

Plot level values of mean σ^0 (dB) were regressed against the corresponding ground-based estimates of plot AGB (Mg ha^{-1}) using ordinary least squares regression. Fitted regression models were of the form:

$$\sigma^0 = a + b(\text{AGB}) + \varepsilon \quad (4.1)$$

where the response variable is σ^0 (dB) in either HH or HV polarisation, a is the regression constant, b is the coefficient of the explanatory variable AGB and ε is the error term. Models were also fitted using the ratio of HH/HV backscatter and the

Radar Forest Degradation Index (RFDI) as the response variables (see Mitchard et al., (2012)). The RFDI was calculated as in Eq. (4.2) and both ratio response variables were calculated in the power domain.

$$\text{RFDI} = \frac{\text{HH}-\text{HV}}{\text{HH}+\text{HV}} \quad (4.2)$$

A polynomial relationship between AGB and backscatter was also investigated; however the second degree polynomial term for AGB was not significant in any of the models in Table 4.2. Transformation of the explanatory variable (AGB) by natural log did not result in an improvement to the R^2 value for any of the models in Table 4.2; therefore all subsequent analyses were performed using the un-transformed data.

Table 4.2: Fitted parameters (± std. error) for each backscatter-AGB model with associated regression statistics.

Response Variable	*a*	*b*(AGB)	R^2	*P* value
HH	-8.034 ± 0.469	-0.017 ± 0.004	0.45	0.000
HV	-16.344 ± 0.420	-0.002 ± 0.004	0.01	0.616
HH/HV	6.804 ± 0.638	-0.016 ± 0.005	0.29	0.005
RFDI	0.744 ± 0.030	-0.001 ± 0.000	0.43	0.000

No significant relationship was found between AGB and HV backscatter (Table 4.2 and Fig. 4.3b.). The dynamic range of the HV response to changes in AGB was extremely small with a difference of just ~1 dB between the lowest and highest plot AGB estimates (Fig. 4.3b). The strongest relationship was found between AGB and σ^0_{HH} ($R^2 = 0.45$) with HH backscatter decreasing as a function of increasing AGB (Fig. 4.3a). In contrast to the HV response, HH backscatter differed by > 4 dB between the lowest and highest plot AGB values (Fig. 4.3a.). There was considerable variability in HH backscatter (~ 6 dB) at the lower range of AGB (8 – 100 Mg ha^{-1}), however this was in part due to the two data-points displaying relatively low HH backscatter (~ 12 dB) at AGB of < 100 Mg ha^{-1} (Fig. 4.3a). The model using the RFDI as the response variable had a similar R^2 to that of the model using σ^0_{HH} (Table 4.2); however this was due to the decline in HH backscatter with increasing AGB and the relatively invariant response of the HV backscatter. As the relationship between the ratio response variables (HH/HV and RFDI) and AGB was

entirely driven by the HH response further analyses used the HH-AGB relationship only.

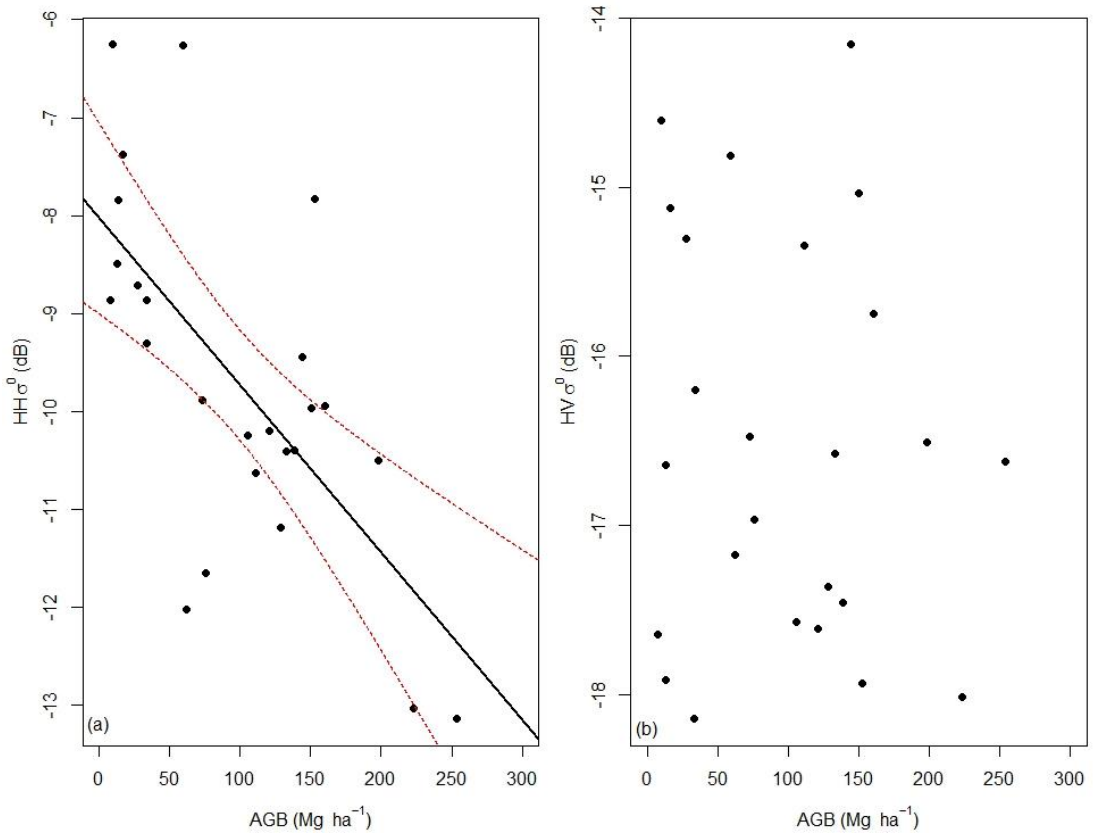

Fig. 4.3. Relationship between L-band HH and HV backscatter (σ^0 in dB) and ground-based estimates of plot AGB (Mg ha^{-1}). The solid black line in (a) represents the ordinary least squares regression line. The dashed red lines in (a) are the 95% confidence interval of the regression line.

The fitted relationship between σ^0_{HH} and AGB was re-arranged to predict AGB from σ^0_{HH} as:

$$AGB = (\sigma^0_{HH} + 8.034) / -0.017 \quad (4.3)$$

The uncertainty on predictions of AGB using Eq. (4.3) had a root mean square error (RMSE) of 76.6 Mg ha^{-1}. Fitted AGB was negative for the five plots with values of σ^0_{HH} greater than the fitted intercept (Fig. 4.3a.). Replacement of these negative values with zero reduced the RMSE by ~18% to 64.4 Mg ha^{-1}. Relatively high RMSE values are not un-expected given that eight of the 25 data-points used to fit the regression fell markedly far from the line of best fit and are not encompassed by the 95% confidence interval of the regression line (Fig. 4.3a.).

4.3.2 Application of regression equation to SAR data

Prior to the application of Eq. (4.3) for the purpose of predicting mangrove AGB along the entire Kenyan coastline; SAR scenes (HH polarisation) were re-sized to 100m resolution in order to reduce speckle in the SAR data. Application of Eq. (4.3) was constrained to σ^0_{HH} values within the limits of the empirical relationship between AGB and HH backscatter. Therefore values of σ^0_{HH} exceeding -8.034 dB (the intercept) were constrained to be -8.034 and values of σ^0_{HH} below -13.14 dB (the lowest HH response from the field plots) to be -13.14 during analysis. The resulting AGB map had values of predicted AGB between 0 and 297 Mg ha^{-1}.

4.3.3 Exclusion of non-mangrove areas

Areas of mangrove forest along the Kenyan coastline were delineated using nine high resolution (2.5m) SPOT-5 images acquired during 2010-2011. Medium resolution (30m) Landsat data acquired during the same time period were used to fill two small gaps in the SPOT data coverage. All optical data were almost entirely cloud free. Object-oriented image analysis techniques (eCognition Developer 64 software, Trimble) were applied to obtain a map showing mangrove extent. This map included different mangrove species and areas of varying densities, but excluded areas of sand and mud banks. In the absence of sufficient field observations along the entire coastline, the classification accuracy was assessed by means of visual inspection. Apart from small patches obscured by cloud and therefore excluded from the mangrove extent map; a few minor classification errors were detected. These included both errors of omission and commission but were estimated to affect < 2% of the total mangrove area along the Kenyan coastline.

The resulting mangrove extent raster file was used to exclude all non-mangrove areas from SAR scenes. The SAR-derived AGB map was transformed into an equal area sinusoidal projection prior to extracting estimates of mean (Mg ha^{-1}) and total (Mt) mangrove AGB for each region and for Kenya as a whole (Table 4.3). Figures 4.5 to 4.7 display maps of AGB for mangroves in the Gazi Bay, Mida Creek, Kiunga NMR and South Lamu regions at a spatial scale of 1ha.

4.3.4 Uncertainty at the regional and national level

The uncertainty on predictions of AGB using Eq. (4.3) is given by the RMSE of the regression (64.4 Mg ha^{-1}) and is applicable at a spatial scale of ~ 0.27 ha (the mean size of the field plots). The uncertainty of the SAR-derived AGB predictions at a spatial scale of 1ha (ε_{pixel}) was estimated using the methodology outlined in Saatchi et al., (2011b) and calculated as:

$$\varepsilon_{\text{pixel}} = \frac{\text{RMSE}_{\text{REG}}}{\sqrt{N}} \quad (4.4)$$

where *N* in this study is the total number of 0.27ha plots contained within a 1 ha pixel (i.e. 1/0.27 = 3.7 plots per 1 ha pixel) and RMSE_{REG} is the RMSE of the regression. Using Eq. (4.4) the mean uncertainty of the SAR-derived AGB prediction for an average 1ha pixel (ε_{pixel}) was 33.5 Mg ha^{-1}.

The total uncertainty in the SAR-derived AGB predictions at the regional and national level (Table 4.3) is comprised of 1) the uncertainty of the ground-based estimates of AGB for the field plots (ε_1) and 2) the uncertainty in the backscatter-AGB relationship (ε_2). The uncertainty in the estimated AGB for each plot as given in Cohen et al., (2013) (which is inclusive of measurement and allometric uncertainty) was used to provide an approximate 95% confidence interval for each of the field plots. The mean 95% confidence interval across all field plots (~ 18% of the estimated AGB) was taken to represent the proportional contribution of ε_1 to the total uncertainty. As many elements contained within the ground-based AGB estimates are potential biases ε_1 was conservatively assumed to be independent of spatial scale. To estimate ε_2 (which is the random error in prediction and was assumed to reduce with increasing spatial scale) Eq. (4.4) was applied where RMSE_{REG} is now the RMSE for an average 1ha pixel as calculated above and *N* is the total number of 1ha pixels (i.e. the total mangrove cover (ha) shown in Table 4.3) at the regional or national level.

The estimated regional and national values of ε_2 (Mg ha^{-1}) were then calculated as a percentage of the corresponding SAR-derived estimates of mean AGB (Mg ha^{-1}) (Table 4.3). Estimated values of ε_2 decrease as *N* increases and therefore the

proportional contribution of ε_2 to the total uncertainty is very small at the regional and national scale, ranging between 0.2 and 1.7% for South Lamu and Kilifi region respectively with a value of 0.1% at the national level. Finally ε_1 and ε_2 were summed to provide an estimate of the total uncertainty (%) of the SAR-derived predictions of mean and total AGB at the regional and national level (Table 4.3). It should be noted that this approach to uncertainty propagation assumes that the various sources of random and systematic errors are uncorrelated.

Table 4.3: SAR-derived estimates of mean AGB (Mg ha^{-1}) and total AGB (Mt ± % uncertainty) for each mangrove region and Kenya as a whole.[a]

Region	Total Cover (ha)	Mean AGB (Mg ha^{-1})	Total AGB (Mt ± % uncertainty)
Gazi Bay	588.3	145.2	0.09 ± 19.4
Mida Creek	1657.7	127.4	0.21 ± 19.1
Mtwapa Creek	512.9	111.3	0.06 ± 19.8
Mwache	2652.5	142.7	0.38 ± 18.9
Vanga	3441.7	132	0.45 ± 18.9
South Coast	2256.1	125.7	0.28 ± 19
South Lamu	26277	104.2	2.74 ± 18.6
Kiunga NMR	4772.9	124.2	0.59 ± 18.8
Kilifi	670.5	74.5	0.05 ± 20.2
Tana River	3362	134.1	0.45 ± 18.9
Kenya	**46,261.4**	**114.9**	**5.32 ± 18.6**

[a] 1 Megatonne (Mt) = 1 million tonnes. Estimates of total mangrove cover (ha) were obtained using the SPOT imagery detailed in section 4.3.3.

The estimates of AGB shown in Table 4.3 were derived using a subset of the data from Cohen et al., (2013) therefore it is not possible to make an independent comparison between the SAR-derived regional and national estimates of AGB presented here with those given in Cohen et al., (2013), derived using a ground-based up-scaling approach. Bearing this caveat in mind, a tentative comparison between the two approaches indicates that at the national level there is some degree of overlap between the uncertainty limits of the ground-based estimate (5.4 and 7.2 Mt) and the upper limit of the SAR estimate (6.3 Mt). At the regional level (see Fig. 4.4) the estimates of mean AGB vary considerably between the two approaches: the SAR-derived estimate of mean AGB is higher than the ground-based estimate for all regions except South Lamu and Kiunga, for which it is lower. For most regions, there is some overlap in the lower and upper uncertainty bounds of the ground-based

and SAR-derived estimates and in the case of South Coast and Vanga there appears to be a particularly close correspondence in the estimates derived using the two approaches. There is however, a marked difference between the ground-based and SAR-derived AGB estimates for the regions Mida Creek and Kiunga which show no overlap in the estimated uncertainty bounds.

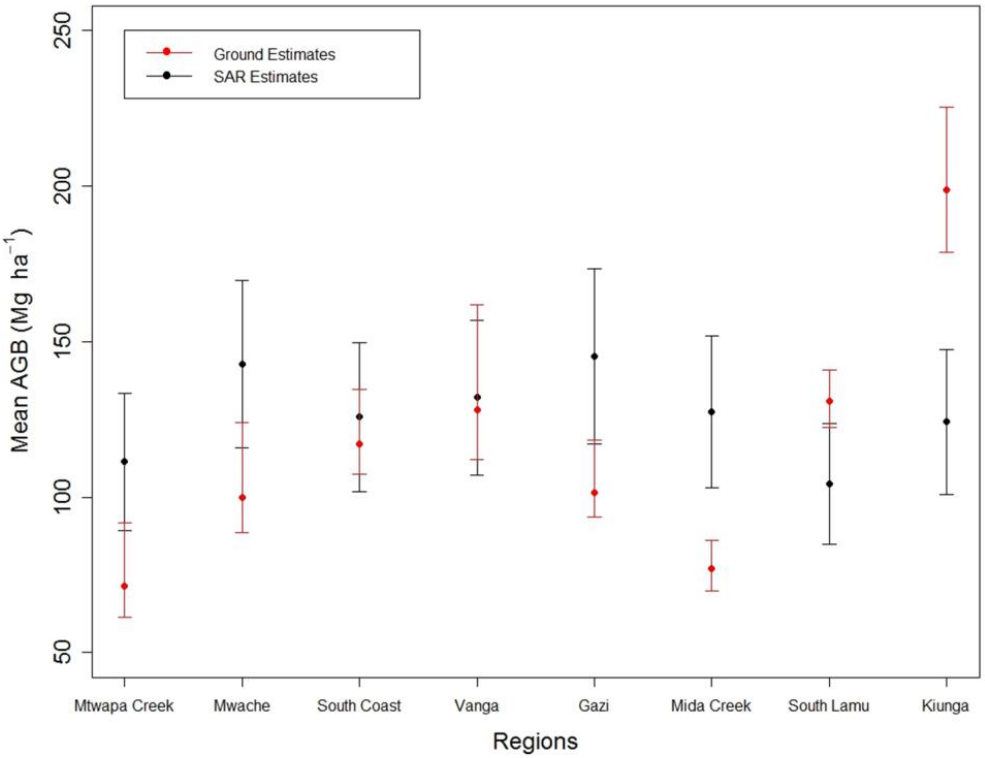

Fig. 4.4: Ground-based vs. SAR-derived estimates of mean AGB (Mg ha^{-1} ± uncertainty) for each mangrove region. The ground-based estimates (± 95% prediction interval) were obtained as described in chapter 2, section 2.2.3.5 and are as shown in Fig. 2.8. Uncertainty around the SAR-derived estimates is the proportional uncertainty as calculated in section 4.3.4 and given in Table 4.3 above.

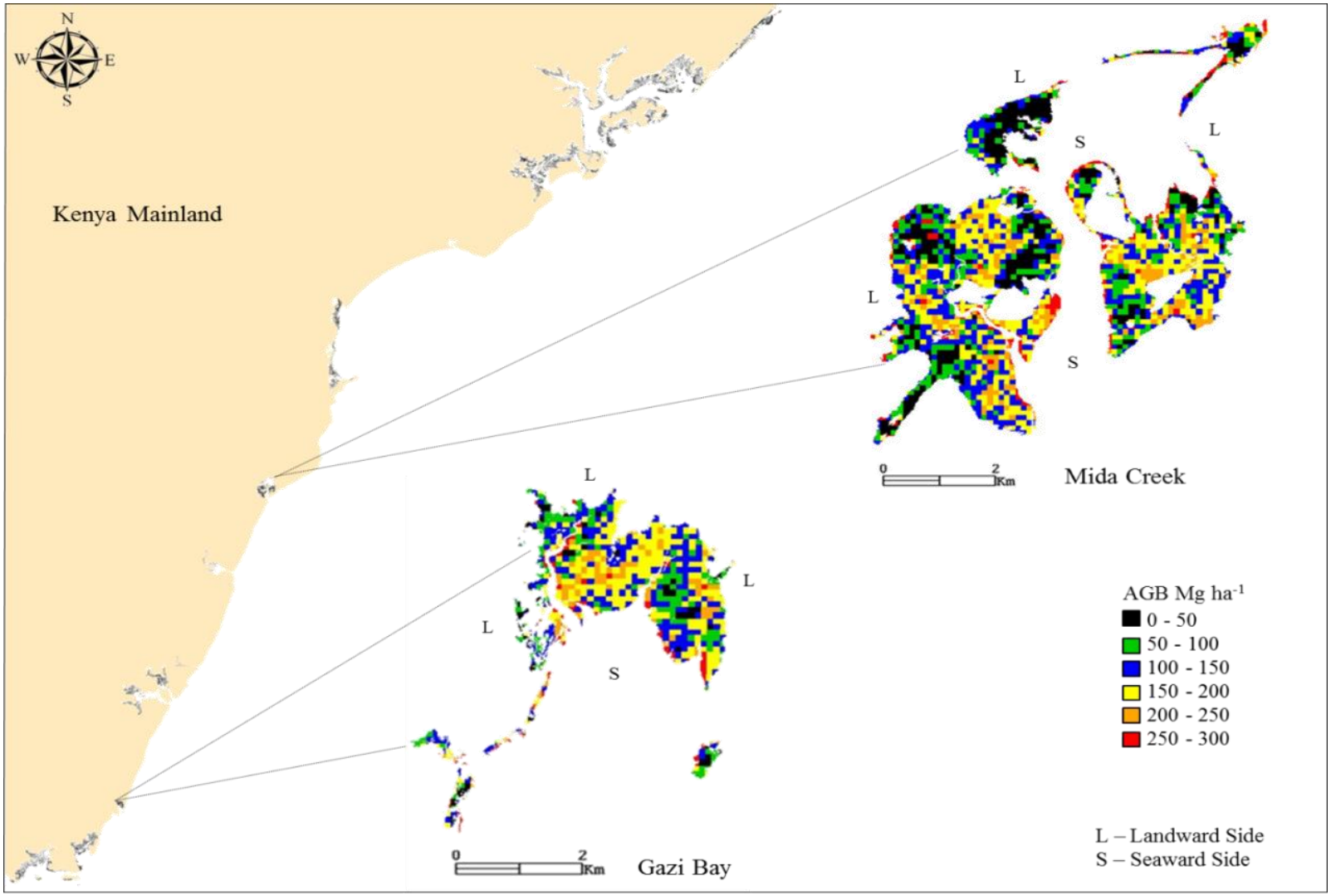

Fig. 4.5. SAR-derived mangrove AGB map for the Gazi Bay and Mida Creek regions. Pixel size = 100m.

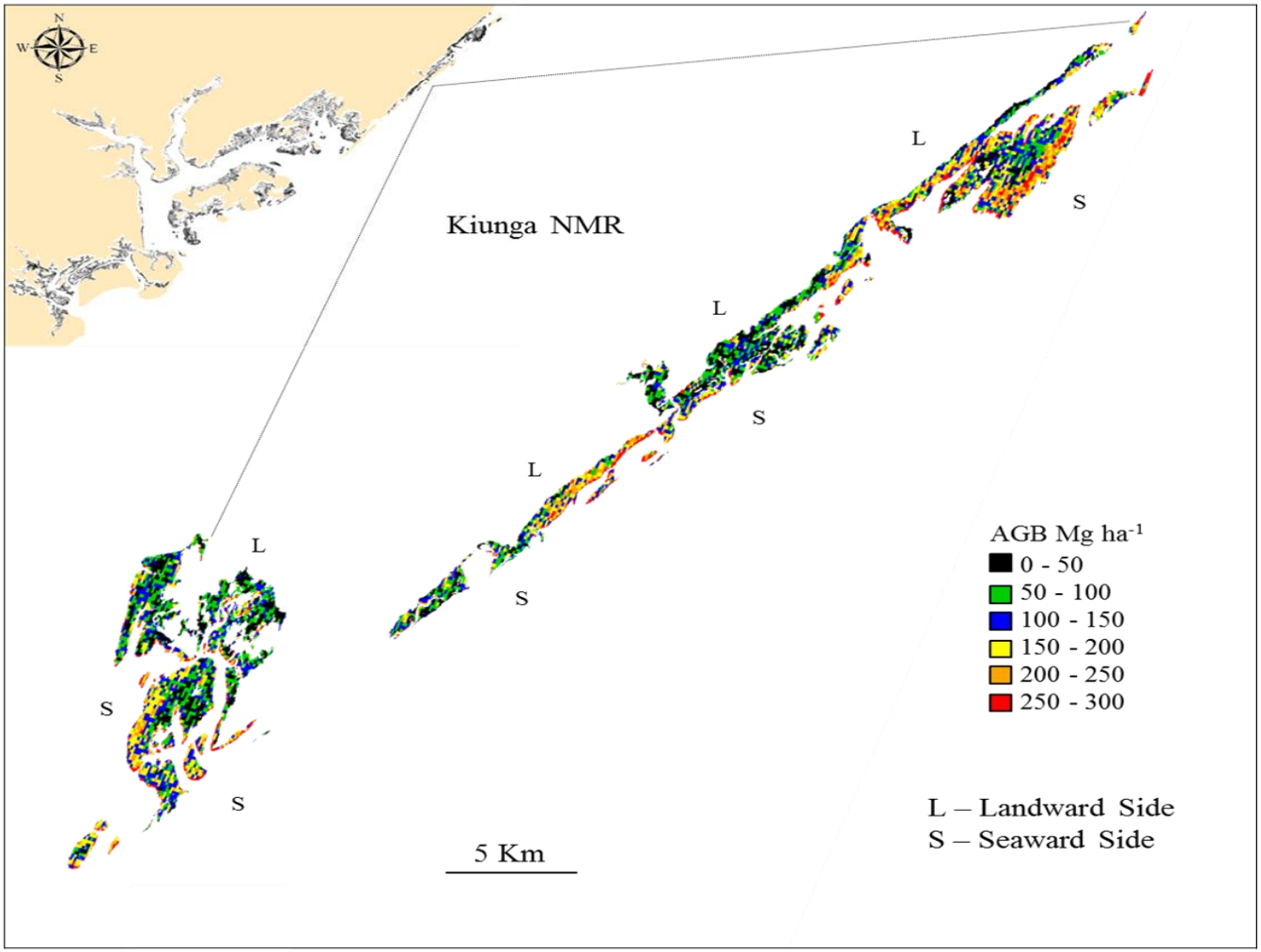

Fig. 4.6. SAR-derived mangrove AGB map for Kiunga National Marine Reserve (NMR). Pixel size = 100m.

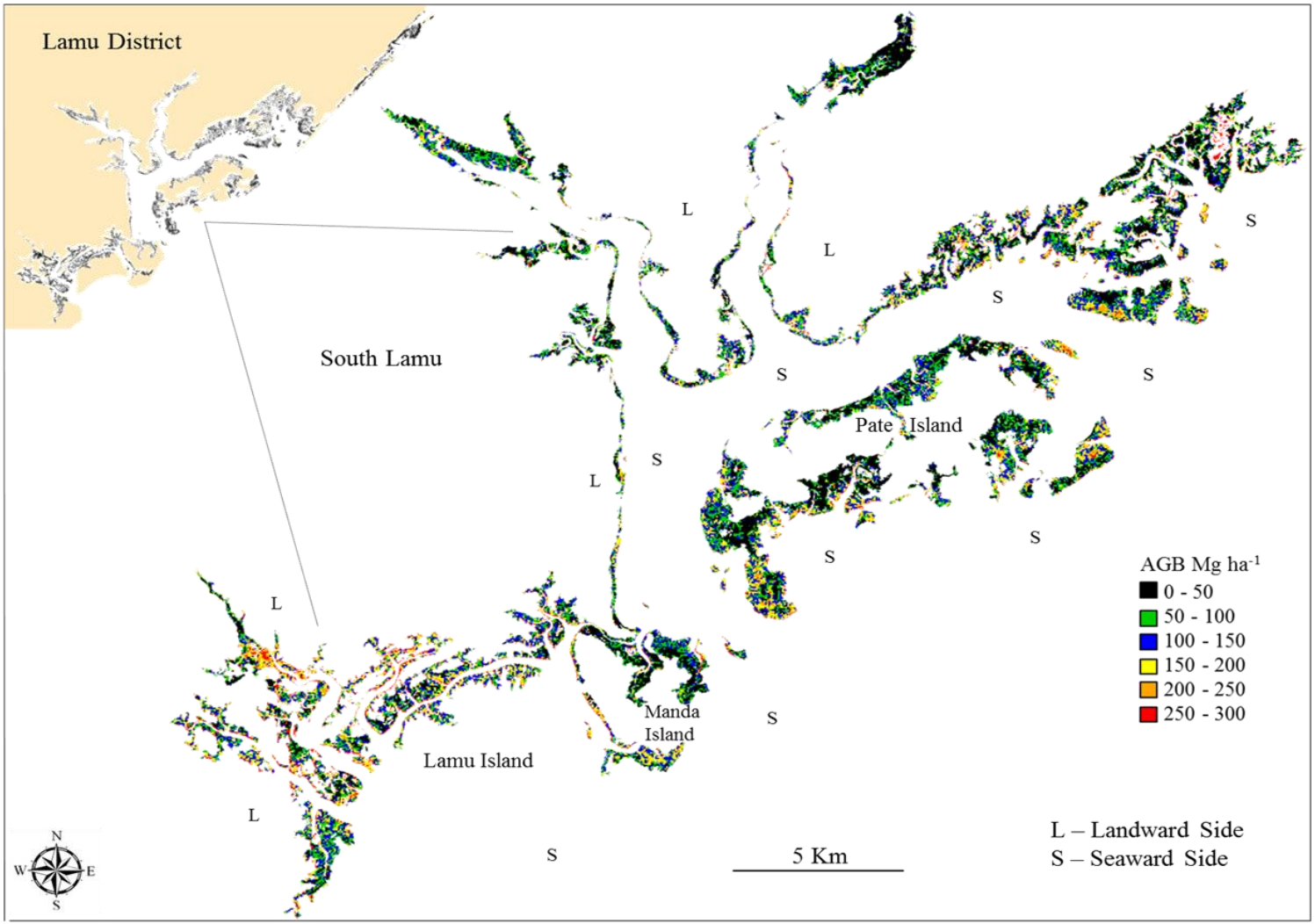

Fig. 4.7. SAR-derived mangrove AGB map for the South Lamu region. Pixel size = 100m.

4.4 Discussion

4.4.1 Backscatter-mangrove AGB relationship

The current study provides an evaluation of the relationship between L-band SAR (ALOS PALSAR) and AGB in Kenyan mangrove forests. Despite the limited number of ground data points (n = 25 plots) there was an observable relationship (R^2 = 0.45) between L-band HH and AGB with σ^0_{HH} found to decrease as a function of increasing AGB. This allowed for the estimation of mangrove AGB along the entire Kenyan coastline (e.g. Figs. 4.5 to 4.7).

The nature of the backscatter-AGB relationship in this study is somewhat unexpected given that most previous studies using L-band SAR for AGB retrieval found a positive backscatter-AGB relationship (for HH and HV) and that L-band in HV polarisation provides the greatest sensitivity to changes in AGB (e.g. Mitchard et al., 2012; Mitchard et al., 2009; Morel et al., 2011; Mougin et al., 1999; Ryan et al., 2012).

A reduction in L-band HH backscatter within tall stature high biomass mangrove stands dominated by *Rhizophora* sp. in Australia has previously been observed by Lucas et al., (2007). However, neither Mougin et al., (1999) nor Carreiras et al., (2012) report a similar reduction in L-band backscatter at high AGB for mangroves in French Guiana and Guinea-Bissau respectively. This is illustrative of the general point that SAR systems do not respond directly to AGB and highlights the importance of considering the influence of forest structural variation when interpreting SAR backscatter from forests (Mitchard et al., 2009; Woodhouse et al., 2012).

In the current study there is a pattern of increasing mean tree height with AGB (Table 4.1) and a reduction in σ^0_{HH} with increasing height (and AGB). In addition, the plots with the highest estimated AGB were dominated by *R. mucronata* (e.g. see Table 4.1 plots 12, 14, 16 and 20) and as such were typified by highly complex prop root systems (e.g. Fig. 4.2a). Therefore, it seems reasonable to suggest that the decrease in σ^0_{HH} with increasing AGB observed in the current study is attributable to greater attenuation of the radar signal by a comparatively dense canopy layer and by

the complexity of the root structure beneath the canopy (Held et al., 2003; Lucas et al., 2007). Indeed, Lucas et al., (2009) used the observed decrease in L-band HH within *Rhizophora* dominated forest as a basis for classifying mangroves in Australia and Belize into high biomass forests (defined in their study as > 10m in height and AGB > ~ 100 – 120 Mg ha^{-1}) with prop roots from those without prop roots and found good correspondence with the results from previous mapping studies in the same regions.

Backscatter at L-band is generally expected to be comparatively lower at lower AGB levels as forest components of a smaller magnitude to that of the wavelength attenuate the signal (Lucas et al., 2007; Proisy et al., 2002). However, in this study σ^0_{HH} was found to be higher at lower AGB (< ~ 50 Mg ha^{-1}). A possible explanation for this may be that in small stature or more open forests (with typically lower AGB) microwaves at longer wavelengths (e.g. L-band) are more likely to interact directly with the underlying surface as there is less attenuation of the incident signal by the canopy (e.g. see Fig. 4.2c). In mangroves the ground surface (mud or sand) can be either inundated with water or can be expected to have high moisture content due to recent tidal inundation. In addition standing pools of water are a common feature in mangroves as is the presence of water in mangrove creeks even at low tide.

Direct scattering from wet and/ or rough ground surfaces and increased double-bounce interactions between the vegetation and ground can result in enhanced backscatter particularly at HH polarisation because such scattering mechanisms do not produce strong depolarisation of the incident signal (Lucas et al., 2010; Mougin et al., 1999; Wang and Imhoff, 1993). Indeed, Lucas et al., (2007) observed an increase in σ^0_{HH} within short stature *Ceriops* dominated mangrove in Australia which they attributed to greater double-bounce interactions. For mangroves in French Guiana, Mougin et al., (1999) found a high ratio of HH/HV backscatter at AGB levels < 140 Mg ha^{-1} suggesting that at low to moderate levels of AGB σ^0_{HH} can dominate the total SAR response if the structure of the forest and the underlying ground conditions are such that strong double-bounce effects and surface scattering occur.

High surface moisture conditions can enhance σ^0_{HH} and σ^0_{HV} by as much as 4 and 2.5 dB respectively (Lucas et al., 2010) however, this enhancement factor is largely moderated by the level of canopy attenuation (Proisy et al., 2002) and thus becomes less pronounced at high AGB levels (Lucas et al., 2010; Quiñones and Hoekman, 2004). Moisture conditions at the time of ALOS PALSAR data acquisition in this study are not known but presumably have influenced to some degree the magnitude of σ^0_{HH} backscatter at lower AGB levels. However, the higher σ^0_{HH} response at low biomass observed in the current study is also a feature of the forest structure. Proisy et al., (2002) found that σ^0_{HH} was enhanced by 3.4 dB in open versus closed mangrove forests in French Guiana which were not tidally inundated at the time of AIRSAR data acquisition. In this study, the plots with the lowest AGB are short stature (mean tree height < 5m) *Ceriops* or *Avicennia* forest with a ground surface characterised by knee roots (*Ceriops* forest) and numerous pneumatophores (*Avicennia* forest) (see Fig. 4.2c and d). These conditions can be expected to produce increased surface and double-bounce scattering and hence an increase in σ^0_{HH} (Lucas et al., 2007). An exception to the overall pattern of higher σ^0_{HH} at lower AGB levels is apparent in the case of plot 5 (Table 4.1 and Fig. 4.2d) which has a σ^0_{HH} value of -7.8 dB and an estimated AGB of ~153 Mg ha^{-1} and as such is positioned far from the regression line shown in Fig. 4.3a. The presence of large trees in combination with a relatively open structure and high surface roughness (i.e. pneumatophores and dead downed wood shown in Fig. 4.2d) could possibly explain the high σ^0_{HH} from this area. However, given the negative relationship between σ^0_{HH} and AGB in this study; the high σ^0_{HH} response from this plot indicates that predictions of AGB made using the current model may, in some cases result in an underestimation of the AGB held in similarly structured mangrove forests.

The insensitivity of L-band HV to changes in AGB (Fig. 4.3b) was surprising as the HV signal is less influenced by surface conditions and is increasingly dominated by volume scattering from vegetation as AGB increases and is therefore usually more sensitive than HH to changes in AGB until saturation at high AGB occurs (Luckman et al., 1997; Mitchard et al., 2012). There is clearly a difference in forest structure (Fig. 4.2a and c) over the range of sampled AGB (~ 7 to 254 Mg ha^{-1}) which is evident in the σ^0_{HH} response; therefore it seems unlikely that the invariant response

of HV in this study can be attributed to homogeneity in forest structure over the range of AGB. A possible explanation may be that for the lowest AGB plots which were either characterised by open short stature (Fig. 4.2c) or dense short stature (Fig. 4.2b) mangroves the HV signal was largely influenced by double-bounce interactions with volume scattering contributing less to the overall signal due to the presence of smaller trees (Kovacs et al., 2008; Proisy et al., 2002). However, with increasing AGB the reduction in double-bounce interactions was not sufficiently compensated by an increase in volume scattering (due to greater attenuation by the more complex canopy and root structure) to produce a perceptible gradient of change in the HV signal.

4.4.2 Evaluation of SAR-derived AGB estimates

This study represents the first attempt at using ALOS PALSAR to map mangrove AGB along the entire Kenyan coastline. The uncertainty of the SAR-derived estimates of mangrove AGB is high at the scale of an average 1 ha pixel (33.5 Mg ha^{-1}) and reflects the underlying uncertainty in the relationship found between σ^0_{HH} and AGB in this study which, in turn, is reflective of the variable influence of factors such as forest structure, moisture and ground conditions on the SAR response. Therefore caution should be applied when considering the detailed AGB maps presented in Figs. 4.5 to 4.7, particularly as there are no existing spatially equivalent AGB mapping studies with which to validate these results.

The proportional uncertainty of the SAR-derived AGB estimates at the regional and national scale accounts for the uncertainties associated with the ground-based approach to AGB estimation and the random errors associated with spatial and structural heterogeneity and geolocation errors which decrease as a function of increasing spatial scale (Mitchard et al., 2012; Saatchi et al., 2011b). The overall uncertainty on predictions at the regional and national scale is reasonably well constrained (~ 18 to 20%) and is comparable to the 25% uncertainty on estimated AGB stocks (derived using ALOS PALSAR) reported by Mitchard et al., (2012) for a large area (~ 50,000 ha) of forest-savanna mosaic in Gabon.

The SAR-derived estimate of mean AGB for Kenyan mangroves (114.9 Mg ha^{-1}) provided in this study is comparable to the estimate of 119 Mg ha^{-1} from Fatoyinbo and Simard (2013) derived using optical (Landsat), space-borne LiDAR (ICESat GLAS) and Shuttle Radar Topography Mission (SRTM) data. However, the SAR-derived estimate of total mangrove AGB for Kenya produced in the current study (5.32 Mt ± 18.6%) is considerably higher than that of the 2.29 Mt estimated by Fatoyinbo and Simard (2013). The main reason for this disparity in estimates appears to be the substantial difference in estimated total mangrove cover between the two studies. The mangrove cover estimate of 19,200 ha given by Fatoyinbo and Simard (2013) for Kenya is considerably lower than the estimate of > 46,000 ha provided in this study and is also considerably lower than other previous estimates of Kenyan mangrove cover (FAO, 2007; Kirui et al., 2012).

In the absence of any previous independent estimates of mangrove AGB at the regional scale the SAR-derived estimates provided here are compared with those obtained in chapter 2 using the ground-based approach (Table 4.3 and Fig. 4.4). In addition to the appreciable difference in the estimated mean AGB for most regions (except South Coast and Vanga) the relative ordering of regions in terms of the level of AGB held within each also appears to differ between the two approaches. For example, the SAR approach estimates that the mean AGB found within mangroves in Mida Creek is higher than that of South Lamu in contrast to the ground-based approach where the reverse is seen (Fig. 4.4).

A possible explanation for the difference between the estimates derived using the two approaches is that the SAR-based approach may be expected to capture the spatial variability in AGB more fully at larger spatial scales. For regions where there is limited field data available (e.g. Mida Creek) the SAR-derived estimate could therefore be more regionally representative. However, the comparatively lower SAR-derived estimate of mean AGB for South Lamu and in particular Kiunga NMR may not adequately reflect the level of mangrove AGB held within these regions. This indicates that further investigation of the backscatter-AGB relationship for Kenyan mangroves is warranted.

4.4.3 Recommendations for further study

Given the unexpected nature of the relationship between L-band SAR and AGB found in this study and the limited number of ground data used to derive the relationship it is strongly recommended that the findings of the current study be validated against new data. The collection of new ground data (wherever possible) should focus on increasing the size of field plots to 0.5 or preferably 1 ha as this has been found to increase the strength and reduce the uncertainty of the backscatter-AGB relationship (Morel et al., 2011; Saatchi et al., 2011a). It has previously been recommended by Lucas et al., (2010) that ALOS PALSAR data be acquired during periods of low moisture conditions (surface and vegetation) in order to increase sensitivity to AGB. Some of the uncertainty in the backscatter-AGB relationship in this study is presumably due to the varying influence of moisture at the time of SAR data acquisition on the magnitude of the backscatter. However, future efforts to acquire 'low moisture' space-borne SAR data over mangrove areas will be challenging due to the need to align satellite observation strategies with variable local tidal regimes. The benefits of integrating existing space-borne SAR and LiDAR data (e.g. ALOS PALSAR and ICESat GLAS) for the purpose of estimating forest AGB at large spatial scales has previously been demonstrated by Mitchard et al., (2012) and the potential use of such a data synergy should be investigated for mangroves.

Acknowledgements

This research was funded by the Natural Environment Research Council (NERC), UK. All ALOS PALSAR data and one SPOT image were provided under the European Space Agency (ESA) Category-1 scheme (Project ID: 8177). We wish to thank Prof. Mark Huxham (Edinburgh Napier University, UK) for allowing the use of additional SPOT imagery which was provided by Spot Image through the Planet Action Initiative as part of a larger project funded by the Ecosystem Services for Poverty Alleviation (ESPA) programme [under the Swahili Seas NE/I003401/1 project]. The ESPA programme is funded by the Department for International Development (DFID), the Economic and Social Research Council (ESRC) and NERC of the UK. All processing of SPOT imagery was undertaken by Dr. Karin

Viergever (Ecometrica, UK). The ground data for this study were collected in collaboration with Kenya Marine and Fisheries Research Institute (KMFRI) and Kenya Forest Service (KFS). Finally, we wish to acknowledge and express our sincere gratitude for the hard work of all those involved in collecting the ground data for this study, in particular Mr Bernard Kivyatu.

5. Discussion

This thesis has focused on producing estimates of the current above-ground (AGB) stocks of Kenyan mangrove forests and quantifying the uncertainty associated with these estimates. The two approaches to AGB estimation detailed and demonstrated in this study (ground and remote sensing) are necessarily linked. Indeed the ground based estimation process is the foundation on which remote sensing efforts to monitor biomass dynamics are built. Therefore, this thesis has placed great emphasis on the need to develop statistically robust methodologies for modelling allometric relationships and for propagating components of uncertainty to estimates of AGB made using allometric models. Consequently, the ground-based estimates of AGB used in the radar remote sensing approach to AGB estimation were fully inclusive of the uncertainty associated with the measurement of inventoried trees and the uncertainty associated with the use of the allometric model.

5.1 Ground-based approach to biomass estimation

One of the key strengths of adopting the mixed-effects approach to modelling the allometric relationship of Kenyan mangroves in chapter 2 was the ability to account for and explicitly model the variability in the relationship due to species and site effects. In this study, between-group variability in the intercept and the slopes of the predictive variables stem diameter and tree height (the random effects terms) accounted for 41% of the total variability in mangrove AGB. It is therefore not surprising that excluding the random effects (from the mixed-effects model) during the biomass estimation process consistently had the largest impact on the magnitude of the predicted uncertainty in chapter 3. Another key strength of using the mixed-effects modelling approach was the ability to generate robust partial pooling estimates of the regression parameters and their uncertainties. Indeed, chapter 3 illustrated the potential for producing unrealistically low estimates of uncertainty as a result of using an allometric model which ignores the structural complexity (i.e. correlations) of the underlying data used to fit the model (e.g. the standard OLS model in this study).

Previous mangrove biomass studies conducted in Kenya have produced allometric equations for selected species at a few sites along the coast. Whilst such equations are useful for some purposes; their application outwith the species and/or sites for which they were developed involves ignoring the uncertainty due to species and site variability in the allometric relationship. In contrast, the generic biomass equation developed in chapter 2 has the potential for broad application to existing or future mangrove inventory data collected in Kenya as it can be used to predict the AGB of new trees where there is no pre-existing knowledge of the specific species-site allometric relationship. However, it is important to note that simply applying the fixed effects estimates (i.e. the generic equation) from Model VIII to estimate AGB without propagating the uncertainty due to the random effects (as detailed in chapter 2, section 2.2.3.4) would produce the kind of under-estimation of uncertainty illustrated in chapter 3 (Fig. 3.3) and would in effect negate one of the main purposes of using the mixed-effects model.

The simulation-based methodology for uncertainty propagation described in chapter 2 allowed for measurement, parameter and residual uncertainty to be propagated to tree, plot and regional scale estimates of AGB. In this way resulting estimates of AGB at all spatial scales were accompanied by a realistic measure of uncertainty. The regional estimates of mean and total AGB (± 95% PIs) produced in chapter 2 represent the most comprehensive attempt to date at summarising current mangrove AGB stocks within Kenya. The ground-based approach used in this study estimated the mean AGB of mangroves in Kenya to be ~ 116 to 154 Mg ha^{-1}. This range encompasses the only other published estimate (to the best of the authors' knowledge) of mean AGB for Kenyan mangroves of 119 Mg ha^{-1} (Fatoyinbo and Simard, 2013).

In considering how best to further constrain the uncertainty of the estimates of mangrove AGB produced in this study there are a variety of issues to address. The presence of large trees within the current inventory dataset had a substantial impact on the magnitude of the predicted uncertainty (chapter 2 and chapter 3). Furthermore, a large proportion of the total AGB of inventoried trees is often held

within relatively few large trees (Brown et al., 1995; Ryan, 2009). It is therefore important to constrain the uncertainty of estimates of AGB for large trees.

In this study, the greater uncertainty in estimating the AGB of large trees (using Model VIII) is in large part reflective of the limited availability of large tree harvest data with which to fit the model. Therefore, any future harvesting of mangroves in Kenya (for the purpose of constructing allometric models) should focus on collecting harvest data for large diameter trees. In the current study limited harvest data for *Xylocarpus* sp. were obtained from a study conducted in South-East Asia by Poungparn et al., (2002). Thus future harvesting of mangroves for allometric studies in Kenya should also prioritise the collection of data from species for which there is currently no existing harvest data namely; *Xylocarpus granatum, Xylocarpus moluccensis, Lumnitzera racemosa* and *Heritiera littoralis*. Current harvest protocols as summarised in Chapter 2, section 2.2.2 can be applied (including the random selection of individuals harvested from the range of diameter size classes present) with slight modification to include the measurement of stem diameter above buttress roots (in the case of *X. granatum* and *H. littoralis*) if these occur > 1.3m above-ground level.

Future harvesting protocols for mangroves in Kenya should also consider sampling the wood density of all harvested trees following the protocols for measurement and calculation of wood density outlined in Williamson and Wiemann, (2010). Previous studies have found wood density to be an important explanatory variable in allometric models (Chave et al., 2005; Komiyama et al., 2008) and the inclusion of wood density data within allometric models for Kenyan mangroves could prove useful in explaining some of the variance which is attributed to the random effects in the current model. Wood density varies at the species level (between and within species), at the site level and at the single tree level between different parts of the same tree (Chave et al., 2006; Sarmiento et al., 2011). Thus, future harvesting protocols could consider sampling the wood density from stem, branch and possibly prop root (in the case of *Rhizophora* sp.) tree components. However, any subsequent allometric model incorporating wood density data (from one or more of these tree components) as a predictive variable would have to be developed with attention to

how the resulting AGB equation(s) could be practically applied to forest inventory data and how the collection of wood density data could be integrated within mangrove forest inventory protocols. Other covariates which could potentially be of use in future allometric modelling studies for Kenyan mangroves include indicators of site condition such as soil nutrient availability, salinity and stocking density. Future work could also explore the use of alternative approaches to modelling the distribution of the variance such as non-linear mixed-effects models or Bayesian hierarchical models.

The methodology used to derive AGB estimates in this study is in line with the IPCC requirements and criteria for higher tier (Tier 2 and 3) reporting of carbon pools (IPCC, 2006; Maniatis and Mollicone, 2010). It is anticipated that the allometric model and methodology for biomass estimation presented in chapter 2 could be utilised within an MRV program for long term monitoring of mangrove AGB stocks in Kenya. In particular the methodology for biomass estimation in chapter 2 could support an MRV program based on estimating changes in AGB carbon pool stocks using the 'Stock-Difference' method which estimates the difference in carbon stocks between two time points (IPCC, 2006). For this purpose it might be advisable to establish a network of permanent sample plots (PSPs) within mangroves along the coastline (according to some stratification system), although the continued representivity of these plots would need to be monitored through time.

In the current study, mangroves along the entire Kenyan coastline were subdivided into spatially discrete 'regions' in order to achieve the main objective of providing a national-scale assessment of current AGB stocks. This type of geographical sub-division was also necessary as it allowed for the collation and use of a large amount of forest inventory data collected by other studies which employed different sampling strategies. The resulting estimates of mean and total mangrove AGB obtained in chapter 2 for each region and for Kenya as a whole were reasonably well constrained. However in order to increase representivity it is recommended that further inventory data be collected in areas where there is either no existing current inventory data or there is limited inventory data available (e.g. Mida Creek and Lamu).

An alternative approach to sub-dividing or stratifying mangroves along the Kenyan coast which would perhaps be more suited to the long-term monitoring of AGB stocks (and other carbon pools) within PSPs and may ensure greater structural representivity would be to stratify mangroves by physiographic and physiognomic type (i.e. fringe, riverine, basin, overwash and dwarf mangrove) as described by Lugo and Snedaker (1974). This would enable the reporting of AGB stocks by mangrove type rather than by location alone. In many cases, further subdivision of these generalised mangrove types may be warranted and could involve the establishment of representative PSPs at different distances from the seaward edge (Kauffman and Donato, 2012).

Conducting forest inventories within mangroves can be challenging as mobility is often extremely difficult due to the combination of thick mud, high density of tree stems and above-ground root structures which are characteristic features of the mangrove environment. In addition, the time available to conduct inventories is often severely constrained due to the prevailing tidal regime. Such conditions often restrict which mangrove areas can be accessed for inventory and are the main reason why the size of plots used in mangrove studies tends to be small (e.g. 10m x 10m). Indeed, in the current study although all efforts were made to limit bias in the positioning of field plots for the collection of inventory data (i.e. random selection of map grid squares) some areas initially identified for sampling were simply inaccessible given the time and resources available. Furthermore, in this study the time taken to establish and census plots of 0.25 and 0.5 ha in size often meant that data collection was undertaken under conditions of incoming tide in order to complete the census of a single large plot within the same day. Whilst such conditions (although undesirable) did not preclude the collection of tree stem diameter and height data required for this study; the time taken to establish (and ensure the accurate establishment of) such large plots would not be practicable if data collection required low tide conditions (e.g. the collection of soil data).

There is no universally applicable protocol which can be adopted for the inventory of mangrove carbon stocks as decisions on how best to stratify the mangrove environment and determine the most appropriate sampling strategy will largely

depend on the overall objectives and scope of the study. If the main focus is to provide an estimate of current AGB stocks only (as in this study) then the use of larger plots is advisable in order to reduce the influence of the uncertainty in estimates of large tree AGB on the overall uncertainty of plot AGB (chapters 2 and 3). Increasing the size of plots is also essential where any kind of remote sensing based approach to AGB estimation is sought (chapter 4). Depending on the stratification system in use, the requirement for larger plot sizes may introduce some degree of sampling bias as often the area over which mangrove forest structural change takes place is very small and therefore finding relatively homogeneous 'units' of forest of a size large enough to accommodate a 0.5 or 1 ha plot may not be possible in some areas of mangrove. However, this is largely unavoidable if study objectives necessitate the use of large plot sizes. In addition, if there has been appropriate stratification at the broad-scale (i.e. regional or national scale) and sufficient sampling is undertaken within each stratum overall then any such sampling bias should, in theory not result in a failure to adequately capture or characterise the variation in whatever forest feature is of interest (e.g. variation in AGB).

If in the future the main study objective became that of providing an estimate of total mangrove carbon stocks (involving the estimation, reporting and long-term monitoring of all five forest carbon pools) then a more appropriate inventory protocol could involve the establishment of smaller PSPs (according to a pre-defined stratification system) and the use of a nested sampling design to measure all carbon pools within each PSP similar to that recommended by Kauffman and Donato (2012). This type of inventory approach could also involve the establishment of a larger 0.5 ha surrounding plot in which to measure large diameter trees if the conditions and/or study objectives required it (Kauffman and Donato, 2012).

In the current study there was some inconsistency in inventory protocol between studies included in this thesis in terms of diameter measurement thresholds with some studies measuring all trees $\geq$ 2.5 cm diameter and some measuring $\geq$ 5 cm. Given the disproportionate contribution of large diameter trees to estimates of total AGB (Brown et al., 1995; Ryan, 2009) the degree of possible under-estimation of AGB in this study due to excluding those trees < 5 cm in diameter is likely

negligible. Thus future inventory studies conducted for the purpose of AGB estimation should consider standardising diameter measurement thresholds at ≥ 5cm or above in an effort to prioritise time and resources on those trees holding the greatest proportion of AGB.

5.2 Remote sensing based approach to biomass estimation

This study represents the first attempt at using SAR for the retrieval of mangrove AGB in East Africa. Despite the limited number of ground data points available in this study there was an observable relationship ($R^2 = 0.45$) found between σ^0_{HH} and mangrove AGB. This relationship was used to map mangrove AGB along the Kenyan coastline and to produce estimates of mean and total AGB for each mangrove region and for Kenya as a whole (chapter 4).

The nature of the relationship between σ^0_{HH} and mangrove AGB found in this study was unexpected given that previous studies have found a positive backscatter-AGB relationship and that L-band in HV polarisation generally provides the greatest sensitivity to changes in AGB (Mitchard et al., 2009; Mougin et al., 1999). The negative relationship between σ^0_{HH} and mangrove AGB found in this study can possibly be attributed to enhanced backscatter at lower AGB due to strong double-bounce and direct surface scattering from short stature/open forests and attenuation of the SAR signal at higher AGB. The insensitivity of σ^0_{HV} to changes in AGB is likely attributable to a reduction in scattering from double-bounce interactions with increasing AGB which was not sufficiently compensated by an increase in volume scattering (i.e. signal losses evened out signal gains). Whilst these mechanisms may explain the SAR response (σ^0_{HH} and σ^0_{HV}) observed in this study; it is important to bear in mind that the resulting empirical HH-AGB relationship is based on a limited number of ground data points and therefore may not fully represent the backscatter-AGB relationship for mangroves in Kenya. In order to validate and reduce the uncertainty in the backscatter-AGB relationship found in this study it is strongly recommended that more field data be collected from all mangrove regions.

Despite the large inventory dataset of 498 plots collated for use in this thesis only the 25 larger plots (0.25 and 0.5 ha plots) were found to be utilizable in the SAR

analysis. Therefore future attempts to validate the radar-derived estimates of AGB presented in this study should focus on the collection of inventory data from plots of a minimum size of 0.25 ha and if possible should try to increase plot sizes to 0.5 or 1 ha. This requirement for larger plots could be aligned with efforts to establish a network of mangrove PSPs for carbon monitoring. The availability of new field data would provide an interesting opportunity to further investigate the backscatter-AGB relationship for Kenyan mangroves utilising data acquired by JAXA's ALOS-2 L-band SAR system (1 to 3 m resolution on the ground) recently launched in May 2014. Furthermore, ESA's Biomass satellite scheduled for launch in 2020 will employ P-band synthetic aperture polarimetric radar (~ 68 cm wavelength) for the explicit purpose of measuring and monitoring the AGB of forests globally and NASA's ICESat-2 mission due for launch in 2017 will operate a space-borne LiDAR system for the same purpose.

The data from such missions, in particular the P-band SAR and LiDAR data will be provided free of charge to the user through ESA and NASA respectively and their potential use (perhaps in synergy) for the long-term monitoring of global forest biomass dynamics is promising. However, it must be noted that the use of such earth observation (EO) data are comparatively more complex than that of more commonly used optical systems; therefore the use of SAR and LiDAR data for AGB estimation within many developing nations may be hampered by the lack of in-country capacity required for the processing, analysis and interpretation of EO data (Cassells et al., 2011).

At the national scale the SAR-derived estimate of mean and total mangrove AGB obtained in chapter 4 was broadly consistent with the corresponding estimates derived using the ground-based statistical up-scaling approach in chapter 2. However, at the regional scale there was a noticeable divergence in the SAR vs. ground-based estimates. In particular there was considerable difference between the SAR-derived estimate of mean AGB for the regions Mida Creek and Kiunga NMR which were substantially higher and lower respectively than the ground-based estimates and showed no overlap in the estimated uncertainty bounds. This disparity in estimates could be in part due to a lack of regional representivity in the field data

which could have affected the ground-based estimates of regional mean AGB. The SAR based approach has in theory captured the spatial variability in AGB at large spatial scales more fully therefore it might be reasonable to suggest that the SAR derived estimates of mean AGB at large spatial scales for some of the regions (i.e. those lacking sufficient number of field data) may be more regionally representative.

The uncertainty in the backscatter-mangrove AGB relationship in this study is reflected in the fairly high uncertainty of the SAR-derived estimates of AGB at the pixel scale. However the uncertainty of the SAR-derived estimates was constrained to between ~ 18 to 20% of the estimated mean and total AGB at the regional and national scale. The procedure for propagating uncertainty to large scale SAR estimates of AGB used in the current study involved a conservative summation of 1) the uncertainty due to the ground-based estimates and 2) the uncertainty due to random errors associated with spatial heterogeneity and geolocation. An alternative approach for future study would be to propagate the various sources of random and systematic error to SAR-derived estimates of AGB at large spatial scales using a simulation-based approach. This could allow for the propagation of asymmetric uncertainties in the ground-based estimates and a more realistic representation of the uncertainty based on multiple realisations of the backscatter-AGB relationship, which could in turn be propagated to large scale estimates of AGB.

5.3 Main implications for REDD+ participation

Current criteria for higher tier REDD+ reporting of forest carbon stocks requires 1) the use of detailed country-specific inventory data to produce estimates of changes to carbon stocks over time, 2) transparent documentation of all datasets and methodologies in use and 3) all carbon stock estimates to be accompanied by an appropriate estimate of uncertainty.

The ground-based approach used in this study to produce estimates of current mangrove AGB stocks in Kenya meets the aforementioned criteria for higher tier REDD+ reporting of this key carbon pool. Although outwith the scope of the current study, the requirement for repeated measurements of AGB carbon stocks through

time could be realised using the ground-based approach as demonstrated here or with modification to accommodate alternative stratification and sampling schemes.

There are currently no specific guidelines for the use of remote sensing in a REDD+ context, however the use of space-borne SAR data will likely play a key role in efforts to provide repeatable long-term monitoring of forest dynamics for REDD+. The potential use of SAR techniques for forest-based applications is widely recognised, as evidenced by the ongoing large investment in the development and operation of current and future SAR satellite missions.

The use of space-borne SAR for AGB retrieval remains promising (particularly the future use of P-band SAR), however the large-scale adoption of this approach for REDD+ purposes may be hampered due to inconsistency in the relationship between backscatter and AGB. Indeed, the nature of the backscatter-mangrove AGB relationship found in this study was unexpected and remains to be validated against an independent dataset. In addition, certain unavoidable features of the mangrove environment (i.e. generally high moisture conditions and structural complexity) which complicate the interpretation of the SAR response may limit the application of SAR techniques for AGB estimation in mangroves. Therefore, whilst the current study has demonstrated some potential in using space-borne SAR data for estimating the AGB of mangroves further investigation of the backscatter- AGB relationship is required prior to adoption of a SAR-based approach to mangrove AGB estimation for REDD+.

Appendix 1: Published version of chapter 2

Forest Ecology and Management 310 (2013) 968–982

Contents lists available at ScienceDirect

Forest Ecology and Management

journal homepage: www.elsevier.com/locate/foreco

Propagating uncertainty to estimates of above-ground biomass for Kenyan mangroves: A scaling procedure from tree to landscape level ☆

R. Cohen [a,*], J. Kaino [b], J.A. Okello [b,c], J.O. Bosire [b], J.G. Kairo [b], M. Huxham [d], M. Mencuccini [a]

[a] School of Geosciences, University of Edinburgh, Crew Building, West Mains Road, Edinburgh EH9 3JN, United Kingdom
[b] Kenya Marine and Fisheries Research Institute, P.O. Box 81651, Mombasa, Kenya
[c] Department of Plant Biology and Nature Management (APNA), Vrije Universiteit Brussels, Pleinlaan 2, 1050 Brussels, Belgium
[d] School of Life, Sport and Social Sciences, Edinburgh Napier University, Edinburgh, United Kingdom

ARTICLE INFO

Article history:
Received 17 June 2013
Received in revised form 20 September 2013
Accepted 22 September 2013
Available online 20 October 2013

Keywords:
Above-ground biomass
Mangrove
Allometric equations
Uncertainty propagation
Mixed-effects models
Kenya

ABSTRACT

Mangroves are globally important carbon stores and as such have potential for inclusion in future forest-based climate change mitigation strategies such as Reduced Emissions from Deforestation and Degradation (REDD+). Participation in REDD+ will require developing countries to produce robust estimates of forest above-ground biomass (AGB) accompanied by an appropriate measure of uncertainty. Final estimates of AGB should account for known sources of uncertainty (measurement and predictive) particularly when estimating AGB at large spatial scales. In this study, mixed-effects models were used to account for variability in the allometric relationship of Kenyan mangroves due to species and site effects. A generic biomass equation for Kenyan mangroves was produced in addition to a set of species-site specific equations. The generic equation has potential for broad application as it can be used to predict the AGB of new trees where there is no pre-existing knowledge of the specific species-site allometric relationship: the most commonly encountered scenario in practical biomass studies. Predictions of AGB using the mixed-effects model showed good correspondence with the original observed values of AGB although displayed a poorer fit at higher AGB values, suggesting caution in extrapolation. A strong relationship was found between the observed and predicted values of AGB using an independent validation dataset from the Zambezi Delta, Mozambique ($R^2 = 0.96$, $p = < 0.001$). The simulation based approach to uncertainty propagation employed in the current study produced estimates of AGB at different spatial scales (tree – landscape level) accompanied by a realistic measure of the total uncertainty. Estimates of mangrove AGB in Kenya are presented at the plot, regional and landscape level accompanied by 95% prediction intervals. The 95% prediction intervals for landscape level estimates of total AGB stocks suggest that between 5.4 and 7.2 megatonnes of AGB is currently held in Kenyan mangrove forests.

1. Introduction

Mangrove forests are now widely recognised as globally important carbon (C) stores (Bouillon et al., 2008; Chmura et al., 2003; Donato et al., 2011; McKee et al., 2007). Despite accounting for just 0.7% of the world's tropical forest cover (Giri et al., 2011) mangroves play a disproportionately important role in the global C cycle. Recent estimates suggest that as much as 20Pg of C is currently being stored in mangrove biomass, sediments and peat world-wide (Donato et al., 2011). Mangroves do not merely sequester and store C they also provide a number of other key ecosystem services which are ecologically and economically important at local, regional and global scales. Such services include but are not limited to; coastal defence (Zhang et al., 2012), fisheries production (Aburto-Oropeza et al., 2008), habitat provision for terrestrial and aquatic fauna (Kathiresan and Bingham, 2001), timber and fuelwood production (Dahdouh-Guebas et al., 2000), pollution abatement (Wickramasinghe et al., 2009) and regulation of sediment exchange between land and sea (Duarte et al., 2005).

The continued degradation and destruction of mangroves world-wide has been highlighted in recent years (Alongi, 2002; Giri et al., 2011). Mangroves are considered to be one of the most threatened ecosystems on the planet with an estimated decline in global cover of ~35% during the period 1980–2000 (Valiela et al., 2001). This decline is largely due to over-exploitation of wood products, conversion to aquaculture, coastal development and human settlement (Primavera, 2005). Although rates of destruction may be slowing in some countries they generally remain high; for example Kenya experienced an estimated mean loss of mangrove cover of ~0.7% yr^{-1} during the period 1985–2010

* Corresponding author. Tel.: +44 (0) 131 650 5103.
E-mail address: Rachel.Cohen@ed.ac.uk (R. Cohen).

0378-1127/$ - see front matter © 2013 The Authors. Published by Elsevier B.V. All rights reserved.
http://dx.doi.org/10.1016/j.foreco.2013.09.047

(Kirui et al., 2012). Continued degradation and loss of mangrove cover not only represents a loss of future C sequestration potential but could result in significant release into the atmosphere of C currently being stored by mangroves (Pendleton et al., 2012).

An estimated 8–20% of annual global anthropogenic CO_2 emissions result from land-use changes occurring primarily in the tropics (van der Werf et al., 2009). This realisation has led to proposals for forest-based climate change mitigation strategies such as Reduced Emissions from Deforestation and Degradation (REDD+). In essence REDD+ envisages achieving CO_2 emissions reductions, forest conservation and sustainable development by placing an economic value on forest carbon storage and facilitating the transfer of funds from developed to developing nations through international trade in carbon credits. Details of how REDD+ will operate at the national and international level under the United Nations Framework Convention for Climate Change (UNFCCC) are still under debate. However many developing nations (including Kenya) are already in the process of formulating national REDD+ readiness strategies in partnership with the World Bank's Forest Carbon Partnership Facility (FCPF). There is definite scope for mangroves to be included in national and/or local scale forest carbon projects operating either under existing voluntary or future compliance carbon markets. Indeed, a recent study by Siikamaki et al. (2012) suggested that at the global scale reducing CO_2 emissions by avoiding further loss of mangroves could prove to be an economically viable option in comparison with the cost of reducing emissions from other sources (e.g. industry) even under scenarios of low mangrove carbon offset supply.

Participation in REDD+ (under the UNFCCC) will require countries to produce accurate estimates of their forest carbon stocks and stock changes through robust Measurement, Reporting and Verification (MRV) programs. The most recent Intergovernmental Panel on Climate Change (IPCC) Guidelines for National Greenhouse Gas Inventories (IPCC, 2006) provide the current methodological framework for REDD+ MRV requirements (Maniatis and Mollicone, 2010). In accordance with these guidelines all estimates should be accompanied by an appropriate measure of uncertainty (95% confidence interval) and should account for and reduce all known sources of uncertainty as far as is possible (IPCC, 2006). Above-ground biomass (AGB) is one of five forest carbon pools (identified by the IPCC) which will be estimable and reportable for REDD+. Providing robust estimates of AGB is important both in terms of future REDD+ reporting but also in providing the link between ground and remote sensing efforts to monitor changes in forest biomass and land cover at local, regional and global scales.

The above-ground biomass of trees is commonly estimated by the use of allometric equations (derived using regression analysis) which relate one or more easily measurable tree variables (e.g., stem diameter at breast height (DBH)) to total above-ground biomass. These equations are then applied to forest inventory data in order to estimate biomass at larger spatial scales. Allometric equations have been developed for a variety of mangrove species occurring across a broad geographical range (Clough and Scott, 1989; Kairo et al., 2009; Komiyama et al., 2005; Poungparn et al., 2002; Soares and Schaeffer-Novelli, 2005). However, African mangroves are under-represented in the current literature with published equations existing for Kenya (Kairo et al., 2009; Kairo et al., 2008; Kirui et al., 2006; Slim et al., 1996; Tamooh et al., 2009) and South Africa (Steinke et al., 1995) only.

Allometric relationships in trees are generally considered to be both species and site-specific. However, the infeasibility of constructing a new allometric equation for every species encountered at every new site has led to increasing interest in the development of generic equations for biomass estimation (Brown et al., 1989; Chave et al., 2005; Zianis and Mencuccini, 2004). Existing generic equations for mangroves have used wood density as the species-specific component of the relationship (Chave et al., 2005; Komiyama et al., 2005). The generic equation developed by Komiyama et al. (2005) was deemed to perform within acceptable levels of precision (as measured by the relative error) in comparison with site-specific equations for selected species (Komiyama et al., 2008).

Uncertainties are introduced at all stages of the biomass estimation process (from single tree to landscape level). Total uncertainty at the single tree level is comprised of uncertainty in the measurement of tree variables (measurement uncertainty) and uncertainty due to the use of the allometric model for predicting the biomass of a new individual (predictive uncertainty) (Chave et al., 2004; Zianis, 2008). These uncertainties are, in turn, propagated to plot and landscape level biomass estimates. Failing to account for uncertainty during the biomass estimation process ultimately leads to an underestimation of the uncertainty on final predictions (Dietze et al., 2008).

Accounting for predictive uncertainty is particularly important in biomass estimation as allometric equations are often applied outwith the data range for which they were originally intended (Chave et al., 2005) and are always applied outside the particular trees (and often sites) from which they were developed. Uncertainty in the parameters of a regression model is often represented by simply quoting the standard error of the allometric constants whilst the coefficient of determination (R^2) is the usual means by which to evaluate both the 'fit' of the model and its predictive power (e.g. Komiyama et al., 2005; Soares and Schaeffer-Novelli, 2005). However, over reliance on the use of R^2 in regression analysis as a measure of model predictive accuracy and for model comparison (between datasets) has been criticised in recent years (Gelman and Pardoe, 2006; Johnson and Omland, 2004). In contrast to model selection criteria such as the Akaike Information Criteria (AIC) (Akaike, 1987) the R^2 statistic is not a direct measure of model predictive accuracy and model selection made solely on the basis of maximising the R^2 statistic can lead to imprecise predictions as no account is taken of model complexity (Johnson and Omland, 2004).

The issue of uncertainty in biomass estimation has been addressed in the literature for forests in general (Brown, 2002; Chave et al., 2004; Ketterings et al., 2001; Parresol, 1999; Phillips et al., 2000; Zianis, 2008). Methodologies for propagating uncertainty have been presented based on summing the variances of component sources of uncertainty (see Chave et al., 2004; Ketterings et al., 2001; Phillips et al., 2000) and simulation techniques such as Monte Carlo (Heath and Smith, 2000; Ryan, 2009). To the best of our knowledge such methodologies have never been applied for the purpose of propagating uncertainty to biomass estimates in mangroves. With this in mind and in the context of future REDD+ requirements for biomass/carbon accounting this study focused on: (1) the development of new allometric equations to estimate the above-ground biomass of Kenyan mangroves using linear mixed-effects models and based on a meta-analysis of all the available harvest data for Kenyan mangrove species (2) demonstrating a simulation based methodology for propagating uncertainty during the biomass estimation process and (3) demonstrating the practical application of said equations and simulations to a large forest inventory dataset spanning the entire Kenyan coastline for the purpose of producing estimates of above-ground biomass at different spatial scales (tree, plot, region and landscape) with an appropriate measure of uncertainty.

2. Methods

2.1. Harvest dataset – model development and validation

The harvest data used in this study is detailed in Table 1 and represents the largest dataset compiled to date for African

mangroves. The bulk of the harvest data originates from the Gazi Bay area (4°25′S, 39°30′E) located ~55 km south of the city of Mombasa in Kenya (Fig. 1) and was made available through collaboration with Kenya Marine and Fisheries Research Institute (KMFRI). The Gazi Bay data has been divided into two sub-sites; Gazi (the area next to Gazi village) and Kinondo (the area next to Kinondo village). An additional study within the Gazi Bay area by Slim et al. (1996) was considered for inclusion but discounted as it was not possible to obtain the raw data. Attempts were made to source additional datasets from outwith Africa in order to expand the range of stem diameter and height data available for each species and also to provide some data for species (e.g. *Xylocarpus* sp.) not included in any of the African studies. An extensive literature search was carried out to look for raw harvest data which were (1) from the same species that occur in Kenya and (2) freely available in the publication. It was only possible to find one study which met both these criteria; that of Poungparn et al. (2002) from South-East Asia.

The harvest dataset used in this study to develop regression models comprises the raw data from 337 individually harvested trees (see Section 2.1.1 for harvest methodology) and includes data for seven of the nine mangrove species known to occur in Kenya. The harvest dataset is unbalanced with very few data points for some species (Table 1). However, *Rhizophora mucronata* and *Avicennia marina* are well represented in the dataset in terms of sample size and these are two of the most dominant and widely distributed mangrove species in Kenya. In common with most allometric studies, there is a paucity of data from large diameter size classes with 97% of the harvested trees in the current dataset <20 cm in diameter. This means that the data range in the harvest dataset does not fully encompass the upper values of diameter and height recorded in the existing forest inventories.

Harvest data from a recent study conducted by WWF, Mozambique and KMFRI in 2011 in the Zambezi Delta, Mozambique (Bosire et al., unpublished results) were used in this study for validation purposes only and were not used to develop regression models (data summarised in Table 1). The Zambezi validation dataset comprises harvest data from 23 trees from six mangrove species occurring in both Mozambique and Kenya.

2.1.1. Summary of harvest methodology

All of the studies listed in Table 1 employed similar methodologies for tree harvesting and determination of total live above-ground biomass (but see individual papers for details). Harvested trees were selected randomly and prior to harvest, the stem diameter (cm) and total height (m) of each tree was recorded. Stem diameter was measured at 1.3 m above-ground (DBH) except in the case of *Rhizophora* trees where the highest prop root occurred >1.3 m above-ground in which case diameter was measured at ~30 cm above the highest prop root. Trees were then harvested at ground level and the fresh weight of component parts (stem, branches, leaves and prop roots in the case of *Rhizophora* sp.) was measured in the field. Sub-samples of component parts were then oven dried to constant weight (80–85 °C in the case of all studies apart from Poungparn et al. (2002) where fresh material was dried at 110 °C) in order to calculate wet-dry weight ratios (conversion factors). Conversion factors were then applied to convert the fresh weight of each tree component to dry weight in kilograms (kg DW) and summed giving total above-ground biomass in kg DW. The study by Kirui (2006) employed a slightly different methodology for determining the total above-ground biomass of multi-stemmed *Avicennia* trees. Each stem arising from a common butt was treated as an individual tree and the biomass of each stem was calculated separately following a procedure outlined in Clough et al. (1997) involving apportionment of the common butt.

2.2. Statistical analyses

2.2.1. Rationale for using mixed-effects models

Ecological datasets often display a complex structure where data from individuals within populations are nested or grouped by one or more factors. Such grouping factors could include for example; the species and/or site which the individual belongs to, an experimental treatment applied to a subset of individuals and time series data. If such correlations or group effects are not accounted for during analysis the standard errors of the regression coefficients will tend to be underestimated due to inflation of the effective sample size (Steele, 2008). Mixed-effects models not only account for but explicitly model the variance due to group effects.

In mixed-effects models the intercept and regression coefficients can be assigned their own probability models and allowed to vary by group (as random effects) around the overall population mean (the fixed effects). This is particularly useful in studies where the main target of inference is the wider population and predictions are sought for new individuals within new groups, with an appropriate measure of predictive uncertainty (Gelman and Hill, 2007). In addition, mixed-effects models deal well with unbalanced datasets (especially common in meta-analysis studies) and provide a more robust estimation of regression coefficients for groups where there is little information (i.e. a small sample size) as additional information on the probability distribution of coefficients can be gained from the dataset as a whole (Dietze et al., 2008).

2.2.2. Model specification and selection process

The power function equation (Eq. (1)) or its linearized form (Eq. (2)) is commonly used as the underlying allometric scaling relationship for biomass regression models (e.g. Brown et al., 1989; Chave et al., 2005; Komiyama et al., 2008; Parresol, 1999).

$$y = ax^b \tag{1}$$

$$\ln(y) = \ln(a) + b\ln(x) + e_i \tag{2}$$

where y is the response variable, x is the predictive variable and a and b are the allometric constants. Specifically, a is the scaling coefficient (or intercept), b is the scaling exponent (or slope) and e_i is the error term which is assumed to be normally distributed $e^i \sim N(0, \sigma^2)$. For mangroves, biomass regression models have been developed using stem diameter (D) as the sole predictive variable (Clough and Scott, 1989; Steinke et al., 1995). However, many studies have found that the inclusion of additional biometric variables (e.g. tree height (H)) either fitted independently or as a combined variable such as $x = D * H$ or $x = D^2 * H$ have improved model fit (Chave et al., 2005; Komiyama et al., 2002; Soares and Schaeffer-Novelli, 2005). The inclusion of wood density as a predictive variable in models has also been recommended (Chave et al., 2005; Komiyama et al., 2005).

In the current study, a linear relationship was obtained between predictive variables (diameter and height) and the response variable (total above-ground biomass (AGB)) after transforming all variables by natural log (Fig. 2) allowing for the use of regression models of the form shown in Eq. (2). Wood density was not included as a potential predictive variable as tree level wood density data were not available in the harvest dataset used for model development. The individual level grouping factor used in the current study was a combined species_site indicator which grouped the harvest data from individuals within each species at each site in the dataset. For example data from *Rhizophora* trees at Kinondo (Table 1) formed the group Rhiz_Kin and so on. In total there were eighteen species_site groupings present within the harvest dataset. It was necessary to combine species and site into one grouping

Table 1
Provenance and summary of the tree harvest dataset used in this study to develop and validate biomass equations for Kenyan mangroves.[a]

Study	Location	Forest type	Species	Stem diameter range (cm)	Height range (m)	Above-ground biomass (kg DW)	Sample size
Lang'at (2008)	Ramisi, Kenya	Plantation (12 yrs old)	*Bruguiera gymnorrhiza*	1.1–4.8	2.7–6.6	0.5–7.3	15
Kairo et al. (2008)	Kinondo (Gazi Bay), Kenya	Plantation (12 yrs old)	*Rhizophora mucronata*	2.4–11.5	3.5–8.9	0.6–68.9	50
Kirui et al. (2006)	Gazi (Gazi Bay), Kenya	Natural	*Rhizophora mucronata*	5.7–21.4	4.3–11.3	13.4–269.5	15
Kirui (2006)	Kipini, Kenya	Natural	*Rhizophora mucronata*	2.3–23.6	2.8–16.1	0.6–383.7	15
			Avicennia marina	2.5–15.8	3.9–11.7	4.6–71.4	28 (19)
	Gazi (Gazi Bay), Kenya	Natural	*Avicennia marina*	3.7–21.8	2.1–11.3	7.2–127.3	51 (15)
Tamooh et al. (2009)	Gazi (Gazi Bay), Kenya	Plantation (6yrs old)	*Rhizophora mucronata*	0.9–6.4	0.8–3.9	0.08–16.2	12
Kairo et al. (2009)	Gazi (Gazi Bay), Kenya	Plantation[b]	*Avicennia marina*	5.2–10.2	4–5.8	6.8–22.5	10
			Sonneratia alba	5.3–11.3	4–5	3.8–9.4	10
			Ceriops tagal	5–5.5	1.8–2.6	1.5–6.1	10
			Rhizophora mucronata	3–8	2.8–5	3–25.8	58
Steinke et al. (1995)	Mgeni estuary, South Africa	Natural	*Bruguiera gymnorrhiza*	3.4–11.5	4.6–13.5	3.2–107.2	12
			Avicennia marina	5.4–9.9	4.9–7.7	5.3–31.9	4
Poungparn et al. (2002)	Thailand	Natural	*Sonneratia alba*	4.2–12.7	3.4–13.4	3.1–79.3	10
			Bruguiera gymnorrhiza	4.8–33.4	9.2–24.9	8.3–943.5	10
			Rhizophora mucronata	4.7–11.2	6.9–16	7.7–73.7	11
			Xylocarpus granatum	3.7–12.7	4.1–8	3.2–66.8	8
	Indonesia	Natural	*Sonneratia alba*	6.7–21.7	7.3–22.6	13.1–256	2
			Bruguiera gymnorrhiza	9.7–48.9	11.1–30.6	54.7–1411.1	4
			Xylocarpus granatum	18.6	13.4	162.2	1
			Xylocarpus moluccensis	11.8	13.5	47.4	1
WWF/KMFRI (Validation Dataset)	Zambezi Delta, Mozambique	Natural	*Ceriops tagal*	5.3–15.4	3.6–6.5	6.55–68.2	3
			Bruguiera gymnorrhiza	5.6–24.6	5.5–8.1	11.7–161.8	4
			Xylocarpus granatum	5.2–14.9	4–7.8	6.7–49	3
			Sonneratia alba	5.9–35	5.9–13.5	8.8–453.4	6
			Avicennia marina	8–28	5.3–13.5	14.9–248	4
			Heritiera littoralis	5–22.5	4.9–9.5	3.9–121.2	3

[a] Above-ground biomass is given in kg dry weight (kg DW) and includes stem, branch, leaf and prop root (in the case of *Rhizophora* sp.) components. An exception is the study by Lang'at (2008) where above-ground biomass comprises stem weight only. In the study by Kirui (2006) sample sizes for *Avicennia* sp. are the total number of stems (treated separately during analysis) and numbers in parentheses are the actual number of harvested trees. The study by Poungparn et al. (2002) included data sourced from other studies; see original paper for details.

[b] Plantation age at time of harvest in Kairo et al. (2009) was 5 years old for *R. mucronata* and *S. alba* and 8 years old for *C. tagal* and *A. marina*.

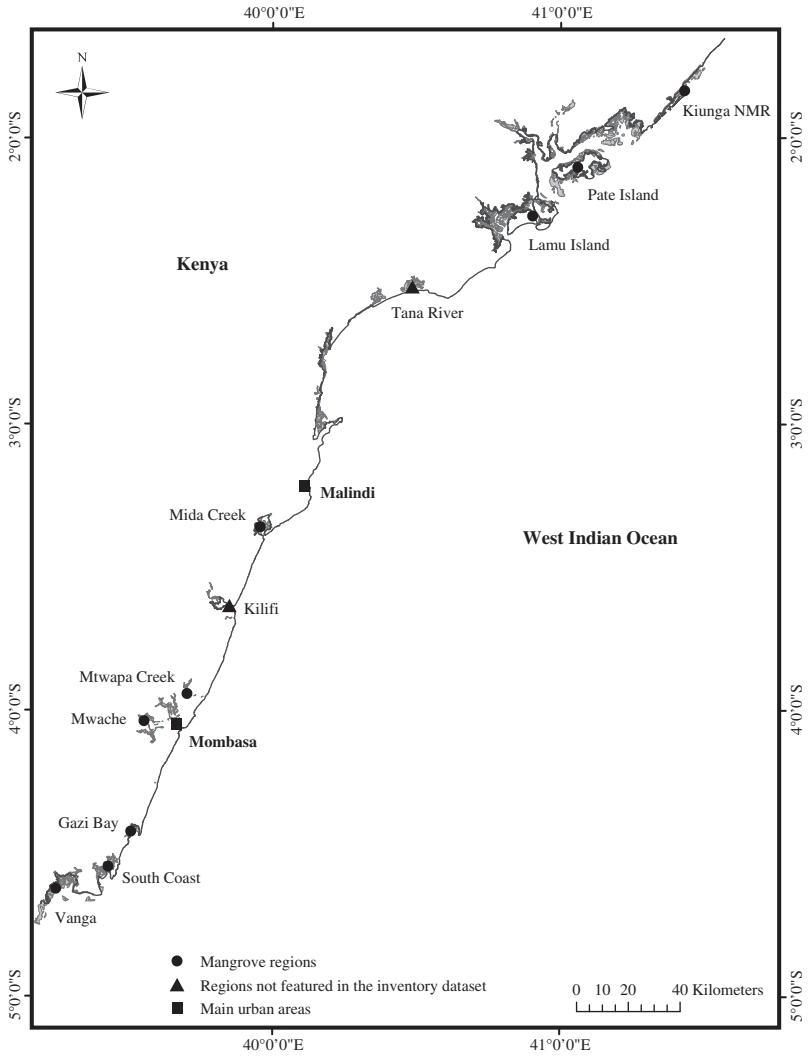

Fig. 1. Kenya coastline showing areas of mangrove forest where inventory data has been collected (dots). Inventory data collected within the general area of Lamu Island and Pate Island constitute the "South Lamu" study region. Kiunga NMR stands for Kiunga National Marine Reserve. Please note that the mangrove area defined as the "Tana River" region in this study spans the official districts of Kilifi and Tana River in Kenya and encompasses the mangroves just North of Malindi to the border of Lamu District. Kenya GIS base-map and mangrove shape-file obtained from the World Resources Institute (available at: <http://www.wri.org/>).

factor due to the unbalanced nature of the harvest dataset which has insufficient replication of species data at each site to allow separation of any possible variation in AGB attributable solely to either factor. In addition, Zianis and Mencuccini (2004) showed that within-species variability in allometric coefficients across sites is just as large as the variability in coefficients across species. Given that the harvest dataset comprises data from various studies any differences between the species_site groupings could also potentially incorporate an effect of study origin. However, harvest methodologies are broadly consistent across studies therefore it is likely the case that the random effects predictions are largely reflective of the differences across groups due to species and site effects.

Linear mixed-effects models were fitted using the lme4 package within R statistical software version 2.15.0 (Bates et al., (2011), http://CRAN.R-project.org/package=lme4). Prior to model fitting the logged predictive variables were centred at their mean to reduce any correlation between intercept and slope coefficients. Models were initially fitted using maximum likelihood (ML) estimation and compared using the Deviance Information Criterion (DIC) as outlined in Gelman and Hill (2007). In order to identify the best fixed and random effects terms for inclusion in the final model eight candidate models were fitted to the data (Table 2). Model notation follows that of Gelman and Hill (2007) where $\ln(y_i)$ is the response (AGB in this study) for the ith individual, α is the intercept, β represents the coefficients for the predictive variables diameter ($\ln(x_i)$) and height ($\ln(z_i)$) and σ_y^2 is the residual or the unexplained 'within-group' variance. The subscript term *j[i]* indexes the ith individual within the jth group and denotes where the intercept or a coefficient has been allowed to vary across groups ($j = 1,..., J$) as a random effect.

Model I was the simplest model and included a random effects term for the intercept only whilst the slopes of both predictive variables were kept constant across groups (Table 2). The inclusion of a random effects term for $\ln(x_i)$ and $\ln(z_i)$ coefficients in models II and III respectively led to a reduction in the DIC value in comparison with model I. In order to ascertain if both diameter and height were needed as predictive variables within the model; models IV and V excluded each variable as a fixed effect (and hence as a random effect) in turn. As shown in Table 2 there is clearly a need to include both variables as fixed effects within the model. This is especially evident in the case of model V where exclusion of diameter from the model had a large impact on the DIC value. Models

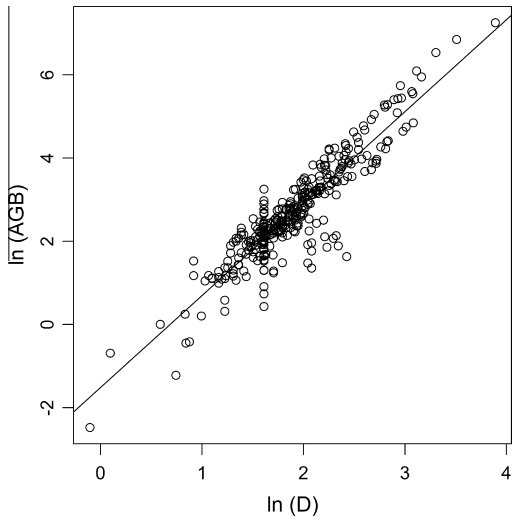

Fig. 2. Relationship between above-ground biomass (AGB) and stem diameter (D) of harvested mangrove trees after transformation by natural log. The vertical arrangement of data points at approximately $\ln(D) = 1.6$ is mostly due to data from the study by Kairo et al. (2009) which focused on harvesting trees from plantation forests of known age whereby a large proportion of data points arising from this study were of similar stem diameter (~5 cm).

Table 2
Comparison of candidate models fitted using maximum likelihood (ML) estimation, with corresponding DIC values.[a]

Model	DIC
I. $\ln(y_i) \sim N(\alpha_{j[i]} + \beta \ln(x_i) + \beta \ln(z_i), \sigma_y^2)$, for $i = 1,\ldots,n$,	274.1
II. $\ln(y_i) \sim N(\alpha_{j[i]} + \beta_{j[i]} \ln(x_i) + \beta \ln(z_i), \sigma_y^2)$, for $i = 1,\ldots,n$,	231.5
III. $\ln(y_i) \sim N(\alpha_{j[i]} + \beta \ln(x_i) + \beta_{j[i]} \ln(z_i), \sigma_y^2)$, for $i = 1,\ldots,n$,	220.3
IV. $\ln(y_i) \sim N(\alpha_{j[i]} + \beta_{j[i]} \ln(x_i), \sigma_y^2)$, for $i = 1,\ldots,n$,	260.5
V. $\ln(y_i) \sim N(\alpha_{j[i]} + \beta_{j[i]} \ln(z_i), \sigma_y^2)$, for $i = 1,\ldots,n$,	603.7
VI. $\ln(y_i) \sim N(\alpha_{j[i]} + \beta_{j[i]} \ln(x_i z_i), \sigma_y^2)$, for $i = 1,\ldots,n$,	299.1
VII. $\ln(y_i) \sim N(\alpha_{j[i]} + \beta_{j[i]} \ln(x_i^2 z_i), \sigma_y^2)$, for $i = 1,\ldots,n$,	240.1
VIII. $\ln(y_i) \sim N(\alpha_{j[i]} + \beta_{j[i]} \ln(x_i) + \beta_{j[i]} \ln(z_i), \sigma_y^2)$, for $i = 1,\ldots,n$,	206.1*

[a] The asterisk symbol denotes that model VIII was the best model overall.

were also fitted using two new combined predictive variables: $\ln(x_i z_i)$ and $\ln(x_i^2 z_i)$, both of which were logged and centred prior to model fitting as before. However, as shown in Table 2 models VI and VII using the combined variables displayed a poorer overall fit in comparison with models II and III (Table 2). Model VIII had the lowest DIC value of all the models under consideration indicating that the inclusion of a random effects term for the coefficients of both $\ln(x_i)$ and $\ln(z_i)$ was needed in order to account for variability in AGB across groups.

Model VIII was considered to be the most appropriate model overall and was subsequently re-fitted using restricted (or residual) maximum likelihood (REML) estimation in order to produce the best unbiased estimates of variance and co-variance parameters (Pinheiro and Bates, 2000). In model VIII the terms α_j, β_{jx} and β_{jz} signify that these parameters have themselves been modelled yielding a partial pooling estimate of α and the coefficients β_x and β_z for each group along with an estimate of the overall population mean and the 'between-group' variance (estimated from the data). The group-level model for model VIII can be written as:

$$\begin{pmatrix} \alpha_j \\ \beta_{jx} \\ \beta_{jz} \end{pmatrix} \sim N\left(\begin{pmatrix} \mu_\alpha \\ \mu_{\beta x} \\ \mu_{\beta z} \end{pmatrix}, \begin{pmatrix} \sigma_\alpha^2 & \rho_1 \sigma_\alpha \sigma_{\beta x} & \rho_2 \sigma_\alpha \sigma_{\beta z} \\ \rho_1 \sigma_\alpha \sigma_{\beta x} & \sigma_{\beta x}^2 & \rho_3 \sigma_{\beta x} \sigma_{\beta z} \\ \rho_2 \sigma_\alpha \sigma_{\beta z} & \rho_3 \sigma_{\beta x} \sigma_{\beta z} & \sigma_{\beta z}^2 \end{pmatrix} \right), \text{ for } j = 1,\ldots,J, \quad (3)$$

where the overall mean across all groups (the fixed effects estimates) for the intercept, slope of $\ln(x_i)$ and the slope of $\ln(z_i)$ are denoted by μ_α, $\mu_{\beta x}$ and $\mu_{\beta z}$ respectively. The between-group variance in the intercept, slope of $\ln(x_i)$ and the slope of $\ln(z_i)$ are given as σ_α^2 and $\sigma_{\beta x}^2$ and $\sigma_{\beta z}^2$ respectively. The parameters ρ_1, ρ_2 and ρ_3 are also estimated as the between-group correlations of the α's and β's (e.g. $\rho_1 \sigma_\alpha \sigma_{\beta x}$ is the correlation between the group intercepts and slopes of $\ln(x_i)$).

2.2.3. Simulation-based approach to biomass estimation

In order to estimate the biomass of mangroves along the entire Kenyan coastline the equations developed in this study were applied to a forest inventory dataset (detailed in Section 2.3) comprising 498 plots inventoried during the period 2007–2012. The modelling process described in Section 2.2.2 generated a mean biomass equation and a suite of specific equations; one for each of the eighteen species_site groups. The mean equation is comprised of the fixed effects estimates and can be regarded as a generic equation for Kenyan mangroves. The group specific equations represent the group departures from the fixed effects estimates (fixed effect estimates ± the group specific random effects) and are only valid for the specific groupings from which they were originally derived. Eight of the group specific equations can potentially be applied to the forest inventory dataset to estimate biomass as the remaining ten equations are only valid for species_site combinations occurring outwith Kenya. Therefore, group specific equations were applied to estimate the biomass of individual trees within the inventory dataset if those trees fell into one of the pre-existing groups identified within the harvest dataset. For example the group specific equation for Rhiz_Kin was applied to inventoried *Rhizophora* trees at Kinondo and so forth. In cases where inventoried trees did not fall into one of the pre-existing groups their biomass was estimated using the generic equation. The simulation-based approach adopted in this study allows for the propagation of measurement, parameter and residual uncertainty to estimates of biomass at the individual tree, plot and regional level.

2.2.4. Simulations for individual tree biomass

The above-ground biomass of each tree in the inventory dataset was simulated 10,000 times using a new set of simulated values for each iteration. In order to propagate measurement uncertainty possible values of stem diameter $\ln(D_{sim})$ and height $\ln(H_{sim})$ for each tree were randomly sampled from a normal distribution with mean equal to the observed value and one standard deviation conservatively assumed to be 5% and 10% of the observed diameter and height respectively. These assumed values of measurement uncertainty are consistent with the findings of previous studies (Chave et al., 2004; Gregoire et al., 1990; Phillips et al., 2000).

To propagate parameter uncertainty, possible values of the fixed effects intercept (α_{fixsim}) and coefficients for stem diameter ($\beta_{xfixsim}$) and height ($\beta_{zfixsim}$) were sampled from a multivariate normal distribution around means equal to μ_α, $\mu_{\beta x}$ and $\mu_{\beta z}$ from model VIII using the variance-covariance matrix of the fixed effects. In cases where the generic equation was applicable (to estimate the biomass of new trees in new groups) simulated values of the random effects for the intercept (α_{ransim}) and the coefficients for stem diameter ($\beta_{xransim}$) and height ($\beta_{zransim}$) were generated by sampling from a multivariate normal distribution around means equal to zero using the variance-covariance matrix of the group level (or mean) random effects (Eq. (3)). In cases where a group specific equation was applicable (to estimate the biomass of new trees in existing groups) possible values of the random effects were simulated as for the generic equation, however values were sampled around means equal to the group specific random effects for the intercept and coefficients and used the variance-covariance matrix

of the group specific random effects. Simulated values were then used in Eq. (4) to calculate AGB biomass ($\ln(AGB_{pred})$) for each tree:

$$\ln(AGB_{pred}) = \alpha_{sim} + ((\beta_{xfixsim} + \beta_{xransim})\ln(D_{sim})) + ((\beta_{zfixsim} + \beta_{zransim})\ln(H_{sim})) \quad (4)$$

where α_{sim} is the un-centred intercept (calculated as shown in Eq. (5)) and corrects for the use of mean centred predictive variables diameter and height during model development (Section 2.2.2).

$$\alpha_{sim} = (\alpha_{fixsim} + \alpha_{ransim}) - ((\beta_{xfixsim} + \beta_{xransim})\bar{x}) - ((\beta_{zfixsim} + \beta_{zransim})\bar{z}) \quad (5)$$

where $\bar{x}$ and $\bar{z}$ are the mean logged values of diameter and height respectively from the harvest dataset. In order to account for residual uncertainty in biomass estimates; possible values of biomass ($\ln(AGB_{Est})$) were randomly sampled from a normal distribution with mean equal to $\ln(AGB_{pred})$ and standard deviation equal to σ_y (the standard deviation of σ_y^2) from model VIII. Values of $\ln(AGB_{Est})$ were then back-transformed by taking the exponent; producing 10,000 estimates of AGB (in kg DW) for each tree. The estimates for all trees within a plot were then summed at each iteration point yielding a distribution of 10,000 possible estimates of total biomass for each plot. The median was taken as the plot level biomass estimate as this provided the most typical value from skewed distributions of the simulations. The quantiles from the distribution of plot estimates were used for calculating the 95% prediction interval (95% PI) at the plot level.

2.2.5. Calculation of regional level prediction intervals

In order to upscale biomass estimates from plot to regional level, plots were first grouped according to the mangrove regions identified in the inventory dataset (Table 3). Plots within Lamu District were further sub-divided into those within Kiunga National Marine Reserve (NMR) and those outwith the reserve (hereafter "South Lamu"). Due to their close geographical proximity plots from Shirazi, Ramisi, Funzi and Bodo were aggregated to form the region "South Coast". The mean biomass estimate was calculated for each iteration (across all plots within a region) yielding a distribution of 10,000 possible mean biomass estimates. The mean of this distribution was taken as the regional level biomass estimate (Mg ha^{-1}) and provides the expected value of AGB taking into account the whole scale of values present in a specific geographical area. The quantiles from the distribution were used to calculate the 95% PI at the regional level.

2.2.6. Model validation

The predictive performance of model VIII was evaluated using a harvest dataset from the Zambezi Delta, Mozambique (Table 1). The simulation process detailed in Section 2.2.4 was repeated for the 23 trees in the Zambezi dataset. For each tree the median fitted value of AGB (kg) was obtained along with the 95% PI for the median.

2.3. Forest inventory dataset

A summary of the forest inventory dataset is provided in Table 3, recent estimates of mangrove cover by region are provided in Table 4 and the location along the Kenyan coastline of each region is shown in Fig. 1. The cover estimates in Table 4 were derived from 2.5 m resolution SPOT remote sensing imagery acquired over the Kenyan coastline during 2009–2011 (see Rideout et al., 2013 for further details). The inventory dataset is a combination of data collected by this and other studies. All studies conducted prior to 2010/2011 had the objectives of characterising and investigating mangrove structural variability and change in the southern coastal region. However, in the current study sampling strategy was tailored (as much as was practicable) towards facilitating both a statistical and remote sensing based approach to biomass estimation along the entire coastline. Thus studies within the inventory dataset differ in terms of sampling strategy and plot size. There is also an obvious bias in total sampling effort towards sites in the south coast (Table 3).

In general all inventory studies followed a standardised methodology of within-plot data collection. In all studies the species, stem diameter and total height of all trees within each plot which met the diameter measurement threshold were recorded. Stem diameter was recorded to the nearest millimetre and was measured at 1.3 m aboveground (DBH) except in the case of *Rhizophora* sp. where stem diameter was measured at ~30 cm above the highest prop root if this occurred above 1.3 m. In cases where trees branched below 1.3 m (common in *Avicennia* sp.) and branches met the diameter measurement threshold; the diameter and height of each branch was recorded separately. In the current study total tree height was measured using an ultrasonic vertex hypsometer (Haglöf, Sweden). In all other studies tree height was measured using a graduated pole.

2.3.1. Mida Creek and Lamu District

Forest inventory data from the Mida Creek area and Lamu District was collected as part of this study during June–August 2010 and 2011. Mida Creek (3°20′S, 40°00′E) is situated mid-way along the Kenyan coast ~23 km south of the town Malindi in Kilifi District. Some of the mangrove forest in this area falls within the boundaries of Watamu Marine National Park (WNMP); however the majority is outwith the protected area. Regardless of location (within or outside of WNMP) harvesting of mangroves is currently prohibited in the Mida Creek area. In total 14 plots within the Mida Creek area were inventoried comprising nine 0.04 ha (20 × 20 m) plots, four 0.25 ha (50 × 50 m) plots and one 0.5 ha (100 × 50 m) plot. None of the inventoried plots were located within the marine park.

The Lamu archipelago extends between 2°22′S, 40°48′E in the South and 1°44′S, 41°30′E in the North and is part of Lamu District. Lamu District currently holds the greatest proportion of remaining mangrove cover in Kenya (Table 4). Mangroves in the extreme north, close to the border with Somalia are part of Kiunga NMR and are considered to be the only remaining examples of relatively "pristine" mangrove forest in Kenya. Forty-one plots within Lamu District were inventoried comprising twenty-five 0.04 ha plots, fifteen 0.25 ha plots and one 0.5 ha plot. Within Lamu District sites visited included: Kiunga NMR ($n = 16$ plots), Pate Island area ($n = 15$) and Lamu Island area ($n = 10$).

Plots inventoried in Mida Creek ($n = 6$) and Lamu District ($n = 8$) during 2010 were all 0.04 ha in size. Plots were positioned at random within *Rhizophora* zones and all trees within each plot with stem diameter ⩾2.5 cm were measured. Plots inventoried during 2011 were a mixture of 0.04 ha plots (Mida Creek: $n = 3$, Lamu District: $n = 17$) located at random within randomly chosen map grid squares (grid resolutions of 500 × 500 metres and 1000 × 1000 m) and larger plots (0.25 ha and 0.5 ha) which were positioned at random within larger areas pre-identified using optical and radar remote sensing imagery. These pre-identified areas were judged to be potentially distinct from each other in terms of forest structure/biomass and also to broadly represent the main levels of structural variation within the study region as a whole. This more targeted plot location strategy was for the purpose of facilitating future remote sensing work. All plots inventoried in 2011 included all trees within each plot which met the criteria of having stem diameter ⩾5 cm.

2.3.2. Gazi Bay

The Gazi Bay inventory consists of 116 plots in total. As part of this study twenty-four 0.01 ha (10 × 10 m) plots were inventoried

Table 3
Provenance and summary of mangrove forest inventory dataset.[a]

Region	Study	Date	No. of plots	Plot size (ha)	Stem diameter range (cm)	Height range (m)
Mida Creek	This study	2010/2011	14	Variable (ranging from 0.01 - 0.5)	2.5–58	1.5–17.7
Lamu District:	This study	2010/2011				
South Lamu			25		2.4–54	1.8–28.5
Kiunga			16		2–49.8	1.3–23.7
Gazi Bay	This study	2010/2011	28		5–64	1.8–20.2
	CAMARV	2009	18	0.01	0.5–51	0.6–15
	UNDP	2009	70	0.01	2.2–63.3	2–21
Mtwapa Creek	Okello (unpublished results)	2010	54	0.01	2.5–46.9	0.5–15
Mwache	Kaino (2013)	2011	67	0.01	2–53	1–15
South Coast:	KMFRI	2007				
Shirazi			43	0.01	5–47.5	2–16
Ramisi			22	0.01	5–48.4	2.5–15
Funzi			24	0.01	5–43.2	1.5–15
Bodo			34	0.01	5–60.5	2–14
Vanga	KMFRI	2012	83	Variable (ranging from 0.0025 - 0.04)	2.5–72.5	1–25

[a] Study abbreviations are as follows; United Nations Development Programme (UNDP); Capacity Building for Mangrove Assessment, Restoration and Validation (CAMARV) and Kenya Marine and Fisheries Research Institute (KMFRI).

Table 4
Mangrove cover estimates for inventory regions derived from high-resolution SPOT satellite imagery.[a]

Region	Mangrove cover estimate (ha)	Proportion of total cover (%)
Mida Creek	1657.8	3.6
South Lamu	26609.1	57.1
Kiunga (NMR)	4763.8	10.2
Gazi Bay	589	1.3
Mwache	2667.1	5.7
Mtwapa Creek	519.4	1.1
South Coast	2253.1	4.8
Vanga	3440	7.4
Kilifi*	640.2	1.4
Tana river*	3433	7.4
Total cover	46572.5	

[a] Regions marked with asterisks' do not feature in the forest inventory dataset. For details of SPOT image processing and analysis see Rideout et al. (2013).

during July 2010 and four 0.25 ha plots were inventoried during August 2011. The smaller plots inventoried in 2010 were positioned randomly within the main identifiable mangrove zones and included all trees DBH $\geqslant$ 5 cm. The larger plots collected in 2011 were positioned using the same procedure as detailed above for the large plots in Section 2.3.1 and included all trees within each plot stem diameter $\geqslant$5 cm.

The remaining plot data (n = 88) from the Gazi Bay area were collected in 2009 as part of two internationally funded short-term projects. Eighteen 0.01 ha plots were inventoried in the area adjacent to Gazi village as part of a project entitled CAMARV (Capacity Building for Mangrove Assessment, Restoration and Valuation in East Africa) funded by the Natural Environment Research Council (NERC) of the United Kingdom. Seventy 0.01 ha plots were inventoried as part of a UNDP-GEF Small Grants Programme project co-ordinated by Gazi Womens Group. In both projects plots were randomly positioned along a transect within each identifiable mangrove zone and all trees within each plot were included in the inventory.

2.3.3. Mwache and Mtwapa Creek

Mwache (4°2′S, 39°33′E) and Mtwapa Creek (3°57′S, 39°43′E) are both examples of peri-urban mangroves due to their close proximity to the city of Mombasa and the town of Mtwapa respectively. Both areas are considered to be degraded due to a combination of sewage pollution, timber over-exploitation and in the case of Mwache; the heavy sedimentation and flooding associated with the *El Niño* event of 1997–1998 (Kitheka et al., 2002). Inventory data from Mtwapa Creek (n = 54) was collected in 2010 as part of a study by Okello (unpublished results). Data from Mwache (n = 67) was collected in 2011 as part of a study conducted by Kaino (2013) and funded by the Western Indian Ocean Marine Science Association (WIOMSA). Both studies used plot sizes of 0.01 ha. Plots at Mtwapa Creek were positioned along transects running perpendicular to the shoreline at ~50 m intervals and all trees with stem diameter $\geqslant$2.5 cm were measured. At the Mwache site plots were positioned along transects running perpendicular to the shoreline at 100 m intervals using a stratified sampling scheme based on observed differences in forest composition and structure. All trees with stem diameter $\geqslant$2 cm within each plot were measured.

2.3.4. South Coast

Forest inventory data from the South Coast (Shirazi, Ramisi, Funzi and Bodo) was collected in 2007 by KMFRI as part of a Kenya government funded project. In total there are data from one hundred and twenty-three 0.01 ha plots comprising; Shirazi (n = 43), Ramisi (n = 22), Funzi (n = 24) and Bodo (n = 34). Plots were positioned at ~20 m intervals along transects running perpendicular to the shoreline and all trees with stem diameter $\geqslant$5 cm were included in the inventory.

2.3.5. Vanga

Mangroves close to the Kenya–Tanzania border were inventoried by KMFRI during January 2012. Plots inventoried within the Vanga mangrove system number 83 in total and are of variable size (sixty-nine 0.01 ha, six 0.04 ha and eight 0.0025 ha (5 $\times$ 5 m) plots). Plots were positioned within each identifiable mangrove zone using a stratified random sampling strategy and all trees $\geqslant$2.5 cm in diameter were recorded.

3. Results

3.1. Model VIII summary and key features

Overall, there is good correspondence between the fitted values of AGB (as estimated from model VIII) and the original observed values of AGB for trees in the harvest dataset (Fig. 3(a) and (b)). The mean absolute error (MAE) in predictions of AGB from model

VIII is 6.3 kg and the mean bias (observed-fitted) in predictions is an underestimate of just 0.06 kg. The model performs well at values of observed AGB $\leqslant$ 50 kg (Fig. 3(b)) which comprise 85% of the total dataset. There is some divergence from the reference line for the few trees in the harvest dataset with higher AGB values (Fig. 3(a)). Poorer model fit at higher AGB is likely due to the paucity of harvest data from larger trees with just 11 out of 337 trees in the dataset having an observed AGB $\geqslant$ 200 kg. Further diagnostic plots (data not shown) revealed no systematic trend in model residuals when plotted against the fitted values and against each of the predictive variables.

Mixed-effects models partition the total variance in the response variable (AGB in this study) between the main components of the model (Fig. 4). The proportional contribution of the random effects terms (σ^2_α, $\sigma^2_{\beta x}$, $\sigma^2_{\beta z}$) and the residual variance (σ^2_y) to the total variance was calculated for each term as:

$$\% \text{ contribution} = ((\sigma^2_\alpha/\text{tot\_var})100) \quad (6)$$

where e.g. σ^2_α is the variance in the model attributed to between-group differences in the intercept and tot_var is the total variance from model VIII calculated as the variance of the logged values of total above-ground biomass of the 337 trees in the harvest dataset. Thus, the contribution to the total variance attributable to the combined fixed effects terms was calculated as:

$$\% \text{ contribution} = (((\text{tot\_var} - (\text{sum}(\sigma^2_\alpha + \sigma^2_{\beta x} + \sigma^2_{\beta z} + \sigma^2_y)))/\text{tot\_var})100) \quad (7)$$

As expected, most of the variability in AGB was accounted for in model VIII by the fixed effects terms (Fig. 4). Together the random effects terms accounted for 41% of the variance in AGB. Between-group variability in the slopes of the predictive variables diameter and height was very similar accounting for 18% and 19% of the total variance respectively. In combination the fixed and random effects explained 94% of the variability in AGB leaving a relatively small residual variance of 6% (Fig. 4).

The random effects represent the group-specific departures (either ±) from the fixed effects estimate of the intercept and the coefficients for diameter and height. There is clearly some between-group variability in the random effects for the eight species_site groups occurring in Kenya (Fig. 5). The 95% PI around the random effects is more constrained for groups with a larger sample size (Fig. 5) and there is some degree of overlap in the prediction intervals between most groups.

The random effects for most groups fall within the bounds of the 95% confidence interval (95% CI) of the fixed effects estimate of each parameter (Fig. 5). However, the predicted random effect for the intercept of group Rhiz_Gaz and the coefficient of height for group Avic_Gaz show no overlap with the fixed effects estimates for these parameters. For group Sonn_Gaz there is a pronounced departure from both the fixed effects estimates and from the predicted random effects for the other groups. Such deviation from the fixed effects estimates suggest that the allometry for these species_site groupings may be distinct from that of the other groups in the harvest dataset and highlights the general need for the inclusion of group effects in regression models.

3.2. Model validation

For harvested trees in the Zambezi Delta predictions of median AGB (±95% PIs) from model VIII correspond well with the original observed values of AGB (Fig. 6). A linear regression between the logged observed values and predicted median values of AGB was used to further assess the predictive ability of model VIII ($R^2 = 0.96$, $p = < 0.001$). The 95% confidence interval for the intercept includes zero (−0.23 ± 0.37) and for the regression slope includes one (1.01 ± 0.09). The uncertainty around predictions is well constrained for trees with lower AGB but increases with increasing predicted AGB.

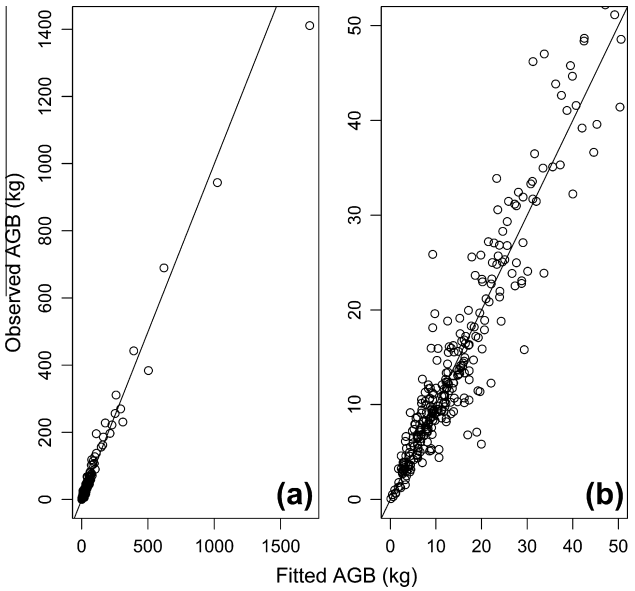

Fig. 3. (a) Total above-ground biomass (AGB) in kg as measured for each tree in the harvest dataset versus the corresponding fitted value (kg) from model VIII and (b) as (a) but re-scaled to show in detail the correspondence between observed and fitted values at the lower range of AGB. The reference lines shown in (a) and (b) represent a 1:1 correspondence between observed and fitted values.

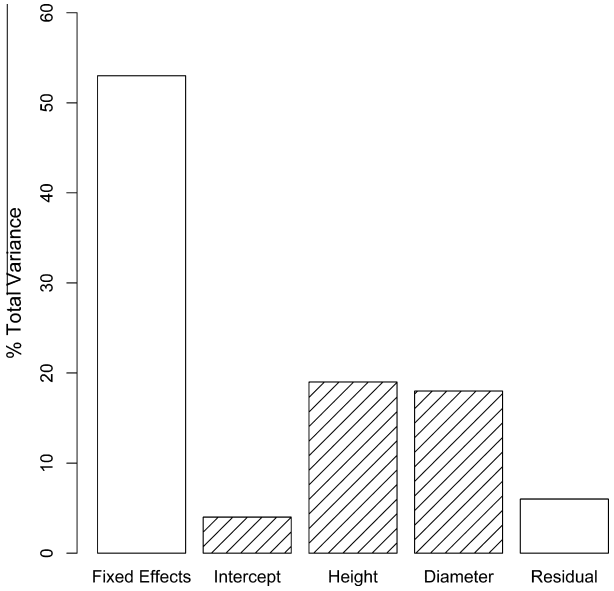

Fig. 4. Proportion of the total variability in AGB of harvested trees associated with the fixed effects terms, the random effects terms (hatched bars) and the remaining unexplained (residual) variance from Model VIII.

3.3. Plot level AGB estimates

Plot level estimates of mangrove AGB vary greatly within and between regions (Fig. 7). Within each study region (except Kiunga) there are two orders of magnitude difference between the smallest and largest plot estimates. If the 95% PIs are considered then the scale of maximum AGB across regions ranges between

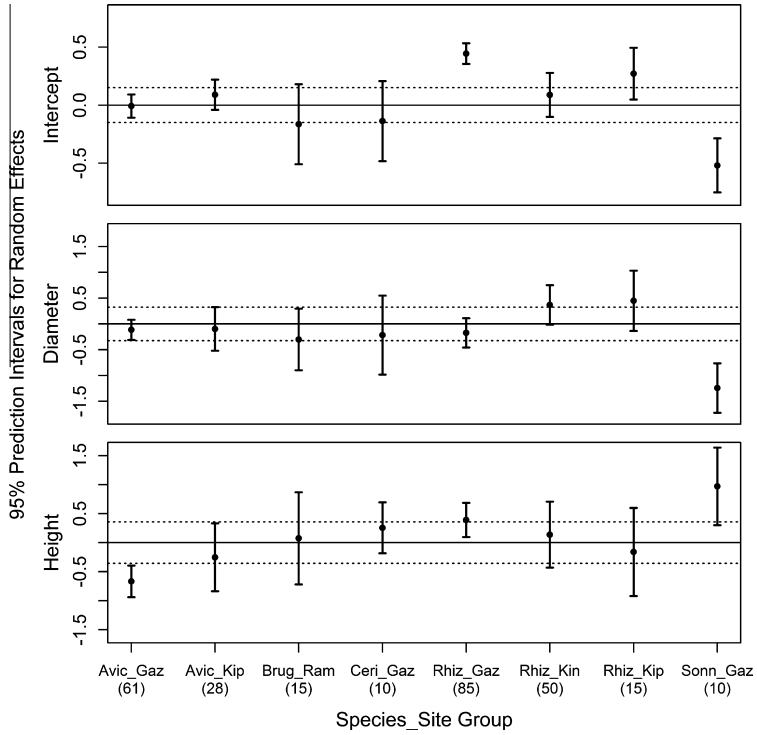

Fig. 5. Group-specific random effects (±95% PI) for the intercept and the coefficients of diameter and height. The solid line at zero represents no departure from the fixed effects estimate for each parameter and the dashed lines on either side are the upper and lower limits of the 95% CI of the fixed effects estimate. Species_site groups correspond to the first four letters of the species followed by the first three letters of the site (see Table 1). Numbers in parentheses denote sample size for each group.

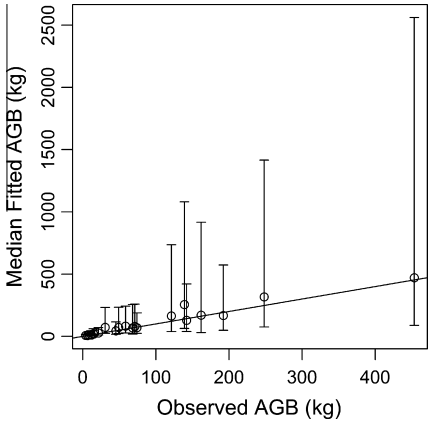

Fig. 6. Total above-ground biomass (AGB) in kg as measured for each tree in the Zambezi harvest dataset versus the corresponding median fitted value (kg ±95% PI) from model VIII. The 95% PI is the difference between the 97.5% and 2.5% quantiles of the simulated distribution of possible values of median AGB for each tree. The reference line represents a 1:1 correspondence between observed and fitted values.

~200 Mg ha^{-1} at Mida Creek to >2000 Mg ha^{-1} at Vanga. For each region the uncertainty in estimates is tightly constrained for plots with low values of AGB but there appears to be a general pattern of larger prediction intervals around estimates for plots with higher AGB (Fig. 7). For some regions there is considerable variation in the PIs of plots with similar median AGB estimates (e.g. see Mwache plots 45 and 46 in Fig. 7). It is likely that larger PIs around the estimates of some plots is not associated with higher biomass *per se* but is due to the presence of large diameter trees in these plots for which the biomass has been estimated with relatively less precision.

3.4. Regional level AGB estimates

As expected, estimates of mean AGB vary amongst the study regions which span the entire Kenyan coastline (Fig. 8). There is a difference of >120 Mg ha^{-1} between the lowest estimate for mangroves at Mtwapa Creek near Mombasa (73 Mg ha^{-1}) to the highest for mangroves within Kiunga NMR (200 Mg ha^{-1}). However, there is a general overlap between the prediction intervals of most regions and the estimates of mean AGB do not differ substantially between the regions Mwache, Gazi, South Coast, Vanga and South Lamu. Uncertainty around the estimates of mean AGB is reasonably well constrained with an absolute difference between upper and lower prediction limits of <50 Mg ha^{-1} for all regions.

The regional level estimates of mean AGB (Fig. 8) and mangrove cover (Table 4) were used in a basic up-scaling exercise in order to give an indication of the total AGB of mangroves within each region and within Kenya as a whole (Table 5). Up-scaled values of total mangrove AGB in megatonnes (Mt) were calculated by multiplying the regional level estimates of mean AGB (Mg ha^{-1}) shown in Fig. 8 by the corresponding estimate of total mangrove cover (ha) for each region (Table 4). There was no inventory data available for mangroves at Kilifi and Tana River therefore it was not possible to estimate mean AGB for these regions. For the purposes of up-scaling it was assumed that the mean AGB of mangroves at Kilifi and Tana River lies somewhere between that of Mtwapa Creek (the lowest regional mean) and Kiunga (the highest regional mean). Thus for sites Kilifi and Tana River two sets of possible values of total AGB ('Low' and 'High') were calculated using the lowest (Mtwapa Creek) and the highest (Kiunga) of the regional level estimates of mean AGB. Consequently there are also two sets of estimates of the total AGB of Kenyan mangroves; one in which the lowest estimates for Kilifi and Tana River were added to the total AGB of the other regions ('Kenya Low') and one in which the

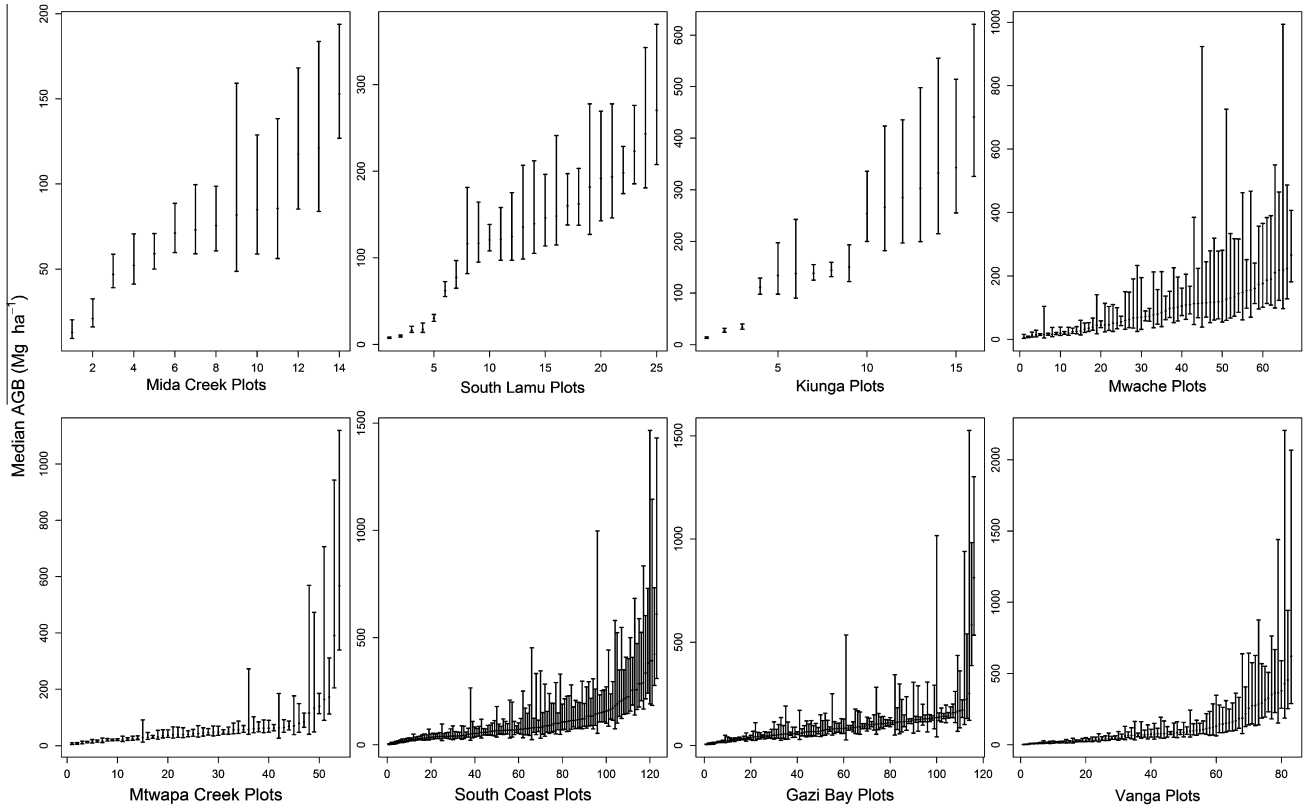

Fig. 7. Estimated median above-ground biomass (AGB) of each plot within the forest inventory dataset (±95% PI). Plots have been grouped according to the eight regions identified in the inventory dataset. For each region plots appear in ranked order from low to high estimated AGB. The 95% PI is the difference between the 97.5% and 2.5% quantiles of the simulated distributions of possible values of median AGB for each plot.

highest estimates were used ('Kenya High'). Lamu District (South Lamu + Kiunga) holds the highest proportion (~69–75% dependent on Kenya total) of mangrove AGB in Kenya (Table 5). Despite having one of the lowest estimates of mean AGB the estimated total AGB of mangroves at Mida Creek is more than double that of Gazi Bay due to the higher mangrove cover at Mida Creek.

The uncertainty around the estimates of total AGB are generally well constrained for all regions (Table 5). However, the Low and High estimates of total AGB for Kilifi and Tana River differ by a factor of ~2.7. This constitutes another level of uncertainty for these regions and consequently the overall total for Kenya which differs by ~8% between Low and High estimates.

4. Discussion

4.1. Applicability and interpretation of Model VIII

This study used mixed-effects modelling to account for both species and site variability in the allometric relationship for mangroves producing a generic equation for Kenyan mangroves and a set of species-site specific equations. The procedure for uncertainty propagation employed in the current study ensures that estimates of AGB at different spatial scales are accompanied by a realistic measure of the total uncertainty. It is important to note that although mangroves have been used as a case study here, the kind of models and methodologies presented can be regarded as broadly applicable to forests in general.

The practical application of the equations developed in the current study is dependent on the target of inference. The set of species-site specific equations are only applicable to four species within the Gazi Bay region and simulations using these equations account for the uncertainty in predicting the AGB of a new tree within a pre-existing group. In contrast, the generic equation has a much broader application as it can be used to predict the AGB of new trees where there is no pre-existing knowledge of the specific species-site allometric relationship: the most commonly encountered scenario in practical biomass studies. The generic equation offers a far better solution than simply disregarding the additional uncertainty involved in applying an equation that was perhaps derived for a different species and/or a different site.

The predictions of AGB from model VIII show good correspondence with the observed values of AGB used to fit the model (Fig. 3). Perhaps more importantly, the median fitted values of AGB (±95% PIs) from model VIII show good overall correspondence with the observed values of AGB for trees within the Mozambican validation dataset (Fig. 6). This would seem to indicate that accounting for variance due to species and site effects in biomass regression models is important if they are to be used effectively elsewhere to predict AGB. Indeed, a large proportion of the total variance in model VIII was attributed to between-group variability in the coefficients of the predictive variables diameter and height (Fig. 4). Both species and site specificity in the allometric relationship for mangroves is indicated by the group-specific random effects (Fig. 5). Most groups show some overlap in predicted random effects but there are some differences between species at the same site (species_Gaz groups) and between sites for the same species (Rhiz_site groups). However the use of a combined species_site grouping factor precludes any conclusion regarding the relative contribution of each factor (species and site) to the total variance in the allometric relationship. It is also not possible to formally assess the potential contribution of a study effect to the predicted random effects in this

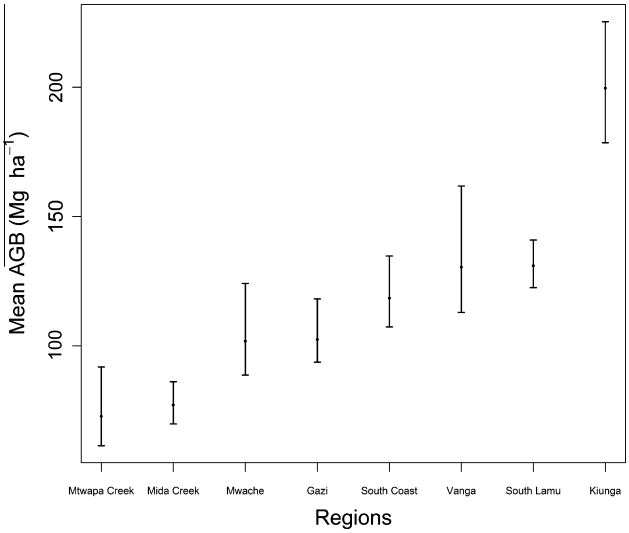

Fig. 8. Estimated mean AGB (±95% PI) of mangroves within each region. The 95% PI is the difference between the 97.5% and 2.5% quantiles of the simulated distribution of possible values of mean AGB for each region.

Table 5
Estimated total mangrove above-ground biomass (AGB) for Kenya and for each region within Kenya.[a]

Region	2.5% Quantile of total AGB (Mt)	Mean of total AGB (Mt)	97.5% Quantile of total AGB (Mt)
Mtwapa Creek	0.032	0.038	0.048
Mida Creek	0.116	0.128	0.143
Mwache	0.237	0.272	0.331
Gazi Bay	0.055	0.060	0.070
South Coast	0.242	0.267	0.304
Vanga	0.388	0.449	0.556
South Lamu	3.260	3.486	3.749
Kiunga	0.851	0.951	1.073
Kilifi (Low)	0.039	0.047	0.059
Kilifi (High)	0.114	0.128	0.144
Tana River (Low)	0.211	0.250	0.315
Tana River (High)	0.613	0.685	0.774
Kenya Total (Low)	5.431	5.947	6.648
Kenya Total (High)	5.908	6.464	7.192

[a] 1 Megatonne (Mt) = 1 million tonnes. The uncertainty around estimates of total AGB for each region is represented by the 2.5% and 97.5% quantiles of the mean.

study. However, as mentioned in Section 2.2.2 any such effect is assumed to be minimal due to the general agreement in methodology across studies included in the harvest dataset. The only study which differed notably in methodology was that of Lang'at (2008) where total above-ground biomass comprised stem weight only (Table 1). In this case the sample size was fairly small (15 trees) and re-fitting model VIII after excluding this dataset did not substantially alter the fixed effects estimates, predicted random effects or residual variance.

In modelling the covariance of the distribution of random effects, the constraints imposed by the mixed-effects model used in the current study on the estimated correlation parameters may be considered too restrictive when more than two coefficients vary by group (Gelman and Hill, 2007). Although outwith the scope of the current paper; an alternative approach for future study would be to use a scaled inverse-Wishart distribution as the prior for modelling the covariance matrix of the random effects in a fully Bayesian model (Dietze et al., 2008; Gelman and Hill, 2007).

Ideally regression models should not be applied outwith the data range for which they were derived (Chave et al., 2005; Chave et al., 2004). The lack of large tree harvest data means that extrapolation is often a practical necessity when estimates of AGB are needed for large trees within forest inventory datasets. In this study, it is assumed that the log-log linear relationship will hold for trees beyond the original data range. It is, however, acknowledged that this may not be the case and that the estimates of AGB for trees outwith the data range recorded in harvest dataset will include additional uncertainty due to extrapolation. Only a very small proportion of trees in the inventory dataset (0.1%) had a recorded diameter exceeding that found within the harvest dataset and none exceeded the height range. However, the effect of having limited information regarding the allometric relationship for large trees is apparent in the poorer model fit at higher AGB values (Fig. 3). It is also apparent (to some degree) in the width of the prediction intervals around the larger trees in the validation dataset and the estimates of AGB at the plot, regional and landscape level. This is presumably due to the fact that by accounting for the covariance of the predictive uncertainty at the single tree level in producing estimates of AGB at aggregated levels (e.g. a plot) the aggregated predictive uncertainty is realistically larger than if the AGB of multiple trees had simply been summed (Wutzler et al., 2008). In addition, the greater width of the PIs for larger trees is an inevitable consequence of using a log-normal model where the variability is related to the mean on the linear scale. An approach to consider for future study would be to investigate the use of alternative distributions for the variability.

The 95% PIs in the current study are generally well constrained given that measurement and predictive uncertainty have been fully propagated to estimates. In addition, prediction intervals take into account both the uncertainty in estimating the conditional mean of the response and the variability in the conditional distribution of the response and as such are generally larger than the frequentist confidence intervals employed to represent uncertainty in most other studies. However, for a few of the plots in the inventory dataset the upper limit of the PI around the median estimate of AGB is exceptionally high (Fig. 7) and exceeds the highest levels of AGB previously reported for mangroves. The effects of both extrapolation and small plot size could possibly explain these extreme upper PI values for selected plots. All of the affected plots measure just 10 $\times$ 10 m and contain two or more large diameter trees which in some cases exceed the maximum diameter (48.9 cm) found in the harvest dataset. The presence of a few large trees in a small plot can skew results, however tree level and sampling uncertainties tend to be reduced in larger plots (Chave et al., 2004).

4.2. Comparison and interpretation of large-scale AGB estimates

Previous allometry/biomass studies conducted in Kenya have focused on the development and application of species-specific allometric equations to mangroves at a particular site. As a result existing published estimates of AGB for Kenyan mangroves are on a species by site basis and in many cases refer to monoculture plantation forest established at Gazi Bay (Kairo et al., 2009; Kairo et al., 2008; Tamooh et al., 2009). Estimates of AGB for natural mangrove forest in Kenya vary considerably between sites but also between studies conducted at the same site. Within the Mida Creek area Gang and Agatsiva (1992) estimated the AGB of *Rhizophora* forest as 11.8 Mg ha^{-1}. However, their estimate is based on the data from just one plot and there is no mention of how this estimate was derived (Gang and Agatsiva, 1992). For the same species at Gazi Bay Slim et al. (1996) and Kirui et al. (2006) produced substantially higher estimates of mean AGB at 249 Mg ha^{-1} (± s.d. 40.1) and 452.02 Mg ha^{-1} respectively. Similar to the study by

Gang and Agatsiva (1992) the estimate of AGB from Slim et al. (1996) was based on the application of their allometric equation to *Rhizophora* trees within one 20 × 20 m mono-specific plot and therefore cannot reasonably be assumed to represent the variability of *Rhizophora* forest within Gazi Bay. The highest estimate from Kirui et al. (2006) is more akin to the level of AGB found in mangroves in South East Asia (Komiyama et al., 2008) and it is not clear how their mean estimate was derived. In contrast to previous studies, this study has focused on providing estimates of mangrove AGB at varying spatial scales. This different approach means that the estimates provided here are not readily comparable with those from previous biomass studies conducted in Kenya. However, to facilitate some kind of comparison the outputs of the simulation procedure (Section 2.2.4) were sub-set to provide an estimate of mean AGB for just *Rhizophora* forest at Gazi Bay of 134.5 Mg ha^{-1} (95% PI range 125.1–146.8 Mg ha^{-1}).

Estimates of biomass density (mean Mg ha^{-1}) at large spatial scales such as those produced in the current study can be regarded as a comparative tool by which to assess the level of AGB at different sites/regions or between countries or forest types. Levels of mean AGB have been found to vary considerably between mangrove forests across the globe (see review by Komiyama et al., 2008) ranging between 31.5 Mg ha^{-1} (± s.d. 2.9) for pioneer mangrove forest in French Guiana (Fromard et al., 1998) to 536.6 Mg ha^{-1} (95% CI range 327.6–743.5 Mg ha^{-1}) for mangroves in Micronesia (Donato et al., 2012). Such broad-scale variability can be attributed to differences in floristic composition, climatic conditions, hydrology, geomorphology, successional stage and disturbance history (Fromard et al., 1998).

The regional estimates of mean AGB (±95% PI) shown in Fig. 8. represent a best attempt at summarising the level of AGB within different mangrove regions in Kenya. The two regions with the lowest estimated mean AGB were Mtwapa Creek (72.8 Mg ha^{-1}, 95% PI range 61.4–91.9 Mg ha^{-1}) and Mida Creek (77.1 Mg ha^{-1}, 95% PI range 69.9–86.2 Mg ha^{-1}) and are comparable to the level of AGB (71–85 Mg ha^{-1}) found in mixed mangrove forests dominated by *R. mucronata* and *A. marina* in Sri Lanka (Amarasinghe and Balasubramaniam, 1992). The estimate for Mida Creek is somewhat lower than expected and could be due to insufficient inventory data from this region (n = 14 plots) but it is also likely reflective of the level of forest degradation in this area due to illegal and poorly managed logging practices (Kairo et al., 2002). The region with the highest estimate of mean AGB was Kiunga NMR (199.6 Mg ha^{-1}, 95% PI range 178.6–225.3 Mg ha^{-1}). This level of AGB is comparable to that reported for mangroves in Micronesia (Donato et al., 2012; Kauffman et al., 2011) and mature coastal mangroves in French Guiana (Fromard et al., 1998) and exceeds the estimate by Donato et al. (2011) of 169.9 Mg ha^{-1} for oceanic mangroves in the Indo-Pacific region.

Although the estimates of AGB produced in this study are statistically robust, it is important to note the underlying assumption that estimates at large spatial scales have been obtained using a sample which is representative of the variability in forest composition and structure within the area in question (Chave et al., 2004). The estimates of mean AGB in this study were derived using all available current inventory data for each region. It seems reasonable to assume that due to the sampling strategy employed (stratified random) and the comparatively large sampling effort (total number of plots sampled) that the mangrove areas in the South of Kenya (Gazi Bay, Mwache, Mtwapa Creek, South Coast and Vanga) have been adequately sampled. In addition, the large within-region variability in estimates of median AGB at the plot level (Fig. 7) would suggest that there has been no sampling bias in terms of plot location, for example by preferentially locating plots in areas likely to yield high biomass and that the range of possible biomass values within each region has been adequately captured.

The regional estimates for Mida Creek and Lamu District (South Lamu and Kiunga) are based on relatively small inventory datasets (n = 14 plots in Mida Creek, 25 in South Lamu and 16 in Kiunga) due to the larger resource requirement and practical difficulties (e.g. accessibility) associated with sampling areas in the North. While the sampling strategies employed in these regions (random and stratified random) are appropriate from a statistical point of view; it is recommended that further data collection is undertaken in order to increase sample size and ensure representivity in these regions. This is particularly important in the case of Lamu District which covers a large geographical area and is worthy of further division into smaller sub-regions. For example, the mangroves of Dodori Creek (Dodori National Reserve, Lamu District) were not sampled in the current study but should probably be considered as a distinct mangrove system.

In considering the regional and Kenya-wide estimates of total AGB provided in Table 5 it is acknowledged that: (1) the estimates of mean AGB (±95% PIs) used in up-scaling are assumed to be regionally representative as discussed above and (2) the uncertainty associated with the estimates of mangrove cover derived from the remote sensing data has not been accounted for. Bearing in mind these caveats the estimates (±95% PIs) shown in Table 5 can still be viewed as a useful comparative overview of the level of total AGB stocks currently held within each region. There is undoubtedly scope for large-scale estimates to be further refined in the future. In particular there is a need for current inventory data to be collected within the regions Kilifi and Tana River (as defined in this study) not only to constrain the regional estimates but also the Kenya-wide estimate of total AGB. In addition, if and when future remote sensing work allows for the detailed mapping of mangrove cover and structural characteristics in each region it may become possible (and desirable) to produce large-scale estimates of AGB based on up-scaling by forest strata.

The stratification of forest cover is recommended for the reporting of forest carbon pools (IPCC, 2006) and there are a variety of stratification options still under consideration for future REDD reporting (Maniatis and Mollicone, 2010). Mangroves are generally considered to display species zonation and have traditionally been stratified by such 'zones' (Hogarth, 1999). However, not all mangroves display well-defined patterns of zonation (e.g. Mida Creek) and other options for stratification for example based on structural characteristics may be more appropriate in some situations. Various remote sensing techniques have been used in recent years to map mangroves at fine to large spatial scales (see review by Kuenzer et al., 2011). Such techniques offer the potential for fast and repeatable estimates of cover, and in the case of radar remote sensing above-ground biomass to be made based on mangrove structural parameters (Fatoyinbo et al., 2008; Held et al., 2003; Lucas et al., 2007).

It is anticipated that if required and pending any further collection of new harvest data, the model and methodology for uncertainty propagation presented in the current study could be used to produce estimates of mean AGB for use in future up-scaling exercises based on some stratification system with only minor modification to the existing procedures.

Acknowledgements

This research was funded by the Natural Environment Research Council (NERC), UK to which we are very grateful. We are also very grateful for the support provided by our collaborating partner Kenya Marine and Fisheries Research Institute (KMFRI) and additional support in the field provided by Kenya Forest Service (KFS). Many thanks to all those who provided the raw data used for model development and application and to WWF, Mozambique/KMFRI for providing us with a validation dataset. Data collection in

Mwache was supported by the WIOMSA-MASMA regional project on "Resilience of mangroves and dependent communities in the WIO region to climate change", Grant No: MASMA/CC/2010/08. Satellite imagery was provided by Spot Image through the Planet Action initiative as part of a larger project funded by the Ecosystem Services for Poverty Alleviation (ESPA) programme [under the Swahili Seas NE/I003401/1 project]. The ESPA programme is funded by the Department for International Development (DFID), the Economic and Social Research Council (ESRC) and the Natural Environment Research Council (NERC) of the UK. Additional SPOT imagery was provided under the European Space Agency (ESA) Category-1 scheme (Project ID: 8177). All processing of satellite imagery was carried out by Dr. Karin Viergever at ecometrica (Edinburgh, UK) and Neha Joshi to whom we are very grateful for lending their expertise. We wish to thank all those involved for their hard work in collecting the inventory data for the current study, in particular Mr Bernard Kivyatu. Many thanks to Mr Luke Smallman (University of Edinburgh, UK) for help with programming in R and to Dr Giles T. Innocent (Biomathematics and Statistics Scotland (BioSS)) for providing statistical advice. Finally, we wish to thank two anonymous reviewers for their comments and suggestions for improvement to the manuscript.

References

Aburto-Oropeza, O., Ezcurra, E., Danemann, G., Valdez, V., Murray, J., Sala, E., 2008. Mangroves in the Gulf of California increase fishery yields. PNAS 105, 10456–10459.

Akaike, H., 1987. Factor analysis and AIC. Psychometrika 52, 317–332.

Alongi, D.M., 2002. Present state and future of the world's mangrove forests. Environ. Conserv. 29, 331–349.

Amarasinghe, M.D., Balasubramaniam, S., 1992. Structural properties of two types of mangrove stands on the northwestern coast of Sri Lanka. Hydrobiologia 247, 17–27.

Bates, D., Maechler, M., Bolker, B., 2011. lme4: Linear mixed-effects models using S4 classes. R package version 0.999375-42. <http://CRAN.R-project.org/package=lme4>.

Bosire, J.O., Bandeira, S., Rafael, J., unpublished results. Coastal climate change mitigation and adaptation through REDD+ carbon programs in mangroves in Mozambique: pilot in the Zambezi Delta. Determination of carbon stocks through localized allometric equations component. WWF report.

Bouillon, S., Borges, A.V., Castaneda-Moya, E., Diele, K., Dittmar, T., Duke, N.C., Kristensen, E., Lee, S.Y., Marchand, C., Middelburg, J.J., Rivera-Monroy, V.H., Smith, T.J., Twilley, R.R., 2008. Mangrove production and carbon sinks: a revision of global budget estimates. Global Biogeochem. Cycles 22.

Brown, S., 2002. Measuring carbon in forests: current status and future challenges. Environ. Pollut. 116, 363–372.

Brown, S., Gillespie, A.J.R., Lugo, A.E., 1989. Biomass estimation methods for tropical forests with applications to forest inventory data. For. Sci. 35, 881–902.

Chave, J., Condit, R., Salomon, A., Hernandez, A., Lao, S., Perez, R., 2004. Error propagation and scaling for tropical forest biomass estimates. Philos. Trans. Roy. Soc. B 359, 409–420.

Chave, J., Andalo, C., Brown, S., Cairns, M.A., Chambers, J.Q., Eamus, D., Fölster, H., Fromard, F., Higuchi, N., Kira, T., Lescure, J.P., Nelson, B.W., Ogawa, H., Puig, H., Riéra, B., Yamakura, T., 2005. Tree allometry and improved estimation of carbon stocks and balance in tropical forests. Oecologia 145, 87–99.

Chmura, G.L., Anisfeld, S.C., Cahoon, D.R., Lynch, J.C., 2003. Global carbon sequestration in tidal, saline wetland soils. Global Biogeochem. Cycles 17.

Clough, B.F., Scott, K., 1989. Allometric relationships for estimating above-ground biomass in 6 mangrove species. For. Ecol. Manage. 27, 117–127.

Clough, B.F., Dixon, P., Dalhaus, O., 1997. Allometric relationships for estimating biomass in multi-stemmed mangrove trees. Aust. J. Bot. 45, 1023–1031.

Dahdouh-Guebas, F., Mathenge, C., Kairo, J.G., Koedam, N., 2000. Utilization of mangrove wood products around Mida Creek (Kenya) amongst subsistence and commercial users. Econ. Bot. 54, 513–527.

Dietze, M.C., Wolosin, M.S., Clark, J.S., 2008. Capturing diversity and interspecific variability in allometries: a hierarchical approach. For. Ecol. Manage. 256, 1939–1948.

Donato, D.C., Kauffman, J.B., Murdiyarso, D., Kurnianto, S., Stidham, M., Kanninen, M., 2011. Mangroves among the most carbon-rich forests in the tropics. Nat. Geosci. 4, 293–297.

Donato, D.C., Kauffman, J.B., Mackenzie, R.A., Ainsworth, A., Pfleeger, A.Z., 2012. Whole-island carbon stocks in the tropical Pacific: implications for mangrove conservation and upland restoration. J. Environ. Manage. 97, 89–96.

Duarte, C.M., Middelburg, J.J., Caraco, N., 2005. Major role of marine vegetation on the oceanic carbon cycle. Biogeosciences 2, 1–8.

Fatoyinbo, T.E., Simard, M., Washington-Allen, R.A., Shugart, H.H., 2008. Landscape-scale extent, height, biomass, and carbon estimation of Mozambique's mangrove forests with Landsat ETM+ and Shuttle Radar Topography Mission elevation data. J. Geophys. Res.-Biogeo. 113.

Fromard, F., Puig, H., Mougin, E., Marty, G., Betoulle, J.L., Cadamuro, L., 1998. Structure, above-ground biomass and dynamics of mangrove ecosystems: new data from French Guiana. Oecologia 115, 39–53.

Gang, P.O., Agatsiva, J.L., 1992. The current status of mangroves along the Kenyan coast – a case-study of Mida Creek mangroves based on remote-sensing. Hydrobiologia 247, 29–36.

Gelman, A., Hill, J., 2007. Data Analysis Using Regression and Multilevel/Hierarchical Models. Cambridge University Press, New York.

Gelman, A., Pardoe, I., 2006. Bayesian measures of explained variance and pooling in multilevel (hierarchical) models. Technometrics 48, 241–251.

Giri, C., Ochieng, E., Tieszen, L.L., Zhu, Z., Singh, A., Loveland, T., Masek, J., Duke, N., 2011. Status and distribution of mangrove forests of the world using earth observation satellite data. Global Ecol. Biogeogr. 20, 154–159.

Gregoire, T.G., Zedaker, S.M., Nicholas, N.S., 1990. Modeling relative error in stem basal area estimates. Can. J. For. Res. 20, 496–502.

Heath, L.S., Smith, J.E., 2000. An assessment of uncertainty in forest carbon budget projections. Environ. Sci. Policy 3, 73–82.

Held, A., Ticehurst, C., Lymburner, L., Williams, N., 2003. High resolution mapping of tropical mangrove ecosystems using hyperspectral and radar remote sensing. Int. J. Remote Sens. 24, 2739–2759.

Hogarth, P.J., 1999. The Biology of Mangroves. Oxford University Press, Oxford.

IPCC, 2006. Guidelines for National Greenhouse Gas Inventories. IGES, Japan.

Johnson, J.B., Omland, K.S., 2004. Model selection in ecology and evolution. Trends Ecol. Evol. 19, 101–108.

Kaino, J., 2013. Structure, biomass and cover change of a peri-urban mangrove forest in Kenya: a case study of Mwache Creek, Mombasa. MSc Thesis. Egerton University, Kenya.

Kairo, J.G., Dahdouh-Guebas, F., Gwada, P.O., Ochieng, C., Koedam, N., 2002. Regeneration status of mangrove forests in Mida Creek, Kenya: a compromised or secured future? Ambio 31, 562–568.

Kairo, J.G., Lang'at, J.K.S., Dahdouh-Guebas, F., Bosire, J., Karachi, M., 2008. Structural development and productivity of replanted mangrove plantations in Kenya. For. Ecol. Manage. 255, 2670–2677.

Kairo, J.G., Bosire, J., Langat, J., Kirui, B., Koedam, N., 2009. Allometry and biomass distribution in replanted mangrove plantations at Gazi Bay, Kenya. Aquat. Conserv.-Mar. Freshw. Ecosyst. 19, S63–S69.

Kathiresan, K., Bingham, B.L., 2001. Biology of mangroves and mangrove ecosystems. Adv. Mar. Biol. 40, 81–251.

Kauffman, J.B., Heider, C., Cole, T.G., Dwire, K.A., Donato, D.C., 2011. Ecosystem carbon stocks of Micronesian mangrove forests. Wetlands 31, 343–352.

Ketterings, Q.M., Coe, R., van Noordwijk, M., Ambagau, Y., Palm, C.A., 2001. Reducing uncertainty in the use of allometric biomass equations for predicting above-ground tree biomass in mixed secondary forests. For. Ecol. Manage. 146, 199–209.

Kirui, B., 2006. Allometric relations for estimating aboveground biomass of naturally growing mangroves, Avicennia marina FORSK (VIERH). and Rhizophora mucronata LAM. along the Kenya coast. MSc. Thesis. Egerton University, Kenya.

Kirui, B., Kairo, J.G., Karachi, M., 2006. Allometric equations for estimating above ground biomass of *Rhizophora mucronata* Lamk. (Rhizophoraceae) mangroves at Gazi Bay, Kenya. WIOJMS 5, 27–34.

Kirui, K.B., Kairo, J.G., Bosire, J., Viergever, K.M., Rudra, S., Huxham, M., Briers, R.A., 2012. Mapping of mangrove forest land cover change along the Kenya coastline using Landsat imagery. Ocean Coast. Manage. http://dx.doi.org/10.1016/j.ocecoaman.2011.12.004.

Kitheka, J.U., Ongwenyi, G.S., Mavuti, K.M., 2002. Dynamics of suspended sediment exchange and transport in a degraded mangrove creek in Kenya. Ambio 31, 580–587.

Komiyama, A., Jintana, V., Sangtiean, T., Kato, S., 2002. A common allometric equation for predicting stem weight of mangroves growing in secondary forests. Ecol. Res. 17, 415–418.

Komiyama, A., Poungparn, S., Kato, S., 2005. Common allometric equations for estimating the tree weight of mangroves. J. Trop. Ecol. 21, 471–477.

Komiyama, A., Ong, J.E., Poungparn, S., 2008. Allometry, biomass, and productivity of mangrove forests: a review. Aquat. Bot. 89, 128–137.

Kuenzer, C., Bluemel, A., Gebhardt, S., Quoc, T.V., Dech, S., 2011. Remote sensing of mangrove ecosystems: a review. Remote Sensing 3, 878–928.

Lang'at, J.K.S., 2008. Assessment of forest structure, regeneration and biomass accumulation of replanted mangroves in Kenya. MSc. Thesis. Egerton University, Kenya.

Lucas, R.M., Mitchell, A.L., Rosenqvist, A., Proisy, C., Melius, A., Ticehurst, C., 2007. The potential of L-band SAR for quantifying mangrove characteristics and change: case studies from the tropics. Aquat. Conserv.-Mar. Freshw. Ecosyst. 17, 245–264.

Maniatis, D., Mollicone, D., 2010. Options for sampling and stratification for national forest inventories to implement REDD+ under the UNFCCC. Carbon Balance Manage. 5, 9.

McKee, K.L., Cahoon, D.R., Feller, I.C., 2007. Caribbean mangroves adjust to rising sea level through biotic controls on change in soil elevation. Global Ecol. Biogeogr. 16, 545–556.

Okello, J.A., unpublished results. Mangrove wood formation as a basis of sustainable wood production in its climate context: The effect of increased sediment accumulation. Ph.D Thesis. Vrije Universiteit, Belgium.

Parresol, B.R., 1999. Assessing tree and stand biomass: a review with examples and critical comparisons. For. Sci. 45, 573–593.

Pendleton, L., Donato, D.C., Murray, B.C., Crooks, S., Jenkins, W.A., Sifleet, S., Craft, C., Fourqurean, J.W., Kauffman, J.B., Marba, N., Megonigal, P., Pidgeon, E., Herr, D., Gordon, D., Baldera, A., 2012. Estimating global "Blue Carbon" emissions from conversion and degradation of vegetated coastal ecosystems. PLoS ONE 7.

Phillips, D.L., Brown, S.L., Schroeder, P.E., Birdsey, R.A., 2000. Toward error analysis of large-scale forest carbon budgets. Global Ecol. Biogeogr. 9, 305–313.

Pinheiro, J.C., Bates, D.M., 2000. Mixed-effects Models in S and S-PLUS. Springer-Verlag, New York.

Poungparn, S., Komiyama, A., Patanaponpaipoon, P., Jintana, V., Sangtiean, T., Tanapermpool, P., Piriyayota, S., Maknual, C., Kato, S., 2002. Site-independent allometric relationships for estimating above-ground weights of mangroves. TROPICS 12, 147–158.

Primavera, J.H., 2005. GLOBAL VOICES OF SCIENCE: mangroves, fishponds, and the quest for sustainability. Science 310, 57–59.

Rideout, A., Joshi, N., Viergever, K., Huxham, M., Briers, R.A., 2013. Making predictions of mangrove deforestation: a comparison of two methods in Kenya. Glob. Change Biol. http://dx.doi.org/10.1111/gcb.12176.

Ryan, C.M., 2009. Carbon cycling, fire and phenology in a tropical savanna woodland in Nhambita, Mozambique. Ph.D. Thesis. University of Edinburgh, Edinburgh, UK.

Siikamaki, J., Sanchirico, J.N., Jardine, S.L., 2012. Global economic potential for reducing carbon dioxide emissions from mangrove loss. PNAS 109, 14369–14374.

Slim, F.J., Gwada, P.M., Kodjo, M., Hemminga, M.A., 1996. Biomass and litterfall of *Ceriops tagal* and *Rhizophora mucronata* in the mangrove forest of Gazi Bay, Kenya. Mar. Freshwater Res. 47, 999–1007.

Soares, M.L.G., Schaeffer-Novelli, Y., 2005. Above-ground biomass of mangrove species. I. Analysis of models. Estuar. Coast. Shelf Sci. 65, 1–18.

Steele, F., 2008. Introduction to multilevel modelling concepts: module 5. University of Bristol Centre for Multilevel Modelling: [online] Learning Environment for Multilevel Methodology and Applications (LEMMA) <http://www.bristol.ac.uk/cmm/>.

Steinke, T.D., Ward, C.J., Rajh, A., 1995. Forest structure and biomass of mangroves in the Mgeni Estuary, South-Africa. Hydrobiologia 295, 159–166.

Tamooh, F., Kairo, J.G., Huxham, M., Kirui, B., Mencuccini, M., Karachi, M., 2009. Biomass accumulation in a rehabilitated mangrove forest at Gazi Bay. In: Hoorweg, J., Muthiga, N. (Eds.), African Studies Collection, vol. 20. African Studies Centre, Leiden, pp. 138–146.

Valiela, I., Bowen, J.L., York, J.K., 2001. Mangrove forests: one of the world's threatened major tropical environments. Bioscience 51, 807–815.

van der Werf, G.R., Morton, D.C., DeFries, R.S., Olivier, J.G.J., Kasibhatla, P.S., Jackson, R.B., Collatz, G.J., Randerson, J.T., 2009. CO_2 emissions from forest loss. Nat. Geosci. 2, 737–738.

Wickramasinghe, S., Borin, M., Kotagama, S.W., Cochard, R., Anceno, A.J., Shipin, O.V., 2009. Multi-functional pollution mitigation in a rehabilitated mangrove conservation area. Ecol. Eng. 35, 898–907.

World Resources Institute. Poverty and ecosystems: Kenya GIS. <http://www.wri.org/>.

Wutzler, T., Wirth, C., Schumacher, J., 2008. Generic biomass functions for Common beech (*Fagus sylvatica*) in Central Europe: predictions and components of uncertainty. Can. J. For. Res. 38, 1661–1675.

Zhang, K.Q., Liu, H.Q., Li, Y.P., Xu, H.Z., Shen, J., Rhome, J., Smith, T.J., 2012. The role of mangroves in attenuating storm surges. Estuar. Coast. Shelf Sci. 102, 11–23.

Zianis, D., 2008. Predicting mean aboveground forest biomass and its associated variance. For. Ecol. Manage. 256, 1400–1407.

Zianis, D., Mencuccini, M., 2004. On simplifying allometric analyses of forest biomass. For. Ecol. Manage. 187, 311–332.

Appendix 2: Chapter 3 OLS model results

Table A2.1: Estimated fixed-effects parameters (± std. error) and associated regression statistics from the ordinary least squares regression model (OLS model) presented in chapter 3 section 3.2.4[a]

a	b_1	b_2	ε	R^2	P value
2.68920 (± 0.02345)	1.77963 (± 0.06327)	0.63810 (± 0.06423)	0.4304	0.88	< 0.001

[a] a is the fitted intercept, b_1 and b_2 are the coefficients for the predictive variables stem diameter and height respectively and ε is the residual variance. Parameter estimates and std. errors are log values.

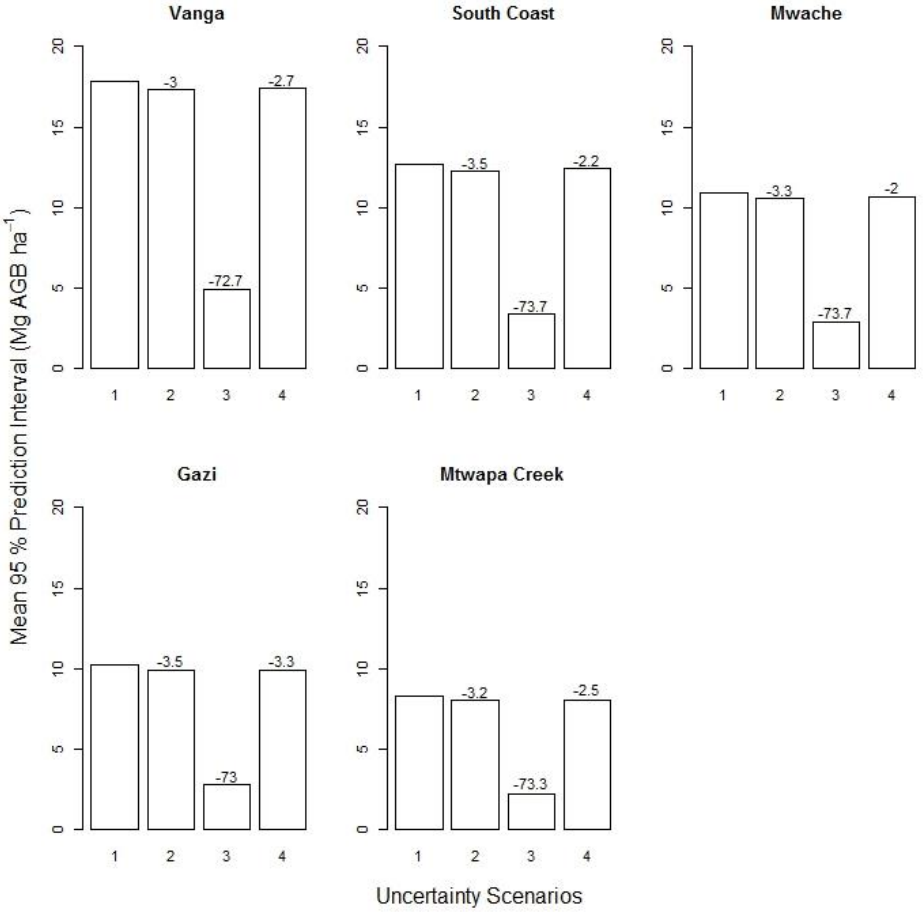

Fig. A2.1: Effect of removing components of uncertainty on the magnitude of the mean 95% prediction interval (95% PI) for an estimate of plot AGB at the regional scale obtained using the OLS model. Numbers above bars represent the percentage decrease in the mean 95% PI under each uncertainty scenario compared to scenario 1. Please note that % changes in the mean PIs between uncertainty scenarios 2 to 4 are not additive.

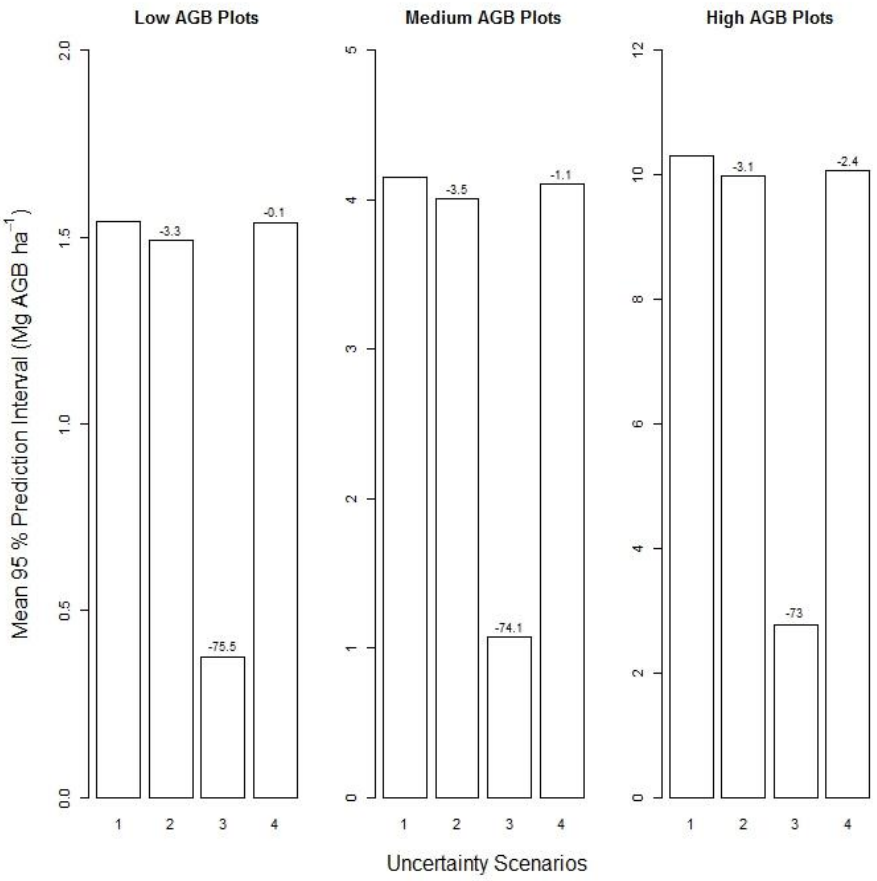

Fig. A2.2**:** Effect of removing components of uncertainty on the magnitude of the mean 95% prediction interval (95% PI) obtained using the OLS model for plots of low, medium and high estimated AGB. Numbers above bars represent the percentage decrease in the mean 95% PI under each uncertainty scenario compared to scenario 1. Please note that % changes in the mean PIs between uncertainty scenarios 2 to 4 are not additive.

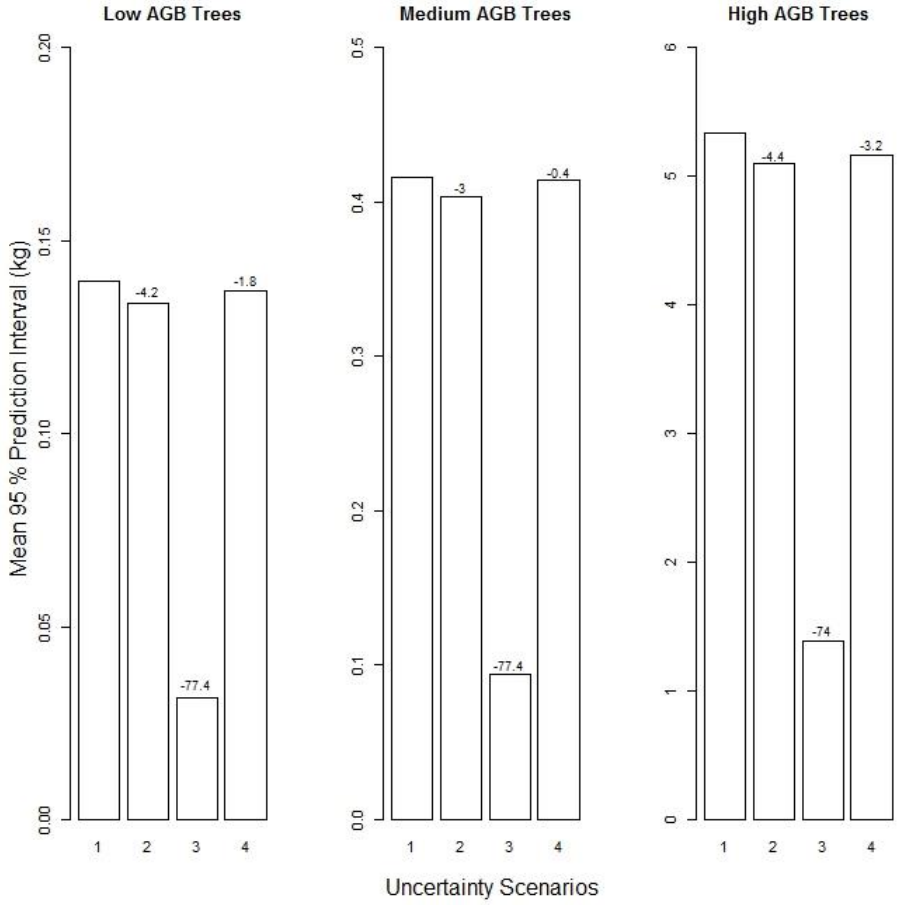

Fig. A2.3: Effect of removing components of uncertainty on the magnitude of the mean 95% prediction interval (95% PI) obtained using the OLS model for trees of low, medium and high estimated AGB. Numbers above bars represent the percentage decrease in the mean 95% PI under each uncertainty scenario compared to scenario 1. Please note that % changes in the mean PIs between uncertainty scenarios 2 to 4 are not additive.

References

Aburto-Oropeza, O., Ezcurra, E., Danemann, G., Valdez, V., Murray, J., Sala, E., 2008. Mangroves in the Gulf of California increase fishery yields. PNAS 105, 10456-10459.

Ahmed, R., Siqueira, P., Hensley, S., Bergen, K., 2013. Uncertainty of Forest Biomass Estimates in North Temperate Forests Due to Allometry: Implications for Remote Sensing. Remote Sensing 5, 3007-3036.

Akaike, H., 1987. Factor analysis and AIC. Psychometrika 52, 317-332.

Alongi, D.M., 2002. Present state and future of the world's mangrove forests. Environmental Conservation 29, 331-349.

Alongi, D.M., 2008. Mangrove forests: Resilience, protection from tsunamis, and responses to global climate change. Estuarine Coastal and Shelf Science 76, 1-13.

Alongi, D.M., 2009. The energetics of mangrove forests. Springer.

Alongi, D.M., Dixon, P., 2000. Mangrove primary production and above- and below-ground biomass in Sawi Bay, southern Thailand. Phuket Marine Biological Center Special Publication 22, 33-38.

Alongi, D.M., Sasekumar, A., Chong, V.C., Pfitzner, J., Trott, L.A., Tirendi, F., Dixon, P., Brunskill, G.J., 2004. Sediment accumulation and organic material flux in a managed mangrove ecosystem: estimates of land-ocean-atmosphere exchange in peninsular Malaysia. Marine Geology 208, 383-402.

Amarasinghe, M.D., Balasubramaniam, S., 1992. Structural properties of two types of mangrove stands on the northwestern coast of Sri Lanka. Hydrobiologia 247, 17-27.

Asner, G.P., Clark, J.K., Mascaro, J., Garcia, G.A.G., Chadwick, K.D., Encinales, D.A.N., Paez-Acosta, G., Montenegro, E.C., Kennedy-Bowdoin, T., Duque, A., Balaji, A., von Hildebrand, P., Maatoug, L., Bernal, J.F.P., Quintero, A.P.Y., Knapp, D.E., Davila, M.C.G., Jacobson, J., Ordonez, M.F., 2012. High-resolution mapping of forest carbon stocks in the Colombian Amazon. Biogeosciences 9, 2683-2696.

Bates, D., Maechler, M., Bolker, B., 2011. lme4: Linear mixed-effects models using S4 classes. R package version 0.999375-42. http://CRAN.R-project.org/package=lme4.

Bosire, J.O., Bandeira, S., Rafael, J., unpublished results. Coastal climate change mitigation and adaptation through REDD+ carbon programs in mangroves in Mozambique: Pilot in the Zambezi Delta. Determination of carbon stocks through localized allometric equations component. WWF report.

Bouillon, S., Borges, A.V., Castaneda-Moya, E., Diele, K., Dittmar, T., Duke, N.C., Kristensen, E., Lee, S.Y., Marchand, C., Middelburg, J.J., Rivera-Monroy, V.H., Smith, T.J., Twilley, R.R., 2008. Mangrove production and carbon sinks: A revision of global budget estimates. Global Biogeochemical Cycles 22.

Bouillon, S., Dehairs, F., Schiettecatte, L.S., Borges, A.V., 2007a. Biogeochemistry of the Tana estuary and delta (northern Kenya). Limnology and Oceanography 52, 46-59.

Bouillon, S., Dehairs, F., Velimirov, B., Abril, G., Borges, A.V., 2007b. Dynamics of organic and inorganic carbon across contiguous mangrove and seagrass systems (Gazi Bay, Kenya). Journal of Geophysical Research-Biogeosciences 112.

Bouillon, S., Moens, T., Dehairs, F., 2004. Carbon sources supporting benthic mineralization in mangrove and adjacent seagrass sediments (Gazi Bay, Kenya). Biogeosciences 1, 71-78.

Brown, I.F., Martinelli, L.A., Thomas, W.W., Moreira, M.Z., Ferreira, C.A.C., Victoria, R.A., 1995. Uncertainty in the biomass of Amazonian forests - an example from Rondonia, Brazil. Forest Ecology and Management 75, 175-189.

Brown, S., 2002. Measuring carbon in forests: current status and future challenges. Environmental Pollution 116, 363-372.

Brown, S., Gillespie, A.J.R., Lugo, A.E., 1989. Biomass estimation methods for tropical forests with applications to forest inventory data. Forest Science 35, 881-902.

Carreiras, J.M.B., Vasconcelos, M.J., Lucas, R.M., 2012. Understanding the relationship between aboveground biomass and ALOS PALSAR data in the forests of Guinea-Bissau (West Africa). Remote Sensing of Environment 121, 426-442.

Cassells, G., Woodhouse, I.H., Patenaude, G., Tembo, M., 2011. Academic and research capacity development in Earth observation for environmental management. Environmental Research Letters 6.

Chapin, F.S., Woodwell, G.M., Randerson, J.T., Rastetter, E.B., Lovett, G.M., Baldocchi, D.D., Clark, D.A., Harmon, M.E., Schimel, D.S., Valentini, R., Wirth, C., Aber, J.D., Cole, J.J., Goulden, M.L., Harden, J.W., Heimann, M., Howarth, R.W., Matson, P.A., McGuire, A.D., Melillo, J.M., Mooney, H.A., Neff, J.C., Houghton, R.A., Pace, M.L., Ryan, M.G., Running, S.W., Sala, O.E., Schlesinger, W.H., Schulze, E.D., 2006. Reconciling carbon-cycle concepts, terminology, and methods. Ecosystems 9, 1041-1050.

Chave, J., Andalo, C., Brown, S., Cairns, M.A., Chambers, J.Q., Eamus, D., Fölster, H., Fromard, F., Higuchi, N., Kira, T., Lescure, J.P., Nelson, B.W., Ogawa, H., Puig, H., Riéra, B., Yamakura, T., 2005. Tree allometry and improved estimation of carbon stocks and balance in tropical forests. Oecologia 145, 87-99.

Chave, J., Condit, R., Salomon, A., Hernandez, A., Lao, S., Perez, R., 2004. Error propagation and scaling for tropical forest biomass estimates. Philosophical Transactions of the Royal Society B 359, 409-420.

Chave, J., Muller-Landau, H.C., Baker, T.R., Easdale, T.A., Ter Steege, H., Webb, C.O., 2006. Regional and phylogenetic variation of wood density across 2456 neotropical tree species. Ecological Applications 16, 2356-2367.

Chmura, G.L., Anisfeld, S.C., Cahoon, D.R., Lynch, J.C., 2003. Global carbon sequestration in tidal, saline wetland soils. Global Biogeochemical Cycles 17.

Ciais, P., Bombelli, A., Williams, M., Piao, S.L., Chave, J., Ryan, C.M., Henry, M., Brender, P., Valentini, R., 2011. The carbon balance of Africa: synthesis of recent research studies. Philosophical Transactions of the Royal Society a-Mathematical Physical and Engineering Sciences 369, 2038-2057.

Clark, D.A., Brown, S., Kicklighter, D.W., Chambers, J.Q., Thomlinson, J.R., Ni, J., 2001. Measuring net primary production in forests: Concepts and field methods. Ecological Applications 11, 356-370.

Clough, B.F., Dixon, P., Dalhaus, O., 1997. Allometric relationships for estimating biomass in multi-stemmed mangrove trees. Australian Journal of Botany 45, 1023-1031.

Clough, B.F., Scott, K., 1989. Allometric relationships for estimating above-ground biomass in 6 mangrove species. Forest Ecology and Management 27, 117-127.

Cohen, R., Kaino, J., Okello, J.A., Bosire, J.O., Kairo, J.G., Huxham, M., Mencuccini, M., 2013. Propagating uncertainty to estimates of above-ground biomass for Kenyan mangroves: a scaling procedure from tree to landscape level. Forest Ecology and Management 310, 968-982.

Collins, J.N., Hutley, L.B., Williams, R.J., Boggs, G., Bell, D., Bartolo, R., 2009. Estimating landscape-scale vegetation carbon stocks using airborne multi-frequency polarimetric synthetic aperture radar (SAR) in the savannahs of north Australia. International Journal of Remote Sensing 30, 1141-1159.

Corbera, E., 2012. Problematizing REDD+ as an experiment in payments for ecosystem services. Current Opinion in Environmental Sustainability 4, 612-619.

Dahdouh-Guebas, F., Jayatissa, L.P., Di Nitto, D., Bosire, J.O., Lo Seen, D., Koedam, N., 2005. How effective were mangroves as a defence against the recent tsunami? Current Biology 15, R443-R447.

Dahdouh-Guebas, F., Mathenge, C., Kairo, J.G., Koedam, N., 2000. Utilization of mangrove wood products around Mida Creek (Kenya) amongst subsistence and commercial users. Economic Botany 54, 513-527.

Day, J.W., Coronado-Molina, C., Vera-Herrera, F.R., Twilley, R., Rivera-Monroy, V.H., Alvarez-Guillen, H., Day, R., Conner, W., 1996. A 7 year record of above-ground net primary production in a southeastern Mexican mangrove forest. Aquatic Botany 55, 39-60.

Dietze, M.C., Wolosin, M.S., Clark, J.S., 2008. Capturing diversity and interspecific variability in allometries: A hierarchical approach. Forest Ecology and Management 256, 1939-1948.

Dittmar, T., Hertkorn, N., Kattner, G., Lara, R.J., 2006. Mangroves, a major source of dissolved organic carbon to the oceans. Global Biogeochemical Cycles 20.

Donato, D.C., Kauffman, J.B., Mackenzie, R.A., Ainsworth, A., Pfleeger, A.Z., 2012. Whole-island carbon stocks in the tropical Pacific: Implications for mangrove conservation and upland restoration. Journal of Environmental Management 97, 89-96.

Donato, D.C., Kauffman, J.B., Murdiyarso, D., Kurnianto, S., Stidham, M., Kanninen, M., 2011. Mangroves among the most carbon-rich forests in the tropics. Nature Geoscience 4, 293-297.

Duarte, C.M., Middelburg, J.J., Caraco, N., 2005. Major role of marine vegetation on the oceanic carbon cycle. Biogeosciences 2, 1-8.

Duke, N.C., Meynecke, J.O., Dittmann, S., Ellison, A.M., Anger, K., Berger, U., Cannicci, S., Diele, K., Ewel, K.C., Field, C.D., Koedam, N., Lee, S.Y., Marchand, C., Nordhaus, I., Dahdouh-Guebas, F., 2007. A world without mangroves? Science 317, 41-42.

Ellison, A.M., 2002. Macroecology of mangroves: large-scale patterns and processes in tropical coastal forests. Trees-Structure and Function 16, 181-194.

FAO, 2007. The world's mangroves 1980-2005. FAO Forestry Paper 153. Food and Agriculture Organization of the United Nations. Rome, FAO.

FAO and JRC, 2012. Global forest land-use change 1990-2005. FAO Forestry Paper No. 169. Food and Agriculture Organization of the United Nations and European Commission Joint Research Centre. Rome, FAO.

Fatoyinbo, T.E., Simard, M., 2013. Height and biomass of mangroves in Africa from ICESat/GLAS and SRTM. International Journal of Remote Sensing 34, 668-681.

Fatoyinbo, T.E., Simard, M., Washington-Allen, R.A., Shugart, H.H., 2008. Landscape-scale extent, height, biomass, and carbon estimation of Mozambique's mangrove forests with Landsat ETM+ and Shuttle Radar Topography Mission elevation data. Journal of Geophysical Research 113.

Fromard, F., Puig, H., Mougin, E., Marty, G., Betoulle, J.L., Cadamuro, L., 1998. Structure, above-ground biomass and dynamics of mangrove ecosystems: new data from French Guiana. Oecologia 115, 39-53.

Gang, P.O., Agatsiva, J.L., 1992. The current status of mangroves along the Kenyan coast - a case-study of Mida Creek mangroves based on remote-sensing. Hydrobiologia 247, 29-36.

Gelman, A., Hill, J., 2007. Data analysis using regression and multilevel/hierarchical models. Cambridge University Press, New York.

Gelman, A., Pardoe, L., 2006. Bayesian measures of explained variance and pooling in multilevel (hierarchical) models. Technometrics 48, 241-251.

Giri, C., Muhlhausen, J., 2008. Mangrove forest distributions and dynamics in Madagascar (1975-2005). Sensors 8, 2104-2117.

Giri, C., Ochieng, E., Tieszen, L.L., Zhu, Z., Singh, A., Loveland, T., Masek, J., Duke, N., 2011. Status and distribution of mangrove forests of the world using earth observation satellite data. Global Ecology and Biogeography 20, 154-159.

Gleason, S.M., Ewel, K.C., 2002. Organic matter dynamics on the forest floor of a Micronesian mangrove forest: an investigation of species composition shifts. Biotropica 34, 190-198.

Government of Kenya, 2003. Geographic dimensions of well-being in Kenya: where are the poor? from districts to locations (volume one). GoK Central Bureau of Statistics. Available at <http://www.econ.worldbank.org/>.

Government of Kenya, 2009. State of the coast report: towards integrated management of coastal and marine resources in Kenya. National Environment Authority (NEMA), Nairobi, Kenya.

Gregoire, T.G., Zedaker, S.M., Nicholas, N.S., 1990. Modeling relative error in stem basal area estimates. Canadian Journal of Forest Research 20, 496-502.

Heath, L.S., Smith, J.E., 2000. An assessment of uncertainty in forest carbon budget projections. Environmental Science and Policy 3, 73-82.

Held, A., Ticehurst, C., Lymburner, L., Williams, N., 2003. High resolution mapping of tropical mangrove ecosystems using hyperspectral and radar remote sensing. International Journal of Remote Sensing 24, 2739-2759.

Henrichs, S.M., 1992. Early Diagenesis of Organic-Matter in Marine-Sediments - Progress and Perplexity. Marine Chemistry 39, 119-149.

Hogarth, P.J., 1999. The biology of mangroves. Oxford University Press, Oxford.

Hutchison, J., Manica, A., Swetnam, R., Balmford, A., Spalding, M., 2013. Predicting global patterns in mangrove forest biomass. Conservation Letters doi:10.1111/conl.12060.

IPCC, 2006. Guidelines for national greenhouse gas inventories. IGES, Japan.

IPCC, 2013. Summary for policymakers. In: Climate Change 2013: the physical science basis. Contribution of working group I to the fifth assessment report of the Intergovernmental Panel on Climate Change. Cambridge University Press, Cambridge, United Kingdom and New York, NY, USA.

Jennerjahn, T.C., Ittekkot, V., 2002. Relevance of mangroves for the production and deposition of organic matter along tropical continental margins. Naturwissenschaften 89, 23-30.

Johnson, J.B., Omland, K.S., 2004. Model selection in ecology and evolution. Trends in Ecology and Evolution 19, 101-108.

Kaino, J., 2013. Structure, biomass and cover change of a peri-urban mangrove forest in Kenya: A case study of Mwache Creek, Mombasa. MSc Thesis. Egerton University, Kenya.

Kairo, J.G., Bosire, J., Langat, J., Kirui, B., Koedam, N., 2009. Allometry and biomass distribution in replanted mangrove plantations at Gazi Bay, Kenya. Aquatic Conservation: Marine and Freshwater Ecosystems 19, S63-S69.

Kairo, J.G., Dahdouh-Guebas, F., Gwada, P.O., Ochieng, C., Koedam, N., 2002. Regeneration status of mangrove forests in Mida Creek, Kenya: A compromised or secured future? Ambio 31, 562-568.

Kairo, J.G., Lang'at, J.K.S., Dahdouh-Guebas, F., Bosire, J., Karachi, M., 2008. Structural development and productivity of replanted mangrove plantations in Kenya. Forest Ecology and Management 255, 2670-2677.

Kathiresan, K., Bingham, B.L., 2001. Biology of mangroves and mangrove ecosystems. Advances in Marine Biology 40, 81-251.

Kauffman, J.B., Donato, D.C., 2012. Protocols for the measurement, monitoring and reporting of structure, biomass and carbon stocks in mangrove forests. Working Paper 86 CIFOR, Bogor, Indonesia.

Kauffman, J.B., Heider, C., Cole, T.G., Dwire, K.A., Donato, D.C., 2011. Ecosystem carbon stocks of Micronesian mangrove forests. Wetlands 31, 343-352.

Ketterings, Q.M., Coe, R., van Noordwijk, M., Ambagau, Y., Palm, C.A., 2001. Reducing uncertainty in the use of allometric biomass equations for predicting above-ground tree biomass in mixed secondary forests. Forest Ecology and Management 146, 199-209.

Kirui, B., 2006. Allometric relations for estimating aboveground biomass of naturally growing mangroves, *Avicennia marina* FORSK (VIERH). and *Rhizophora mucronata* LAM. along the Kenya coast. MSc. Thesis. Egerton University, Kenya.

Kirui, B., Kairo, J.G., Karachi, M., 2006. Allometric equations for estimating above ground biomass of *Rhizophora mucronata* Lamk. (Rhizophoraceae) mangroves at Gazi Bay, Kenya. Western Indian Ocean Journal of Marine Science 5, 27-34.

Kirui, K.B., Kairo, J.G., Bosire, J., Viergever, K.M., Rudra, S., Huxham, M., Briers, R.A., 2012. Mapping of mangrove forest land cover change along the Kenya coastline using Landsat imagery. Ocean and Coastal Management 83, 19-24.

Kitheka, J.U., Ongwenyi, G.S., Mavuti, K.M., 2002. Dynamics of suspended sediment exchange and transport in a degraded mangrove creek in Kenya. Ambio 31, 580-587.

Komiyama, A., Jintana, V., Sangtiean, T., Kato, S., 2002. A common allometric equation for predicting stem weight of mangroves growing in secondary forests. Ecological Research 17, 415-418.

Komiyama, A., Ong, J.E., Poungparn, S., 2008. Allometry, biomass, and productivity of mangrove forests: A review. Aquatic Botany 89, 128-137.

Komiyama, A., Poungparn, S., Kato, S., 2005. Common allometric equations for estimating the tree weight of mangroves. Journal of Tropical Ecology 21, 471-477.

Kovacs, J.M., Vandenberg, C.V., Wang, J., Flores-Verdugo, F., 2008. The use of multipolarized spaceborne SAR backscatter for monitoring the health of a degraded mangrove forest. Journal of Coastal Research 24, 248-254.

Kristensen, E., 2007. Carbon balance in mangrove sediments; the driving processes and their controls. In: Tateda, Y. (Ed.), Greenhouse Gas and Carbon Balances in Mangrove Coastal Ecosystems. Gendaitosho, Kanagawa, Japan, pp. 61-78.

Kristensen, E., Bouillon, S., Dittmar, T., Marchand, C., 2008. Organic carbon dynamics in mangrove ecosystems: A review. Aquatic Botany 89, 201-219.

Kuenzer, C., Bluemel, A., Gebhardt, S., Quoc, T.V., Dech, S., 2011. Remote sensing of mangrove ecosystems: a review. Remote Sensing 3, 878-928.

Laffoley, D., Grimsditch, G., 2009. The management of natural coastal carbon sinks. IUCN, Gland, Switzerland., 53pp.

Lang'at, J.K.S., 2008. Assessment of forest structure, regeneration and biomass accumulation of replanted mangroves in Kenya. MSc. Thesis. Egerton University, Kenya.

Lee, S.Y., 1995. Mangrove Outwelling - a Review. Hydrobiologia 295, 203-212.

Leimgruber, P., Kelly, D.S., Steininger, M.K., Brunner, J., Muller, T., Songer, M., 2005. Forest cover change patterns in Myanmar (Burma) 1990-2000. Environmental Conservation 32, 356-364.

Li, X., Yeh, A.G.O., Wang, S., Liu, K., Liu, X., Qian, J., Chen, X., 2007. Regression and analytical models for estimating mangrove wetland biomass in South China using Radarsat images. International Journal of Remote Sensing 28, 5567-5582.

Lucas, R., Armston, J., Fairfax, R., Fensham, R., Accad, A., Carreiras, J., Kelley, J., Bunting, P., Clewley, D., Bray, S., Metcalfe, D., Dwyer, J., Bowen, M., Eyre, T., Laidlaw, M., Shimada, M., 2010. An Evaluation of the ALOS PALSAR L-Band Backscatter-Above Ground Biomass Relationship Queensland, Australia: Impacts of Surface Moisture Condition and Vegetation Structure. IEEE Journal of Selected Topics in Applied Earth Observations and Remote Sensing 3, 576-593.

Lucas, R.M., Bunting, P., Clewley, D., Proisy, C., Souza Filho, P.W.M., Viergever, K., Woodhouse, I.H., Ticehurst, C., Carreiras, J., Rosenqvist, A., Accad, A., Armston, J., 2009. Characterisation and monitoring of mangroves using ALOS PALSAR data. Japan Aerospace Exploration Agency (JAXA) Earth Observation Research Center (EORC): Kyoto and Carbon Initiative - Phase 1 report. <http://www.eorc.jaxa.jp/>.

Lucas, R.M., Mitchell, A.L., Rosenqvist, A., Proisy, C., Melius, A., Ticehurst, C., 2007. The potential of L-band SAR for quantifying mangrove characteristics and change: case studies from the tropics. Aquatic Conservation: Marine and Freshwater Ecosystems 17, 245-264.

Luckman, A., Baker, J., Kuplich, T.M., Yanasse, C.D.F., Frery, A.C., 1997. A study of the relationship between radar backscatter and regenerating tropical forest biomass for spaceborne SAR instruments. Remote Sensing of Environment 60, 1-13.

Lugo, A.E., Snedaker, S.C., 1974. The ecology of mangroves. Annual Review of Ecology and Systematics 5, 39-64.

Maniatis, D., Mollicone, D., 2010. Options for sampling and stratification for national forest inventories to implement REDD+ under the UNFCCC. Carbon Balance Management 5, 9.

Mazda, Y., Magi, M., Nanao, H., Kogo, M., Miyagi, T., Kanazawa, N., Kobashi, D., 2002. Coastal erosion due to long-term human impact on mangrove forests. Wetlands Ecology and Management 10, 1-9.

McKee, K.L., Cahoon, D.R., Feller, I.C., 2007. Caribbean mangroves adjust to rising sea level through biotic controls on change in soil elevation. Global Ecology and Biogeography 16, 545-556.

McLeod, E., Salm, R.V., 2006. Managing mangroves for resilience to climate change. IUCN, Gland, Switzerland.

Middleton, B.A., McKee, K.L., 2001. Degradation of mangrove tissues and implications for peat formation in Belizean island forests. Journal of Ecology 89, 818-828.

Mitchard, E.T.A., Saatchi, S.S., White, L.J.T., Abernethy, K.A., Jeffery, K.J., Lewis, S.L., Collins, M., Lefsky, M.A., Leal, M.E., Woodhouse, I.H., Meir, P., 2012. Mapping tropical forest biomass with radar and spaceborne LiDAR in Lope National Park, Gabon: overcoming problems of high biomass and persistent cloud. Biogeosciences 9, 179-191.

Mitchard, E.T.A., Saatchi, S.S., Woodhouse, I.H., Nangendo, G., Ribeiro, N.S., Williams, M., Ryan, C.M., Lewis, S.L., Feldpausch, T.R., Meir, P., 2009. Using satellite radar backscatter to predict above-ground woody biomass: A consistent relationship across four different African landscapes. Geophysical Research Letters 36.

Morel, A.C., Saatchi, S.S., Malhi, Y., Berry, N.J., Banin, L., Burslem, D., Nilus, R., Ong, R.C., 2011. Estimating aboveground biomass in forest and oil palm plantation in Sabah, Malaysian Borneo using ALOS PALSAR data. Forest Ecology and Management 262, 1786-1798.

Mougin, E., Proisy, C., Marty, G., Fromard, F., Puig, H., Betoulle, J.L., Rudant, J.P., 1999. Multifrequency and multipolarization radar backscattering from mangrove forests. IEEE Transactions on Geoscience and Remote Sensing 37, 94-102.

Mumby, P.J., Edwards, A.J., Arias-Gonzalez, J.E., Lindeman, K.C., Blackwell, P.G., Gall, A., Gorczynska, M.I., Harborne, A.R., Pescod, C.L., Renken, H., Wabnitz, C.C.C., Llewellyn, G., 2004. Mangroves enhance the biomass of coral reef fish communities in the Caribbean. Nature 427, 533-536.

Mutai, C.C., Ward, M.N., 2000. East African rainfall and the tropical circulation/convection on intraseasonal to interannual timescales. Journal of Climate 13, 3915-3939.

Nellemann, C., Corcoran, E., Duarte, C.M., Valdés, L., De Young, C., Fonseca, L.a., Grimsditch, G.E., 2009. Blue carbon. A Rapid Response Assessment. United Nations Environment Programme, GRID-Arendal.

Okello, J.A., unpublished results. Mangrove wood formation as a basis of sustainable wood production in its climate context: The effect of increased sediment accumulation. Ph.D Thesis. Vrije Universiteit, Belgium.

Ong, J.E., Gong, W.K., Wong, C.H., 2004. Allometry and partitioning of the mangrove, Rhizophora apiculata. Forest Ecology and Management 188, 395-408.

Parresol, B.R., 1999. Assessing tree and stand biomass: A review with examples and critical comparisons. Forest Science 45, 573-593.

Patenaude, G., Milne, R., Dawson, T.P., 2005. Synthesis of remote sensing approaches for forest carbon estimation: reporting to the Kyoto Protocol. Environmental Science and Policy 8, 161-178.

Peel, M.C., Finlayson, B.L., McMahon, T.A., 2007. Updated world map of the Köppen-Geiger climate classification. Hydrology and Earth System Sciences 11, 1633-1644.

Pendleton, L., Donato, D.C., Murray, B.C., Crooks, S., Jenkins, W.A., Sifleet, S., Craft, C., Fourqurean, J.W., Kauffman, J.B., Marba, N., Megonigal, P., Pidgeon, E., Herr, D., Gordon, D., Baldera, A., 2012. Estimating global "Blue Carbon" emissions from conversion and degradation of vegetated coastal ecosystems. PLoS ONE 7.

Phillips, D.L., Brown, S.L., Schroeder, P.E., Birdsey, R.A., 2000. Toward error analysis of large-scale forest carbon budgets. Global Ecology and Biogeography 9, 305-313.

Pinheiro, J.C., Bates, D.M., 2000. Mixed-effects models in S and S-PLUS. Springer-Verlag, New York.

Polidoro, B.A., Carpenter, K.E., Collins, L., Duke, N.C., Ellison, A.M., Ellison, J.C., Farnsworth, E.J., Fernando, E.S., Kathiresan, K., Koedam, N.E., Livingstone, S.R., Miyagi, T., Moore, G.E., Ngoc Nam, V., Ong, J.E., Primavera, J.H., Salmo, S.G., III, Sanciangco, J.C., Sukardjo, S., Wang, Y., Yong, J.W.H., 2010. The Loss of Species: Mangrove Extinction Risk and Geographic Areas of Global Concern. PLoS ONE 5, e10095.

Poungparn, S., Komiyama, A., Patanaponpaipoon, P., Jintana, V., Sangtiean, T., Tanapermpool, P., Piriyayota, S., Maknual, C., Kato, S., 2002. Site-independent allometric relationships for estimating above-ground weights of mangroves. TROPICS 12, 147-158.

Primavera, J.H., 2005. GLOBAL VOICES OF SCIENCE: mangroves, fishponds, and the quest for sustainability. Science 310, 57-59.

Proisy, C., Mougin, E., Fromard, F., Trichon, V., Karam, M.A., 2002. On the influence of canopy structure on the radar backscattering of mangrove forests. International Journal of Remote Sensing 23, 4197-4210.

Quiñones, M.J., Hoekman, D.H., 2004. Exploration of factors limiting Biomass estimation by polarimetric radar in tropical forests. IEEE Transactions on Geoscience and Remote Sensing 42, 86-104.

R Development Core Team, 2012. R: A language and environment for statistical computing. R Foundation for Statistical Computing, Vienna, Austria. ISBN 3-900051-07-0, URL http://www.R-project.org/.

Rahman, M.M., Sumantyo, J.T.S., 2013. Retrieval of tropical forest biomass information from ALOS PALSAR data. Geocarto International 28, 382-403.

Rignot, E., Way, J.B., Williams, C., Viereck, L., 1994. Radar Estimates of aboveground biomass in boreal forests of interior Alaska. IEEE Transactions on Geoscience and Remote Sensing 32, 1117-1124.

Rodriguez, W., Feller, I.C., 2004. Mangrove landscape characterization and change in Twin Cays, Belize using aerial photography and IKONOS satellite data. Atoll Research Bulletin.

Ross, M.S., Ruiz, P.L., Telesnicki, G.J., Meeder, J.F., 2001. Estimating above-ground biomass and production in mangrove communities of Biscayne National Park, Florida (U.S.A). Wetlands Ecology and Management 9, 27-37.

Ryan, C.M., 2009. Carbon cycling, fire and phenology in a tropical savanna woodland in Nhambita, Mozambique. Ph.D. Thesis. University of Edinburgh, Edinburgh, UK.

Ryan, C.M., Hill, T., Woollen, E., Ghee, C., Mitchard, E., Cassells, G., Grace, J., Woodhouse, I.H., Williams, M., 2012. Quantifying small-scale deforestation and forest degradation in African woodlands using radar imagery. Global Change Biology 18, 243-257.

Saatchi, S., Marlier, M., Chazdon, R.L., Clark, D.B., Russell, A.E., 2011a. Impact of spatial variability of tropical forest structure on radar estimation of aboveground biomass. Remote Sensing of Environment 115, 2836-2849.

Saatchi, S.S., Harris, N.L., Brown, S., Lefsky, M., Mitchard, E.T.A., Salas, W., Zutta, B.R., Buermann, W., Lewis, S.L., Hagen, S., Petrova, S., White, L., Silman, M., Morel, A., 2011b. Benchmark map of forest carbon stocks in tropical regions across three continents. PNAS 108, 9899-9904.

Saenger, P., Snedaker, S.C., 1993. Pantropical Trends in Mangrove Aboveground Biomass and Annual Litterfall. Oecologia 96, 293-299.

Sarmiento, C., Patiño, S., Paine, C.E.T., Beauchêne, J., Thibaut, A., Baraloto, C., 2011. Within-individual variation of trunk and branch xylem density in tropical trees. American Journal of Botany 98, 140-149.

Shimada, M., Isoguchi, O., Tadono, T., Isono, K., 2009. PALSAR Radiometric and Geometric Calibration. IEEE Transactions on Geoscience and Remote Sensing 47, 3915-3932.

Siikamaki, J., Sanchirico, J.N., Jardine, S.L., 2012. Global economic potential for reducing carbon dioxide emissions from mangrove loss. PNAS 109, 14369-14374.

Slim, F.J., Gwada, P.M., Kodjo, M., Hemminga, M.A., 1996. Biomass and litterfall of *Ceriops tagal* and *Rhizophora mucronata* in the mangrove forest of Gazi Bay, Kenya. Marine and Freshwater Research 47, 999-1007.

Smith, J.E., Heath, L.S., 2001. Identifying influences on model uncertainty: An application using a forest carbon budget model. Environmental Management 27, 253-267.

Soares, M.L.G., Schaeffer-Novelli, Y., 2005. Above-ground biomass of mangrove species. I. Analysis of models. Estuarine Coastal and Shelf Science 65, 1-18.

Steele, F., 2008. Introduction to multilevel modelling concepts: module 5. University of Bristol Centre for Multilevel Modelling: [online] Learning Environment for Multilevel Methodology and Applications (LEMMA) available at: <http://www.bristol.ac.uk/cmm/>.

Steinke, T.D., Ward, C.J., Rajh, A., 1995. Forest structure and biomass of mangroves in the Mgeni Estuary, South-Africa. Hydrobiologia 295, 159-166.

Streck, C., 2012. Financing REDD+: matching needs and ends. Current Opinion in Environmental Sustainability 4, 628-637.

Tamooh, F., Huxham, M., Karachi, M., Mencuccini, M., Kairo, J.G., Kirui, B., 2008. Below-ground root yield and distribution in natural and replanted mangrove forests at Gazi bay, Kenya. Forest Ecology and Management 256, 1290-1297.

Tamooh, F., Kairo, J.G., Huxham, M., Kirui, B., Mencuccini, M., Karachi, M., 2009. Biomass accumulation in a rehabilitated mangrove forest at Gazi Bay, in: Hoorweg, J., Muthiga, N. (Eds.), African Studies Collection vol. 20. African Studies Centre., Leiden, pp. 138-146.

Twilley, R.R., Chen, R.H., Hargis, T., 1992. Carbon Sinks in Mangroves and Their Implications to Carbon Budget of Tropical Coastal Ecosystems. Water Air and Soil Pollution 64, 265-288.

UNEP, 2014. UNEP Risoe CDM/JI Pipeline Analysis and Database, April 1st 2014. Available at <http://www.cdmpipeline.org>

Valentini, R., Arneth, A., Bombelli, A., Castaldi, S., Gatti, R.C., Chevallier, F., Ciais, P., Grieco, E., Hartmann, J., Henry, M., Houghton, R.A., Jung, M., Kutsch, W.L., Malhi, Y., Mayorga, E., Merbold, L., Murray-Tortarolo, G., Papale, D., Peylin, P., Poulter, B., Raymond, P.A., Santini, M., Sitch, S., Laurin, G.V., van der Werf, G.R., Williams, C.A., Scholes, R.J., 2014. A full greenhouse gases budget of Africa: synthesis, uncertainties, and vulnerabilities. Biogeosciences 11, 381-407.

Valiela, I., Bowen, J.L., York, J.K., 2001. Mangrove forests: One of the world's threatened major tropical environments. BioScience 51, 807-815.

van Breugel, M., Ransijn, J., Craven, D., Bongers, F., Hall, J.S., 2011. Estimating carbon stock in secondary forests: Decisions and uncertainties associated with allometric biomass models. Forest Ecology and Management 262, 1648-1657.

van der Werf, G.R., Morton, D.C., DeFries, R.S., Olivier, J.G.J., Kasibhatla, P.S., Jackson, R.B., Collatz, G.J., Randerson, J.T., 2009. CO2 emissions from forest loss. Nature Geoscience 2, 737-738.

van Zyl, J.J., 1993. The effect of topography on radar scattering from vegetated areas. IEEE Transactions on Geoscience and Remote Sensing, on 31, 153-160.

Venter, O., Koh, L.P., 2012. Reducing emissions from deforestation and forest degradation (REDD+): game changer or just another quick fix? Year in Ecology and Conservation Biology 1249, 137-150.

Wang, Y., Imhoff, M.L., 1993. Simulated and observed L-HH radar backscatter from tropical mangrove forests. International Journal of Remote Sensing 14, 2819-2828.

Wickramasinghe, S., Borin, M., Kotagama, S.W., Cochard, R., Anceno, A.J., Shipin, O.V., 2009. Multi-functional pollution mitigation in a rehabilitated mangrove conservation area. Ecological Engineering 35, 898-907.

Williamson, G.B., Wiemann, M.C., 2010. Measuring wood specific gravity…Correctly. American Journal of Botany 97, 519-524.

Woodhouse, I.H., Mitchard, E.T.A., Brolly, M., Maniatis, D., Ryan, C.M., 2012. CORRESPONDENCE: Radar backscatter is not a 'direct measure' of forest biomass. Nature Climate Change 2, 556-557.

World Resources Institute. Poverty and ecosystems: Kenya GIS data available at: <http://www.wri.org/>.

Wutzler, T., Wirth, C., Schumacher, J., 2008. Generic biomass functions for Common beech (*Fagus sylvatica*) in Central Europe: predictions and components of uncertainty. Canadian Journal of Forest Research 38, 1661-1675.

Zapata-Cuartas, M., Sierra, C.A., Alleman, L., 2012. Probability distribution of allometric coefficients and Bayesian estimation of aboveground tree biomass. Forest Ecology and Management 277, 173-179.

Zhang, K.Q., Liu, H.Q., Li, Y.P., Xu, H.Z., Shen, J., Rhome, J., Smith, T.J., 2012. The role of mangroves in attenuating storm surges. Estuarine Coastal and Shelf Science 102, 11-23.

Zianis, D., 2008. Predicting mean aboveground forest biomass and its associated variance. Forest Ecology and Management 256, 1400-1407.

Zianis, D., Mencuccini, M., 2004. On simplifying allometric analyses of forest biomass. Forest Ecology and Management 187, 311-332.